Theses, Dissertations and Capstones

2016

Adult neural stem cell differentiation and signaling is disrupted by low-level silver nanoparticle exposure in vitro

Robert Jefferson Cooper
cooper239@marshall.edu

ADULT NEURAL STEM CELL DIFFERENTIATION AND SIGNALING IS DISRUPTED
BY LOW-LEVEL SILVER NANOPARTICLE EXPOSURE *IN VITRO*.

A thesis submitted to
the Graduate College of
Marshall University
in partial fulfillment of
the requirements for the degree of
Master of Science
in
Biological Sciences
by
Robert Jefferson Cooper
Approved by
Dr. Nadja Spitzer, Committee Chairperson
Dr. Guo-Zhang Zhu
Dr. Lawrence Grover

Marshall University
May 2016

APPROVAL OF THESIS

We, the faculty supervising the work of Robert Jefferson Cooper, affirm that the thesis *Adult Neural Stem Cell Differentiation and Signaling is Disrupted by Low-Level Silver Nanoparticle Exposure in Vitro*, meets the high academic standards for original scholarship and creative work established by the Department of Biological Sciences and the College of Science. This work also conforms to the editorial standards of our discipline and the Graduate College of Marshall University. With our signatures, we approve the manuscript for publication.

May 6, 2016

Dr. Nadja Spitzer, Department of Biological Sciences   Committee Chair   Date
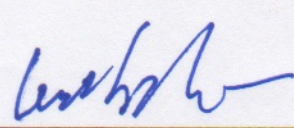
5-6-2016

Dr. Guo-Zhang Zhu, Department of Biological Sciences   Committee Member   Date

5/6/16
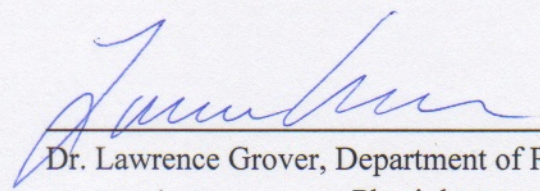
Dr. Lawrence Grover, Department of Pharmacology,   Committee Member   Date
Physiology, and Toxicology

iii

ACKNOWLEDGEMENTS

CONTENTS

LIST OF TABLES

LIST OF FIGURES

LIST OF ABBREVIATIONS

Ag^+	ionic silver
AgNP	silver nanoparticles
Ag_2S-NP	silver sulfide (Ag_2S) nanoparticles
APC	adenomatus polyposis coli
ATP	adenosine triphosphate
bFGF	basic fibroblast growth factor
BrdU	bromodeoxyuridine
BSA	bovine serum albumin
cAMP	cyclic adenosine monophosphate
CNS	central nervous system
CREB	cAMP response element-binding protein
CSF	cerebrospinal fluid
DCX	doublecortin
DMEM	Dulbecco's modified eagle medium
DOM	dissolved organic matter
DTE	dithioerythritol
DTT	dithiothreitol
EDTA	ethylenediaminetetraacetic acid
EGF	epidermal growth factor
EGTA	ethylene glycol tetraacetic acid
ERK	extracellular signal-regulated kinase
FOXO	forkhead box type O
GABA	γ-aminobutyric acid
GAPDH	glyceraldehyde 3-phosphate dehydrogenase
GFAP	glial fibrillary acidic protein
$GSK3\beta$	glycogen synthase kinase 3β
HRP	horse radish peroxidase
ICC	immunocytochemistry
IHC	immunohistochemistry
IP injection	intraperitoneal injection
LV	lateral ventricle
OB	olfactory bulb
MAP2	microtubule-associated protein 2
MAPK	mitogen-activated protein kinase
NCAM	neural cell adhesion molecule
NEAA	non-essential amino acids
NGS	normal goat serum
NSC	adult neural stem cells
PBS	phosphate buffered saline
RMS	rostral migratory stream
ROS	reactive oxygen species
RT-PCR	reverse transcription polymerase chain reaction
SVZ	subventricular zone
TCF/LEF	T-cell factor/lymphoid enhancement factor

ABSTRACT

Silver nanoparticles (AgNP) are an emerging environmental contaminant with unique chemical and physical properties. They are utilized in products like medical dressings and children's toys for their antimicrobial action. Though AgNP's bioaccumulative nature and high-level toxicity are established, low-level effects from chronic exposure to AgNP-containing products and environmental AgNP remain unclear. This study uses adult neural stem cells, a model for neural cell function and neurodevelopment, to assess changes in cell differentiation and behavior following low-level AgNP exposure. *In vitro*, low-level AgNP produced dose- and time-dependent formation of co-localized f-actin inclusions and β-catenin puncta. Neurite extension and arborization were also reduced, indicating that AgNP disrupt cytoskeleton dynamics and β-catenin signaling. *In vivo*, AgNP treatment caused accumulation and persistence of Ag in brains at levels comparable to *in vitro* studies without overt toxicity. Together, this indicates that low-level AgNP exposure from consumer products may impair normal brain function and neurodevelopment.

CHAPTER 1: BACKGROUND AND SIGNIFICANCE

1.1 ADULT NEURAL STEM CELLS

Stem cells occupy multiple niches in the adult body, maintaining populations and aiding in repair and upkeep. Only recently has the idea of stem cells existing in the postnatal brain taken root. Initial work revealed their presence in the hippocampus of postnatal rat brains (Altman and Das, 1965). However, at the time it was thought that these cells merely proliferated and underwent apoptosis without differentiating. Soon thereafter, evidence was found to indicate that these adult neural stem cells (NSC) also existed in the olfactory ventricles of neonate rats (Altman and Das, 1966). Even more astonishing, NSC migrate to the olfactory bulb and differentiate into granule cells (Altman and Das, 1966). However, the authors concluded that these NSC were only capable of becoming short-axon neurons, and that any cells with longer extensions were formed during prenatal development. Subsequent work identified similar processes in neonate guinea pigs (Altman and Das, 1967), demonstrating that postnatal neurogenesis occurs in the brains of multiple rodent species, not only rats. Postnatal neurogenesis has since been documented in many organisms, including fish (Anderson and Waxman, 1985), reptiles (Garcia-Verdugo et al., 1989; Wang and Halpern, 1988), birds (Alvarez-Buylla, 1990; Alvarez-Buylla and Nottebohm, 1988; Alvarez-Buylla et al., 1990), and terminally-ill human cancer patients (Eriksson et al., 1998), indicating that postnatal neurogenesis is not a rodent- or even mammal-specific process.

Analysis of the structure of the neurogenic niche in the subventricular zone (SVZ) led to the discovery of distinct subpopulations of cells, existing side-by-side at various stages of differentiation (Doetsch et al., 1997) (Figure 1). So-called B2 astrocytes have been identified as the stem cells in the SVZ niche (Doetsch et al., 1999), with their proliferative activity, expression

of stem markers, and localization to the SVZ differentiating them from regular B1 astrocytes. B2 astrocytes give rise to Type C cells, or rapidly dividing transit-amplifying cells (Doetsch et al., 1997) that differentiate into Type A cells. Type A cells are migratory neural progenitor cells positive for polysialylated neural cell adhesion molecule (NCAM) and β-tubulin III (Doetsch and Alvarez-Buylla, 1996). NCAM is associated with endogenous repair following nervous injury (Caubit et al., 1993), plasticity, and learning (Cremer et al., 1994), and β-tubulin III is a marker for immature neuronal precursor cells. Type A cells move through the rostral migratory stream sheathed in a guiding scaffold of B1 astrocytes and begin differentiation into neuronal or glial phenotypes (Luskin, 1993; Luskin and Boone, 1994). Once they arrive at the olfactory bulb, Type A cells complete differentiation and integrate into existing circuitry (Doetsch et al., 1997).

Early evidence of adult neurogenesis function came from research with songbirds. Neurons generated from NSC were suggested to be instrumental in learning (Nordeen and Nordeen, 1990; Nottebohm, 1989). Specifically, they were believed to aid in the wiring of new motor pathways and enable animals to learn new songs. Further, newly-generated neurons were believed to be involved in modulation of these pathways by altering the wiring between various song nuclei and the central efferent motor pathway during seasonal changes (Alvarez-Buylla, 1992). Later work used bromodexoyuridine (BrdU), a thimidine analog that labels dividing cells, and found that mice with access to running wheels have higher numbers of BrdU-positive cells, indicating greater NSC proliferation and elevated levels of neurogenesis following exercise memory (van Praag et al., 1999). Further, their hippocampal neurons exhibited enhanced long term potentiation, a synaptic-strengthening process associated with the ability to learn (van Praag et al., 1999). Therefore, mice with increased neurogenesis exhibited an increased ability to learn.
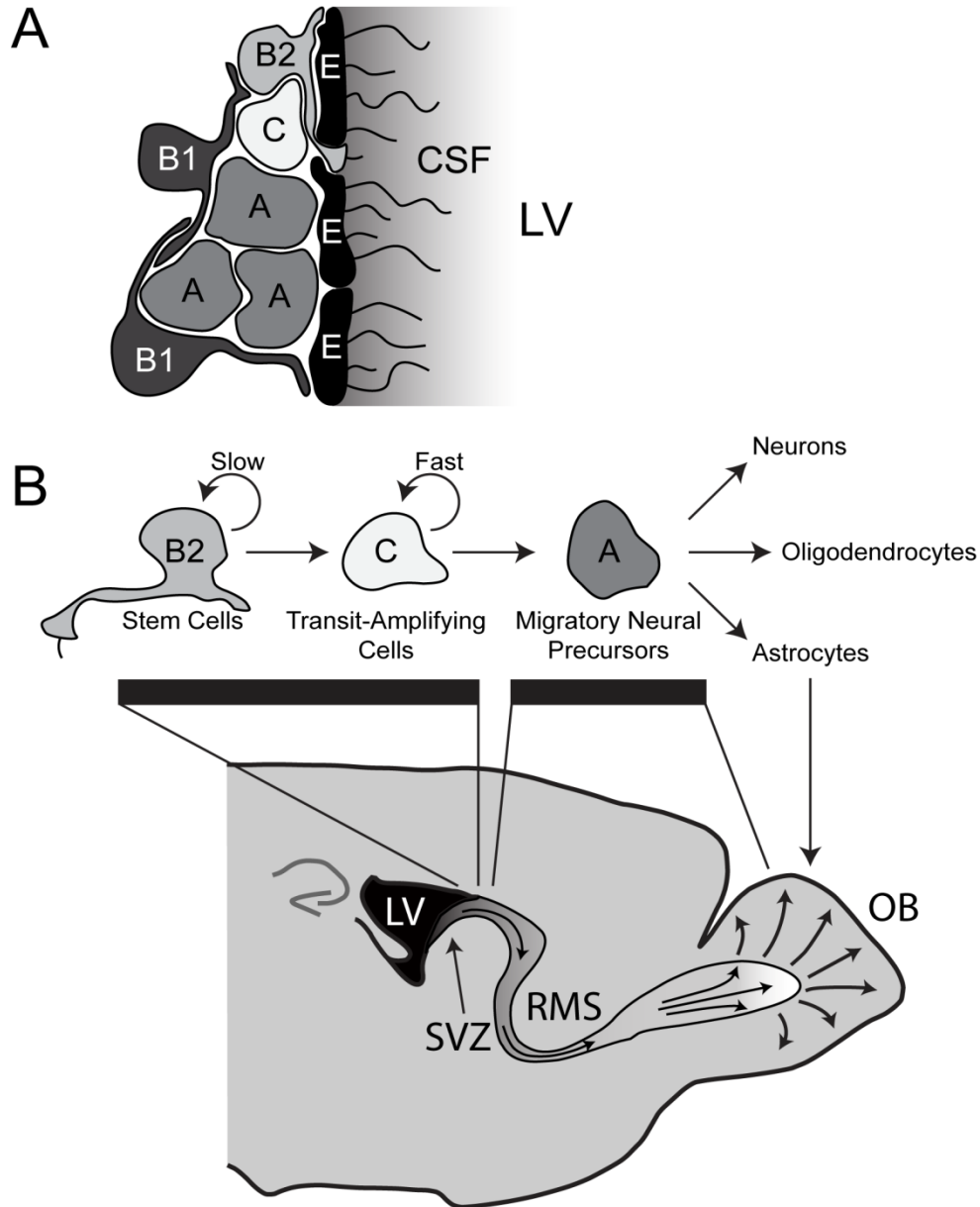
Figure 1: **Schematic representation of NSC differentiation and localization in the adult rodent brain. A**: Organization of astrocytes (B1) and stem (B2), transit-amplifying (C), and migratory precursor (A) cells adjacent to ependymal cells (E) lining the lateral ventricle (LV) filled with cerebrospinal fluid (CSF). Coronal view. **B**: Stem cells, also called B2 astrocytes, slowly undergo asymmetric proliferation in the subventricular zone (SVZ) of the lateral ventricles, undergoing self-maintenance and producing rapidly dividing C-type cells. C-type cells differentiate into A-type cells, migratory neural precursor cells that migrate down the rostral migratory stream (RMS). There, they are sheathed in B1 astrocytes acting as a scaffold to guide A-type cells to their destination. En route, A-type cells continue differentiating. They arrive in the olfactory bulb (OB) after several days and complete differentiation into neurons, oligodendrocytes, or astrocytes, and integrate into existing circuitry. Sagittal view. Illustration © Robert Cooper, 2016.

This finding implicated adult neurogenesis as a part of healthy brain function, and a component of learning and memory.

Adult neurogenesis is involved in several other basic processes, chief among them mood stability (Gage, 2000). Stress decreases adult neurogenesis (Tanapat et al., 1998), and this decrease is thought to be linked to mood disorders such as depression (Jacobs et al., 2000). Antidepressant treatment increases NSC proliferation and neurogenesis (Malberg et al., 2000), and neurogenesis is sensitive to serotonergic (Benninghoff et al., 2010; Gerard et al., 1994) and dopaminergic (Baker et al., 2004; Sui et al., 2012) signaling, two pathways commonly targeted by mood-altering drugs. However, some argue that neurogenesis is not directly involved in depression, nor is its dysfunction necessary for a depressive state (Jedynak et al., 2014). Still, the general consensus seems to be that neurogenesis is somehow involved in mood stability, but the mechanism by which neurogenesis alters mood is poorly understood (Miller and Hen, 2015).

NSC are also involved in endogenous repair following brain injury. Numerous studies have observed marked increases in hippocampal and SVZ neurogenesis following traumatic brain injury in rats (Chirumamilla et al., 2002; Dash et al., 2001; Rice et al., 2003; Sun et al., 2005a). In the SVZ, NSC from post-ischemic rats migrate at a greater rate than those from normal brains (Zhang et al., 2007). Further, SVZ NSC in brain slices taken from post-ischemic rats migrate towards sites of damage instead of towards the olfactory bulb, continuing to undergo cell division once they reach their target (Zhang et al., 2007). Postmortem brains from humans with traumatic brain injury showed an accumulation of cells at the edges of the damaged regions expressing NSC markers (Zheng et al., 2013). Finally, application of bFGF, a growth factor known to enhance NSC proliferation, increased these effects and improved recovery rates of subjects (Sun et al., 2009), demonstrating increased successful repair. Overall, these studies

clearly demonstrate that NSC in the adult brain play a role in the body's attempts at endogenous brain repair following injury.

NSC can also be a useful tool. They can be isolated from neurogenic niches of rodents, generally the SVZ, and induced to continuously proliferate in culture in the presence of EGF and bFGF (Reynolds and Weiss, 1992; Wachs et al., 2003) (Figure 2). The resulting neurospheres of cells are composed of a heterogeneous mixture of subpopulations of stem cells in various stages of differentiation (Mokry et al., 1995, 1996). Undifferentiated NSC dominate within neurospheres, and are capable of maintaining their 'stem-ness' for at least two years (Zhou and Chiang, 1998), possibly longer. Importantly, when neurospheres are subjected to growth factor withdrawal and presented with an extracellular matrix such as laminin (Reynolds and Weiss, 1992; Wachs et al., 2003), they will attach, cease proliferating, and individual NSC will begin differentiating and migrating away from the neurosphere. These neurosphere-derived NSC are capable of differentiating into mature phenotypes such as oligodendrocytes, astrocytes, and GABAergic, dopaminergic, and serotonergic neurons (Zhou and Chiang, 1998).

Differentiating cultured adult SVZ NSC recapitulate many of the same pathways present during neurodevelopment and adult neurogenesis (Ge et al., 2008), while producing functional neural cells. Therefore, cultured SVZ NSC offer an invaluable tool to study changes to NSC both *in vitro* and *in vivo*. *In vitro*, changes in NSC fate, behavior, and signaling can be easily and rapidly observed. These results can then be used as predictors to inform studies investigating the same types of cells *in vivo*, or those examining NSC-related processes such as repair and learning. Finally, as SVZ NSC become functionally viable neurons and glia *in vitro* and lack many of the sustainability issues of primary culture, they can be utilized as a rapid, renewable

5
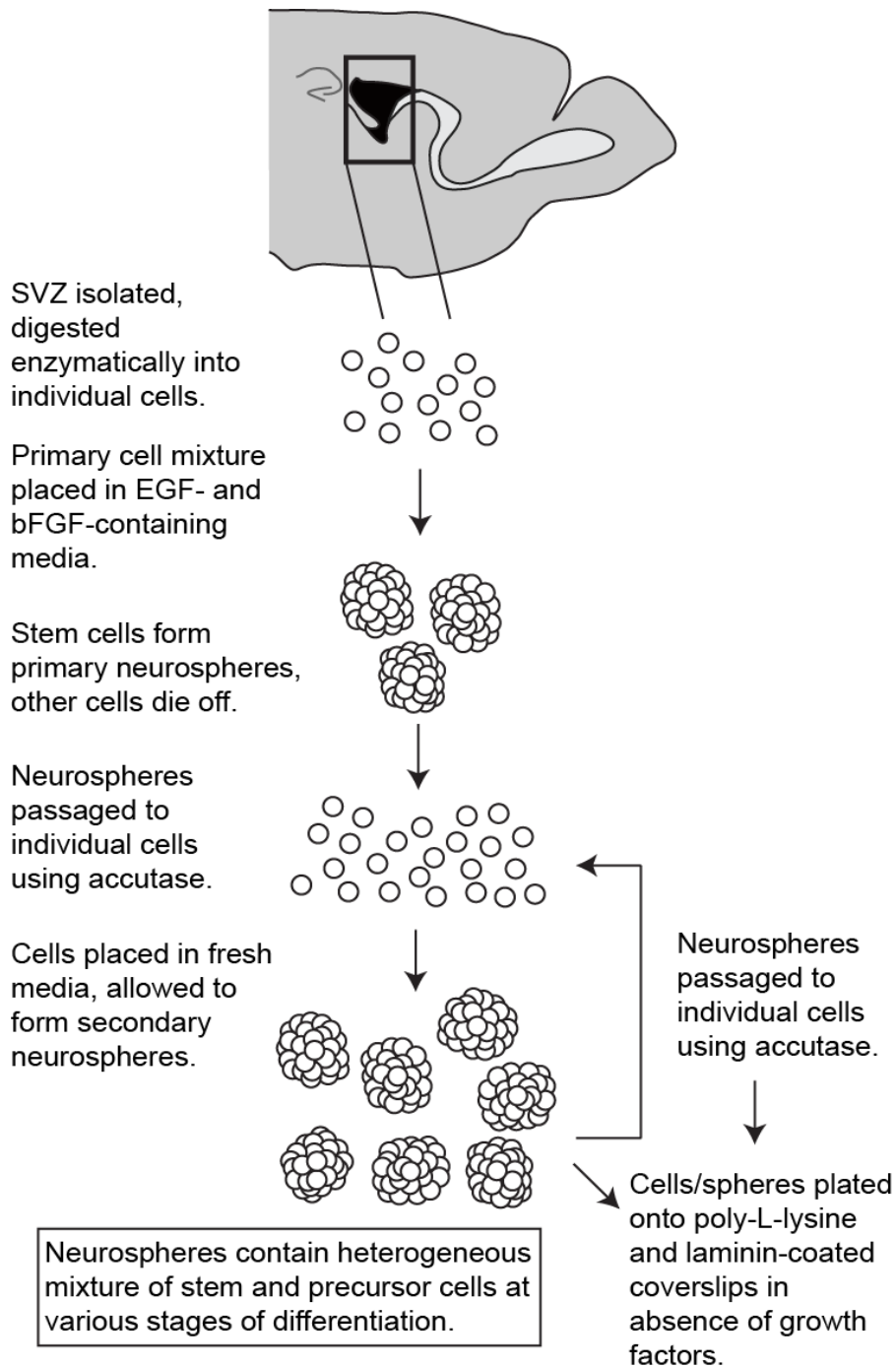
Figure 2: **Schematic representation of NSC isolation, neurosphere formation and maintenance, and differentiation.** The SVZ is removed and enzymatically digested. The resulting mixture of cells is placed in media containing EGF and bFGF. Primary neurospheres will form from any stem cells, and other cell types will die off. Primary neurospheres are passaged into individual cells again and maintained in growth factors to form secondary neurospheres. Cells in secondary spheres will differentiate following growth factor withdrawal and introduction of an extracellular matrix, such as poly-L-lysine and laminin. Illustration © Robert Cooper, 2016.

source of neural cells to investigate general neural cell and brain function.

Therefore, SVZ NSC offer an excellent, sensitive model system to investigate the effects of environmental contaminants on adult neurogenesis and overall brain health at low concentrations. *In vitro* work will allow for the identification of changes to cell behavior and fate following low-level silver nanoparticle exposure, and allow for targeted experiments to determine a molecular mechanism of any observed effects. Further, this will target *in vivo* experiments and provide a framework upon which to build them, allowing for the construction of a comprehensive picture of low-level silver nanoparticles' effects.

1.2 SILVER NANOPARTICLES

Silver is a toxic heavy metal that has been used for centuries as an agent to both prevent and treat disease (Moyer et al., 1965; Ricketts et al., 1970; Russell and Hugo, 1994), usually in the form of colloidal elemental (Ag^0) or ionic (Ag^+) silver. Ionic silver is now known to possess oligodynamic activity, effective in fighting viral, fungal, and bacterial infections (Guggenbichler et al., 1999). Several mechanisms have been proposed for its action. The most prominent is that Ag^+ interacts with the proteins involved with respiration and ATP synthesis in the plasma membrane of bacteria (Bragg and Rainnie, 1974). Another proposed mechanism is direct disruption of the plasma membrane's integrity, causing the cells to lyse (Jung et al., 2008). Finally, Ag^+ interacts with DNA (Guggenbichler et al., 1999; Kargov et al., 1986) and ribosomal machinery (Yamanaka et al., 2005) directly to disrupt normal transcription and translation of genes associated with metabolism.

In addition, there is a body of research showing that Ag^+ can exhibit toxic effects on eukaryotic organisms as well. Predominantly, it seems that the mechanism for these effects is to interact with the Na^+/K^+-ATPase and prevent its activity, thereby causing an ion gradient

imbalance within the cells that ultimately leads to either the detriment or death of the organism (Hussain et al., 1994). Ag^+-mediated disruption of Na^+/K^+-ATPase has been demonstrated in several organisms, including water fleas (Bianchini and Wood, 2003), sea slugs, shrimp (Bianchini et al., 2005), and fish (Atli and Canli, 2013). Ag^+ also interacts with other ion pump ATPases, such as the Ca^{2+}-ATPase and Mg^{2+}-ATPase, to disrupt their activity (Atli and Canli, 2013). Further, it competes for Na^+ channels to gain entry to cells, simultaneously bypassing membranes and disrupting the normal ion flow (Bury and Wood, 1999). Indeed, it is possible that this is the mechanism by which Ag^+ is capable of bypassing biological defenses in the human body such as the blood-brain barrier (Rungby and Danscher, 1983; Van Breemen and Clemente, 1955). Never the less, silver remains an attractive antimicrobial agent, as effective antimicrobial concentrations appear to be below those that can cause toxicity in multicellular organisms. With the advent of nanotechnology and silver nanoparticles, silver has seen a sharp increase in its use.

Though exact definitions vary, the most unifying definition of silver nanoparticles (AgNP) is structures of elemental silver with at least one dimension between 1-100nm (Kruszewski et al., 2011). Due to their small size, AgNP have very high surface area-to-volume ratios, thus providing AgNP novel physical and chemical properties. As an example, spherical 40nm AgNP having a surface area-to-volume ratio of 1.5×10^8, and one gram of these particles theoretically contains approximately $14.3m^2$ of available surface area. As with Ag^+, the most exploited of AgNP's properties is their potent antimicrobial action (Baker et al., 2005; Panacek et al., 2006; Samuel and Guggenbichler, 2004; Sondi and Salopek-Sondi, 2004). Originally envisioned as a coating for medical catheters (Samuel and Guggenbichler, 2004), AgNP have since been used in other medical applications such as burn dressings, sutures, and surgical

equipment (Chen and Schluesener, 2008). They have also become popular in consumer products, conferring antimicrobial properties to products ranging from toys and food packaging to washing machines and water filtration systems (Cushen et al., 2013; Quadros et al., 2013; Silvestry-Rodriguez et al., 2007; von Goetz et al., 2013). However, the potential biological impacts of AgNP to non-target organisms are still poorly understood.

Initial research investigated whether, like Ag^+, AgNP can exert toxic effects on eukaryotic cells. Early studies in germline stem cells revealed a concentration-dependent loss of viability (significant above 10μg/mL) when exposed to 15nm AgNP, while equal quantities of Ag^+ exerted no overt toxic effects (Braydich-Stolle et al., 2005). Presently, some studies have found no difference between AgNP and Ag^+ toxicity or effects (De Matteis et al., 2015; Hadrup et al., 2012), stating that any toxic action of AgNP is due to release of Ag^+ from their surface, while others have identified effects of AgNP separate from Ag^+ (Garcia-Reyero et al., 2014; Xu et al., 2014). Current consensus seems to be that AgNP effects are mediated in part by released Ag^+, but that AgNP also have unique properties unto themselves.

In vivo experiments have pointed to several novel properties of AgNP. Where Ag^+ is thought to cross membranes by competing for cation channels (Bury and Wood, 1999), AgNP have been shown to simply pass through membranes and biological defenses such as the blood-brain barrier (Tang et al., 2008; Tang et al., 2010) and placenta (Melnik et al., 2013). Once there, AgNP accumulate in tissues such as the brain, kidney, gonads, and liver (Lee et al., 2013), with especially high retention times in the gonads (Lee et al., 2013) and brain (Lankveld et al., 2010; Wen et al., 2016). Indeed, a four-month recovery study following one month of AgNP treatment did not reach a half-life of brain Ag content by its conclusion (Lee et al., 2013).

Not only do AgNP persist in tissues, they also persist in the environment. A study found that, in water with high levels of chloride ions, AgNP quickly agglomerated and dropped out of suspension (Tugulea et al., 2014). However, in the presence of dissolved organic matter, AgNP could remain available for at least nine months, even in strongly chlorinated water (Tugulea et al., 2014). Other studies have shown that AgNP persistence is dependent upon pH and sunlight conditions, as low pH or low sunlight encourages particle oxidation and dissolution to Ag^+, whereas high pH or high sunlight encourages reduction of Ag^+ onto the surface of AgNP (Yu et al., 2014). Ag^+ in the environment may even form new AgNP under reductive conditions (Zhang et al., 2015c). Ultimately, AgNP fate in the environment is highly variable, with factors such as local water chemistry (Yin et al., 2015c; Zhang et al., 2015a), nanoparticle coating (Jang et al., 2014; Yin et al., 2015b), particle size (Angel et al., 2013; Dobias and Bernier-Latmani, 2013), sunlight availability, and dissolved organic matter (Tugulea et al., 2014; Zhang et al., 2015c) each having a dramatic impact (Figure 3). A 20-year study analyzing AgNP fate in a watershed system showed that local concentrations of AgNP and AgNP-derived compounds could vary by up to nine orders of magnitude between treatment sites (Dale et al., 2015).

Despite this abundance of experimental data, little to no research examines levels of AgNP in the environment itself. One study, performed in various Colorado rivers and streams, showed up to four orders of magnitude difference between AgNP concentrations at different sites (0.1ng/L to 1.8μg/L), with the highest being a river downstream from an industrial complex (Wen et al., 2002). Conversely, significantly more research has been done examining exposure levels due to release from medical or consumer products. Burn dressings have been found to release approximately 0.6μg/day (Bidgoli et al., 2013), and AgNP-containing throat sprays were found to release 0.24-0.26ng AgNP per use (Quadros and Marr, 2011). Exposure from food

Engineered particles introduced into system; specific shapes, sizes, coatings, and composition.

Low pH, low sunlight, low DOM

High pH, high sunlight, high DOM

Ag+ Ag+ Ag+ Ag+ Ag+ Ag+ Ag+ Ag+ Ag+ Ag+ Ag+ Ag+ Ag+ Ag+ Ag+ Ag+

Naturally formed or re-formed particles; variable size, shape, coating, and composition.

Silver ions and significantly smaller particles.

Particle agglomeration

High Cl-, high sulfide, high thiol-containing groups

Removal from water column

Figure 3: **Schematic representation of AgNP behavior in aquatic environments.** Briefly, when AgNP are introduced to the environment, their fate depends largely on local chemistry and physical properties. Low pH, low sunlight levels, and low levels of dissolved organic matter (DOM) contribute to particle oxidation, and therefore breakdown and dissolution. Conversely, high pH, high sunlight, and high concentrations of DOM contribute to ion reduction, and therefore particle formation or growth. However, if large particles remain under growth conditions, they may agglomerate and become too large to remain suspended in the water column. Alternatively, if there is an abundance of chloride, sulfide, or thiol-containing groups, Ag^+ ions can be removed from the water column. Together, this makes AgNP levels within the environment highly variable depending upon local fluctuations in any of these factors, complicating efforts to quantify environmental AgNP concentrations.
Illustration © Robert Cooper, 2016.

packaging has been estimated to be between 0.06-13µg/kg/day (Cushen et al., 2013, 2014).

Similarly, release of AgNP from several baby products has been assessed, with a plush toy

releasing up to 18.5mg/kg product, and a blanket up to 4.8mg/kg product (Quadros et al., 2013).

Finally, analysis of various household products such as shirts, toothpaste, shampoo, and

detergent each release anywhere from 22 to 43.3mg/kg product (Benn et al., 2010). Attempts

have been made to model AgNP exposure from the environment (Blaser et al., 2008; Money et

al., 2014; Whiteley et al., 2013), but it is clear that exposure depends on differences in daily

interaction with AgNP-containing products. Further, the bioaccumulative nature of AgNP (Lee et

al., 2013) complicates attempts at estimation. Still, it is clear that the ubiquitous nature of AgNP

within society ensures at least some level of daily exposure, whether from shedding of AgNP-

containing products or from environmental sources. This leads to accumulation of low levels of

AgNP within tissues, especially the brain, where they can cause unknown physiological changes.

Therefore, it is a priority to understand the effects of low-level AgNP exposure on brain cell

function and general brain health.

1.3 SILVER NANOPARTICLES AND NEURAL STEM CELLS

The effects of high levels of AgNP on biological systems are well-documented (reviewed

in Bartlomiejczyk et al., 2013). At 5µg/mL and above, AgNP cause significant loss of cell

viability *in vitro* (summarized in Table 1), break down the cytoskeleton in neuroblastoma cells

(Schrand et al., 2008) and cultured neurons (Xu et al., 2013), and damage DNA in embryonic

stem cells and embryonic fibroblasts (Ahamed et al., 2008). Ultimately, high levels of AgNP

lead to apoptosis and necrosis of cells *in vitro* (Arora et al., 2008; Haase et al., 2012; Kim et al.,

2012). However, their effects at lower concentrations are poorly understood. AgNP exposure can

result in the production of reactive oxygen species (ROS), either through the downregulation or

12

Table 1: **Summary of *in vitro* AgNP toxicity data in mammalian cells.** Multiple values are given for minimum toxic concentration where different assays produced differing results.

Size	Coating	Cell Type Used	Time	Minimum Toxic Conc.	Source
15nm	None	C18-4 immortalized germline stem cells	48hr	10μg/mL	(Braydich-Stolle et al., 2005)
15nm	None	BRL-3A rat liver-derived	24hr	5μg/mL (MTT) 10μg/mL (LDH)	(Hussain et al., 2005)
100nm				5μg/mL (MTT) 10μg/mL (LDH)	
15nm	None	PC12 cells	24hr	10μg/mL	(Hussain et al., 2006)
7-20nm	None	A431 human skin carcinoma HT-1080 human fibrosarcoma	24hr	6.25μg/mL 6.25μg/mL	(Arora et al., 2008)
15nm 30nm 55nm	None	Alveolar macrophages	24hr	5μg/mL 10μg/mL 50μg/mL	(Carlson et al., 2008)
7-10nm	None	HepG2 human heptoma	24hr	1.5μg/mL	(Kawata et al., 2009)
20nm	CKK-peptide	Primary neuronal culture (rat)	7d 14d 21d	20μg/mL 5μg/mL* 5μg/mL*	(Haase et al., 2012)
40nm			7d 14d 21d	>100μg/mL 10μg/mL 10μg/mL	
14nm	PVP	PC12 cells	48hr	10μmg/mL	(Hadrup et al., 2012)
20nm	None	Primary cortical neurons (rat)	72hr	1μg/mL (immediate) 10μg/mL (4d post-culture) 5μg/mL (10d post-culture)	(Xu et al., 2013)
10nm	Citrate	PC12 cells	4d	3μM (6x10^{10}AgNP/mL) (~0.33μg/mL)	(Powers et al., 2011)
46nm	None	Human mesenchymal stem cells	1hr 3hr 24hr	10μg/mL 10μg/mL 10μg/mL	(Hackenberg et al., 2011)

lowest concentration tested

disruption of antioxidant enzymes within the cell or production of ROS at the nanoparticle surface (Manke et al., 2013). In high concentrations, this can result in oxidative stress, ultimately leading to cell dysfunction and death (Haase et al., 2012; Jiang et al., 2013; Kim et al., 2008b). Normally, minute modulations of intracellular ROS levels are involved in maintenance of NSC proliferation and fate decision during NSC differentiation (Le Belle et al., 2011; Prozorovski et al., 2015; Vieira et al., 2011). Therefore, changes to intracellular ROS following low-level AgNP exposure may be capable of altering NSC behavior.

Interestingly, low levels of AgNP (0.1-0.2μM, 12hr) increase neural differentiation of SH-SY5Y neuroblastoma cells, and cause an increase in ERK, Akt, and ROS signaling (Dayem et al., 2014). ERK activation promotes NSC proliferation and neuronal differentiation (Huang et al., 2014; Liu et al., 2014), and Akt activation enhances NSC proliferation and survival during differentiation (Conti et al., 2001; Jin et al., 2005). Similarly, ROS signaling is a key regulator of neural stem cell maintenance and differentiation (Le Belle et al., 2011; Ryu et al., 2015; Vieira et al., 2011), and is coupled with Wnt/β-catenin signaling (Braunschweig et al., 2015). Wnt/β-catenin signaling is another intracellular signaling pathway involved generally in metabolism and cytoskeleton regulation, while also playing roles in promoting NSC proliferation and modulating differentiation (Kuwabara et al., 2009; Mu et al., 2010; Wexler et al., 2009; Wheelock and Knudsen, 1991; Wisniewska, 2013).Together, this provides good evidence for the ability of AgNP to alter physiological functions within NSC even with low-level exposures. Further, changes to NSC behavior may interfere with adult neurogenesis, and result in a disruption of basic processes such as learning and memory.

1.4 SPECIFIC AIMS

AgNP are ubiquitous in the environment, and are known to bypass biological defenses such as a blood-brain barrier and accumulate in tissues, especially the brain. It is known that AgNP at high concentrations can damage the cytoskeleton and DNA, and induce oxidative stress, apoptosis, and necrosis. However, less is known about effects of AgNP at concentrations more in line with those found in the environment or accumulated in tissues. Therefore, as NSC are an excellent, accessible model of adult neurogenesis, neurodevelopment, and neural cells in general, this work investigates changes to proliferation, differentiation, and activity of NSC in response to low-level AgNP exposure.

Specific Aim 1 is to investigate changes to NSC differentiation and behavior *in vitro* following low-level AgNP exposure. Isolated neurospheres of NSC (Figure 2) were plated onto poly-L-lysine and laminin-coated coverslips, allowed to differentiate, and exposed to 40nm citrate-stabilized, spherical AgNP at a concentration of 0.05-2.0μg/mL for 48 hours. Immunocytochemistry assessed changes to expression of differentiation markers, while staining of the cytoskeleton allowed visualization of morphology. Time-lapse microscopy immediately following AgNP exposure investigated changes to cell behavior, especially the cytoskeleton-dependent processes neurite extension and arbor development. Finally, comet assay was used to ensure that the concentrations of AgNP used in this study are, in fact, not toxic to the cells. Together, these experiments highlighted changes to AgNP fate and behavior following low-level AgNP exposure.

Specific Aim 2 is to determine the cellular signaling pathways altered by low-level AgNP. Protein isolated from differentiated NSC exposed to low-level AgNP was probed by Western blot for changes in ERK or Akt signaling, as both can be altered by AgNP (Dayem et

al., 2014). Additionally, β-catenin signaling, the canonical mediator of Wnt signaling, was investigated due to its link to ROS signaling in NSC (Braunschweig et al., 2015). Immunocytochemistry was also used to probe β-catenin localization, as β-catenin's cellular distribution impacts its signaling. Together, these experiments highlighted which pathways are targeted for disruption by low-level AgNP.

Specific Aim 3 is to investigate *in vivo* effects of low-level AgNP and functional changes to cells generated from NSC exposed to low-level AgNP. For *in vivo* experiments, equal numbers of male and female rats were given AgNP daily at a dosage shown previously to not exert overt toxic effects (100mg/kg/day) for 28 days. Half of each group was collected immediately following treatment, with the other half allowed 28 days of recovery without treatment. BrdU was given at 14, 7, 2, and 1 days pre-collection to visualize new cells. Cerebella were collected and analyzed for silver content. Fixed brains were sliced and analyzed for fate markers using immunohistochemistry to determine number of proliferating cells, cell position, and cell fate. For cell function experiments, patch clamp electrophysiology was used to assess changes in voltage-activated currents in differentiated NSC. Together, these experiments aimed to showcase AgNP's ability to bypass bodily defenses and accumulate in tissues, and subsequently alter cell behavior and activity even at levels that exert no toxic effects.

Overall, this study investigates changes to NSC proliferation, migration, differentiation, maturation, and integration at multiple levels following low-level AgNP exposure. As these processes are all vital for adult neurogenesis, disruption of even one of them could point to a corresponding disruption of adult neurogenesis and therefore healthy brain function. This, in turn, could lead to deficits in basic activities such as learning, memory, and the brain's ability to repair itself. Therefore, this research informs future investigations into the low-level effects of

AgNP on the brain and begins the much-needed process of filling gaps in the knowledge base. This is especially prudent as, due to the relative novelty of AgNP, little to no legislation or regulation exists governing their use.

Though AgNP have chemical and physical properties distinct from the Ag^+ released from their surface, whether the detrimental effects of AgNP are mediated by Ag^+ release or AgNP-unique processes remains unknown. Ag^+ enters cells by means of cation channels, but AgNP can penetrate membranes and bypass biological defenses *in vivo* and *in vitro* while remaining in nanoparticle form (Tang et al., 2008). This has led to an argument that AgNP effects are mediated mainly by AgNP's ability to easily cross membranes and deliver Ag^+ into the cell (Hsiao et al., 2015). Alternatively, Ag^+ in biological conditions can form AgNP in the presence of reducing sugars like glucose (Hansen and Thunemann, 2016), meaning that any Ag^+ released into cells might be easily re-formed back into nanoparticles. Ultimately, this work does not differentiate effects that are mediated by AgNP or Ag^+ released from those AgNP. There is enough evidence that AgNP migrate to and persist in tissues intact to justify studying changes to NSC differentiation, signaling, and behavior following direct exposure to AgNP.

CHAPTER 2: LOW-LEVEL SILVER NANOPARTICLES DISRUPT CYTOSKELETON AND NEURITE DYNAMICS IN DIFFERENTIATING CULTURED NEURAL STEM CELLS.

2.1 INTRODUCTION

The adult brain contains pools of adult neural stem cells (NSC) that proliferate and differentiate into mature neural phenotypes throughout life (Altman and Das, 1965; Eriksson et al., 1998; Gage, 2000). They are primarily localized to specialized niches, one of which is the subventricular zone (SVZ) of the lateral ventricles (Alvarez-Buylla and Nottebohm, 1988; Luskin, 1993). There, NSC proliferate, begin the process of differentiation, and migrate down the rostral migratory stream towards the olfactory bulb (Doetsch et al., 1997; Luskin, 1993; Luskin and Boone, 1994). Once in the olfactory bulb, they complete differentiation and integrate into existing circuits, primarily as GABAergic interneurons (Gerard et al., 1994; Scheffler et al., 2005). This process of adult neurogenesis continues throughout life, and is important in basic processes such as learning, memory, and endogenous repair (Snyder et al., 2001; van Praag et al., 1999; Zhang et al., 2007; Zheng et al., 2013). It is therefore considered to be a part of healthy brain function. Further, NSC can be isolated from the SVZ and maintained in culture as neurospheres, organized spheres of progenitor cells (Doetsch et al., 2002; Reynolds and Weiss, 1992; Wachs et al., 2003). Cells in neurospheres can be induced to differentiate by growth factor withdrawal in the presence of an extracellular matrix, and will follow the same molecular programs seen in adult neurogenesis and development (Ge et al., 2008). In doing so, they produce functional neurons and glia. Therefore, SVZ-derived NSC are a useful *in vitro* model system to investigate changes in neurodevelopment, adult neurogenesis, and general brain function following endogenous or exogenous physiological insults.

In this study, SVZ-derived NSC are used to investigate the effects of the emerging environmental contaminant silver nanoparticles (AgNP). AgNP are nano-scale (1-100nm) in at least one dimension (Kruszewski et al., 2011), which gives them a high surface area to volume ratio and novel chemical and physical properties that differentiate them from ionic or colloidal silver (Braydich-Stolle et al., 2005; Garcia-Reyero et al., 2014; Tang et al., 2008). One of these properties is potent antimicrobial effects (Pal et al., 2007; Samuel and Guggenbichler, 2004; Sondi and Salopek-Sondi, 2004), resulting in AgNP-containing products ranging from burn dressings and catheter coatings to food packaging and children's toys (Benn et al., 2010; Cushen et al., 2013; Quadros et al., 2013; Zhang et al., 2012). AgNP are known to cross or disrupt biological membranes such as the blood-brain barrier (Tang et al., 2008), and accumulate in various tissues, especially the brain (Lee et al., 2013). In culture, AgNP damage the cytoskeleton and DNA (Ahamed et al., 2008; Schrand et al., 2008; Xu et al., 2013), and induce oxidative stress, apoptosis, and necrosis (Arora et al., 2008; Haase et al., 2012; Hadrup et al., 2012; Kim et al., 2009).

Many studies have showcased AgNP's toxic potential (Arora et al., 2008; de Lima et al., 2012; Kruszewski et al., 2011; Li et al., 2014). However, concentrations of AgNP used in these studies, sometimes as high as 100μg/mL (Haase et al., 2012), are generally well in excess of those thought to be relevant to actual exposure levels, estimates of which are generally within the range of 0.06-13μg/day for single sources (Cushen et al., 2014; Quadros and Marr, 2011; Tulve et al., 2015). Given that AgNP can persist in the environment for extended periods of time (Dale et al., 2015; Tugulea et al., 2014) and accumulate in tissues (Lee et al., 2013), measurements of true exposure are difficult at best. This is further complicated by the presence of AgNP in numerous consumer products encountered every day (Tulve et al., 2015; von Goetz et al., 2013;

Yang and Westerhoff, 2014), making exposure even more variable with lifestyle and location (Wen et al., 2002). For this study, low-level AgNP concentrations that do not significantly reduce viability of cultured neurons (<5μg/mL) (Haase et al., 2012; Xu et al., 2013) and neuron-like cell lines (<5-10μg/mL) (Hadrup et al., 2012; Hussain et al., 2005), and that are in line with levels seen in brains following oral exposure in rats (0.2-0.5μg/mL) (Lee et al., 2013) were chosen. The aim was to investigate how low, environmentally-relevant levels of AgNP can induce changes to NSC behavior and differentiation, and therefore neurogenesis and normal brain function.

2.2 MATERIAL AND METHODS

2.2.1 SVZ-NSC Isolation and Maintenance of Progenitor Cells

Stem cells were isolated from female young adult (3-6 months old) Sprague-Dawley rats (Hilltop Lab Animals, Scottsdale, PA) according to established protocols (Muraoka et al., 2008; Reynolds and Weiss, 1992; Wachs et al., 2003). Rats were deeply anesthetized with inhaled isoflurane (Kent Scientific Corp., Torrington, Connecticut) and decapitated. The brain was removed and placed in cold phosphate-buffered saline 1 (PBS1, in mM: NaH_2PO_4, 2.69 (Sigma, St. Louis, Missouri, United States); Na_2HPO_4, 11.9 (AMRESCO, Solon, Ohio); NaCl, 137 (Fisher, Fair Lawn, New Jersey); KCl, 27 (AMRESCO); pH 7.4) containing 1% penicillin-streptomycin (P/S; Life Technologies, Grand Island, New York) before the subventricular zone was isolated. The tissue was chopped in PBS1 plus 4.5g/L glucose (Sigma) with a scalpel blade, then enzymatically digested in fresh PDD (0.01% papain (Fisher); 0.01% DNase I (Sigma); 0.1% Dispase II (Sigma); 12.4mM $MgSO_4$ (Sigma)) for 40 minutes with trituration every 10 min. After digestion, cells were collected by centrifugation, washed three times with DMEM/F12 (Life Technologies) and suspended in Neurosphere medium (DMEM/F12 + Glutamate, non-

essential amino acids (NEAA), P/S, B27, 20ng/ml EGF, 5ng/ml bFGF, (all from Life Technologies) and 1.25U/ml Heparin sodium (Sigma)). Fungizone antimycotic (Life Technologies) was included in the medium for the first week of culture. Fresh medium was added every 2-3 days and neurospheres formed within two weeks of culture in non-TC flasks at 37^oC, 5% CO_2. Cells in neurospheres were dissociated with accutase (Life Technologies) before reaching a diameter greater than 500μm (every 7-14 days), passaged cells giving rise to new neurospheres.

2.2.2 *In Vitro* Differentiation of SVZ-NSCs and Exposure to AgNP

To induce differentiation of NSC, undifferentiated neurospheres (passage 4-18) were collected by centrifugation, washed to remove growth factors, and plated on poly-L-lysine (0.01%) and laminin (10μg/mL) coated coverslips or wells in 24-well plates in differentiation medium (Neurobasal (Life Technologies), 2% B27 (Life Technologies), 1% NEAA, 1% Glutamax (Life Technologies), and 1% P/S) lacking EGF and bFGF. After being allowed to attach and differentiate for 2-3 days, medium was replaced with fresh medium containing 0, 0.05, 0.1, 0.5, 1.0, or 2.0 μg/mL AgNP stabilized in 2mM citrate (Sigma). Filter-sterilized 2mM sodium citrate was used as a vehicle control. Cells were incubated for 48 hours for dose-response experiments. For time-response experiments, media was replaced with fresh and stock AgNP solution was added to individual wells at the appropriate time (24hr, 6hr, 2hr, 1hr) for a final working concentration of 1.0μg/mL AgNP in each well.

2.2.3 B35 Cell Culture

Undifferentiated B35 neuroblastoma cells (ATCC, Manassass, Virginia), a model of neurite extension and cell migration, were maintained in TC-coated flasks in growth medium (DMEM, 10% fetal bovine serum, 1% P/S) and passaged at 90-95% confluence using trypsin. To induce differentiation, cells were plated in 24-well plates coated with poly-L-lysine and laminin

in serum-free medium. Cells were allowed to adhere and differentiate for two days before

exposure to 1.0μg/mL AgNP in serum-free medium.

2.2.4 Immunocytochemistry

Immunocytochemistry was used to label cells for markers of differentiation state and cell

fate. Cells were washed with PBS1, fixed on coverslips with 4% paraformaldehyde for 15min,

washed with phosphate buffered saline 2 (PBS2; 100mM sodium phosphate, 150mM NaCl, pH

7.4) and then permeabilized with 0.3% Triton-X/PBS2 for 10 minutes. Preparations were

blocked with 5% bovine serum albumin (BSA, Fisher) and 10% normal goat serum (NGS, Life

Technologies) for one hour before being incubated overnight with primary antibodies (1:500)

specific to cell fate marker proteins. No-primary control preparations were included in each

experiment. Primary antibodies were mouse-α-MAP2 (Millipore, Darmstadt, Germany), rabbit-

α-MBP (Millipore), mouse-α-β-tubulin III (Phosphosolutions, Aurora, Colorado), mouse -α-

GFAP (Abcam, San Francisco, California), and rabbit-α-DCX (Abcam). Secondary antibodies

(1:500) were goat-α-mouse or goat-α-rabbit Alexa 488 (Life Technologies), and were co-

incubated with phalloidin-Alexa 568 (1:100; Life Technologies) overnight in 5% BSA and 1%

NGS solution. Cells were counterstained with DAPI and washed with D.I. H_2O before being

mounted on slides using Prolong Gold (Life Technologies). Slides were allowed to cure at room

temperature overnight and stored at 4^oC. Images were acquired using epifluorescent microscopy.

2.2.5 Comet Assay

Comet assay was used to confirm that levels of AgNP used in this experiment do not

induce significant DNA damage, and therefore apoptosis or necrosis, in cultured NSC. Solutions

for alkaline comet assay (Singh et al., 1988) were prepared in advance and stored at 4^oC.

Undifferentiated neurospheres were plated on plastic 6-well plates coated with poly-L-lysine and

laminin in differentiation medium as described above (see 2.2.2). After the 2-3 day attachment period, media was replaced with either unaltered media (for positive and negative control) or media containing 1μg/mL or 2μg/mL AgNP for 24hr. Flamed slides were dipped in molten normal melt agarose (10mg/mL in water) and stored flat at room temperature overnight. Slides were pre-warmed to 37^oC before use. Cells were lifted by scraping and collected by centrifugation. Resulting pellets were suspended in 500μL either PBS1 or 200μM H_2O_2 (positive control only) on ice for 20min. Cells were once again collected by centrifugation and resuspended in 20μL PBS1 at 37^oC. 10μL of this suspension was mixed with 90μL of molten low-melt agarose (LMA; 0.6mg/mL in PBS1, final 0.55mg/mL) at 37^oC and gently spread over pre-warmed slides. Slides were placed on an ice block in 4^oC for at least 30 minutes, until LMA layer had solidified, before being immersed in lysis buffer at 4^oC (0.1M EDTA (Sigma); 2.5M NaCl (Fisher); 0.2M NaOH (AMRESCO); 10mM Tris (AMRESCO); 1% Triton-X; pH 10) in dark for 1hr. Slides were moved to electrophoresis buffer (0.3M NaOH; 1mM EDTA; pH 13) in the dark, 1hr to allow for DNA denaturing. Slides were moved to a horizontal gel aparatus in fresh electrophoresis bufffer and run at 1V/cm and 300mA for 30 minutes. Slides were then immersed in neutralization buffer (0.4M Tris, pH 7.5) at room temperature four times 5min, before being washed in diH$_2$O two times 5min. Finally, slides were dehydrated in 70% ethanol for 5min and allowed to dry at 37^oC for 15 minutes. Slides were covered with 60μL each of 1μg/mL DAPI, coversliped, and imaged after 30min using an epifluorescent microscope. 10x10 tilescans were taken from the center of each slide, with at least 50 cells per sample.

2.2.6 AgNP Enhancement for Light Microscopy Visualization

AgNP enhancement experiments examined localization of AgNP within NSC. Cells were cultured and exposed to AgNPs for two days before fixation and permeabilization as described

above for immunocytochemistry (see 2.2.4). Following permeabilization, cells were treated with phalloidin-Alexa 568 in PBS2 for 20 minutes, washed with PBS2, and images were recorded using epifluorescent microscopy. Image XY locations were saved, and then cells were treated with the Aurion R-Gent SE-LM Silver Enhancement kit (Electron Microscopy Sciences, Hatfield, Pennsylvania), as per the manufacturer's instructions. Images were collected again from cells in the saved XY positions with transmitted light immediately after enhancement.

2.2.7 Time Lapse Microscopy

Time lapse experiments were performed to assess cell behavior immediately following low-level AgNP exposure. Cells were grown in differentiation conditions for 2-3 days on poly-L-lysine and laminin-coated 24-well tissue culture plate. Medium was replaced with either AgNP-containing medium (1.0μg/mL) or control medium. Immediately following media replacement, cells were moved to a stage-top incubator at $37^{o}C$ and 5% CO_2 and images were collected using transmitted light. Images of B35 cells were collected every hour for 24 hours, and images of SVZ-NSCs were collected every 15 minutes for 6 hours, with at least two positions collected per well in every experiment.

2.2.8 RT-PCR

RT-PCR was used to assess transcription of NSC markers by cells within neurospheres. Undifferentiated neurospheres were collected by centrifugation. Total RNA was isolated from cells using an Ambion PureLink kit with on-column DNA treatment (Life Technologies) followed by reverse transcription of 2μg of RNA to cDNA using an ABI high-capacity RT kit (Life Technologies). No RT control reactions were run in parallel for each sample. PCR reactions were run using Taq polymerase (Bioexpress, Kaysville, UT), and primers for DCX (F: TTGGACATTTTGACGAACGA, R: CCCTTCTTCCAGTTCATCCA; NM_053379; 353bp

(Liu et al., 2009a)), GFAP (F: TAAGCTAGCCCTGGACATCG, R:

TTTCTCGGATCTGGAGGTTG; NM_010277; 110bp (Liu et al., 2009a)), Sox2 (F:

ACCAGCTCGCAGACCTACAT, R: TAGGAGTGGGAGGAAGAGGTA; NM_001109181;

154bp (Liu et al., 2009a)), Nestin (F: AGAGAAGCGCTGGAACAGAG, R:

AGGTGTVTGCAACCGAGAGT; 234bp (Sun et al., 2011)) or GAPDH (F:

GATGCTGGTGCTGAGTATGTCG, R: GTGGTGCAGGATGCATTGCTCTGA; 197bp)(All

5'→3'). PCR products were separated by 10% poly-acrylamide gel electrophoresis, stained with

ethidium bromide, and imaged under UV.

2.2.9 Imaging

A Leica DM6000B microscope was used to obtain epifluorescent and transmitted light

images with 10x and 20x objectives. Images were acquired using LAS AF software (Leica,

Buffalo Grove, Illinois). Adjustments to brightness and contrast were performed only on entire

images using ImageJ (NIH, Bethesda, Maryland). For the enhancement assay, open source

software (GIMP) was used to manually align the images and the transmitted light images were

color-reversed to allow overlaying in ImageJ and simultaneous visualization of silver

enhancement and actin staining. All figures were created using Adobe Illustrator.

2.2.10 Data Analysis

For ICC, cells were counted in ImageJ. Neurites were analyzed with the freeware ImageJ

extension NeuronJ(Meijering et al., 2004). Comet assay data were analyzed with the freeware

ImageJ extension OpenComet (Gyori et al., 2014). Data in bar graphs are presented as mean ±

standard deviation of at least three independent experiments as detailed. Graphs were generated

and statistical significance was determined using Prism (Graphpad, San Diego, CA). Following

one-way ANOVA tests, Tukey's multiple comparisons test was used to determine significance

between groups. Additionally, the more conservative Sidak's multiple comparisons test confirmed significance levels. Following two-way ANOVA tests, Sidak's multiple comparisons test was used to determine significance between groups.

2.3 RESULTS

2.3.1 Characterization of SVZ-Derived NSC and Assessment of AgNP Toxicity.

Cells from the SVZ of young adult rats formed free-floating spheres in media containing EGF or bFGF (Figure 4A). The cells in these spheres regularly express the neural stem cell markers Sox2, nestin, doublecortin (DCX), and glial fibrillary acidic protein (GFAP)(Figure 4B). When plated on an extracellular matrix (laminin) in media lacking growth factors, the cells in the spheres attach, migrate away, and differentiate into mature lineages with complex morphologies. These differentiating cells express the neuronal precursor marker β-tubulin III (Figure 4C), the mature neuronal marker microtubule-associated protein 2 (MAP2; Figure 4D), and the oligodendrocyte marker myelin basic protein (MBP; Figure 4E).

Though proposed AgNP exposure levels for this study are below those found to be toxic in other studies (Table 1), different cell types have different tolerances for AgNP, with size and coating playing a large role in toxicity. Comet assay of the two highest exposure levels chosen for this study revealed no statistically significant change in the distribution of Olive moment, a metric used to quantify the amount of DNA damage (Olive et al., 1990), between negative control cells and those treated with 1 or 2μg/mL 40nm AgNP (Figure 4F). Conversely, all conditions had a significantly greater proportion of cells with an Olive moment of 0-10 than positive control, in which apoptosis was induced with H_2O_2 (Figure 4F).
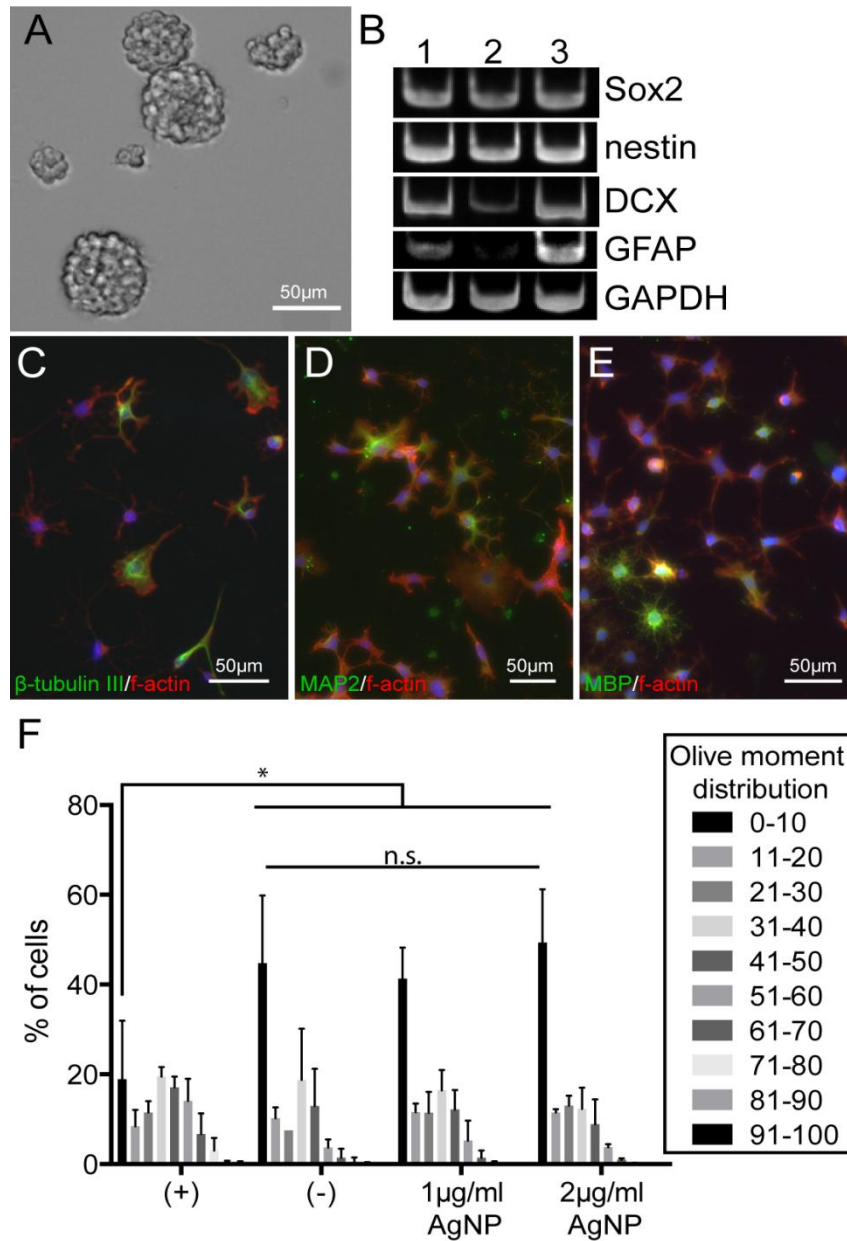
Figure 4: **SVZ-derived NSC express stem markers, differentiate into neurons and glia, and do not experience genotoxicity from low-level AgNP exposure.** Isolated cells proliferate and form free-floating spheres in culture (A). RT-PCR demonstrated expression of stem cell markers in three separate cell lines (B). NSC in spheres can be induced to differentiate *in vitro*, extending neurites, forming complex morphologies, and expressing markers (green) of early neurons (β-tubulin III; C), mature neurons (Map2; D), and oligodendrocytes (MBP; E). After 24hr AgNP exposure, cells' Olive moment distribution is not significantly altered from negative control, while AgNP-treated and control cells have a significantly greater proportion of cells with Olive moments between 0-10 than H_2O_2-treated positive controls, indicating low DNA damage (F; $p<0.05$; *$p<0.0001$, Sidak's multiple comparisons; 908-1607 cells per condition across 3 separate experiments). Nuclei are blue (DAPI). Comet assay data courtesy of Dr. Nadja Spitzer.

2.3.2 AgNP Exposure Induces Formation of f-Actin Inclusions That Do Not Co-localize With AgNPs.

Following 48hr exposure, cells exposed to low levels of AgNP formed punctate f-actin inclusions (Figure 5B, 2.2C, arrows) that did not localize to a specific cellular compartment. Very few control cells contained these inclusions (Figure 5A, arrows), while there was a marked increase in their appearance in AgNP-exposed cells (Figure 5B, 2.2C, 2.2E, arrows). Quantification of the proportion of cells containing these inclusions showed that 1µg/mL AgNP exposure induced a significantly higher number of cells to form inclusions compared to vehicle and media controls (Figure 5F). Additionally, inclusion formation was found to increase in a dose-dependent (Figure 5G) and time-dependent manner (Figure 5H).

To ensure that inclusions were not a result of AgNP sequestration within the cell, a nanoparticle enhancement assay was performed in tandem with f-actin staining. Control cells (Figure 5I, arrows) showed no visible enhancement following treatment, whereas AgNP-treated cells (Figure 5J, arrows) showed numerous enhanced nanoparticles following treatment. Increased contrast allowed visualization of cells among enhanced nanoparticles (Figure 5K). AgNP-treated cells are observed to contain both f-actin inclusions (Figure 5L, arrows) and enhanced AgNP (Figure 5M, arrowheads). However, when these two images are merged (Figure 5N), a vast majority of enhanced AgNP do not co-localize with f-actin inclusions, and most f-actin inclusions to not contain enhanced AgNP. Several co-localizations were observed (double arrowheads), but these are thought to have been non-specific occurrences, given their rarity. Taken together, these results suggest that inclusions are formed through AgNP-mediated disruption of some cellular mechanism, not sequestration of AgNP within cells.

28
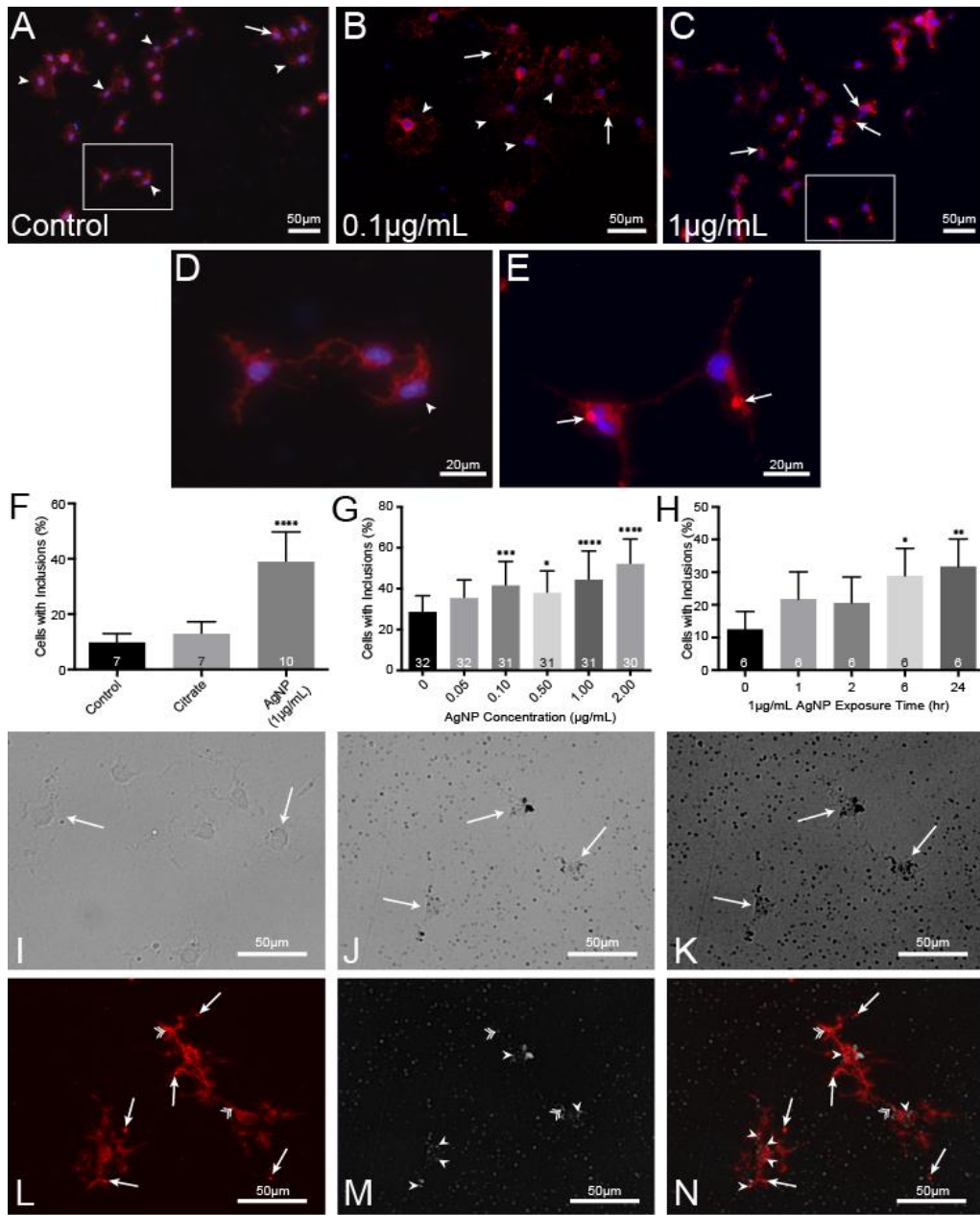
Figure 5: **Low-level AgNP induce formation of f-actin inclusions in differentiating NSC.** Control cells (A) appear uniform (arrowheads) and rarely contain f-actin inclusions (arrows) compared to AgNP-treated cells (B, C). Inclusions lack localization specific cellular compartments. After 48hr, significantly more AgNP-treated cells contain inclusions than vehicle or media controls (F). Inclusion incidence is dose (G) and time-dependent (H). ($p<0.05$, ANOVA; *$p<0.05$, **$p<0.01$, ***$p<0.001$, ****$p<0.0001$; Tukey's multiple comparisons; $n≥3$; numbers in bars are independent coverslips) After enhancement, control cells (I, arrows) do not change, while enhanced AgNP appear among AgNP-treated cells (J, arrows). Higher contrast visualizes cells (K). When f-actin staining (L) and color-reversed enhancement (M) are merged (N), few inclusions (L, N, arrows) co-localize with AgNP (M, N, arrowheads), though incidental co-localization was observed (double arrowheads).

2.3.3 Low-level AgNP Exposure Disrupts Neurite Extension, Dynamics, and Arborization.

In time lapse experiments using the B35 neuroblastoma cell line, exposure to 1µg/mL AgNP was found to significantly reduce maximum neurite length (Figure 6A), indicating a possible disruption of neurite dynamics. Indeed, when experiments were replicated with SVZ NSCs, control cells (Figure 6B) possessed long, variable neurites that were consistently well-arborized. Conversely, cells exposed to 1µg/mL AgNP (Figure 6C) began similarly to control cells, but rapidly experienced a reduction of neurite length and arborization. When the neurites and degree of arborization of these neurites was quantified (Figure 6E-H), SVZ NSC exhibited an similar trend to B35 neuroblastoma cells, with a significant reduction in maximum neurite length overall (Figure 6D).   Interestingly, analysis of individual time points revealed that this trend towards shorter neurites is affected by exposure time. Control cells possess neurites of highly variable, dynamic lengths that constantly extend and retract throughout the experiment (Figure 6E), whereas AgNP-exposed cells' neurites collapse after treatment and never recover, with neurites generated after the start of data collection failing to extend as far as control (Figure 6F). The neurites of control cells also have highly variable arborization (Figure 6G), whereas AgNP-exposed cells possess neurites that begin variably-arborized, but by the conclusion of the experiment have neurites with almost no branching at all (Figure 6H).

2.4 DISCUSSION

The toxic action of AgNP *in vitro* is well documented (Bartlomiejczyk et al., 2013; Kruszewski et al., 2011). However, significantly less is known about how cells respond at lower, concentrations. It is known that AgNP at concentrations that do not cause overt toxicity in animals bypass bodily defenses such as the blood-brain barrier (Tang et al., 2008) and accumulate significantly in tissues, especially the brain (Lee et al., 2013). Therefore, it is
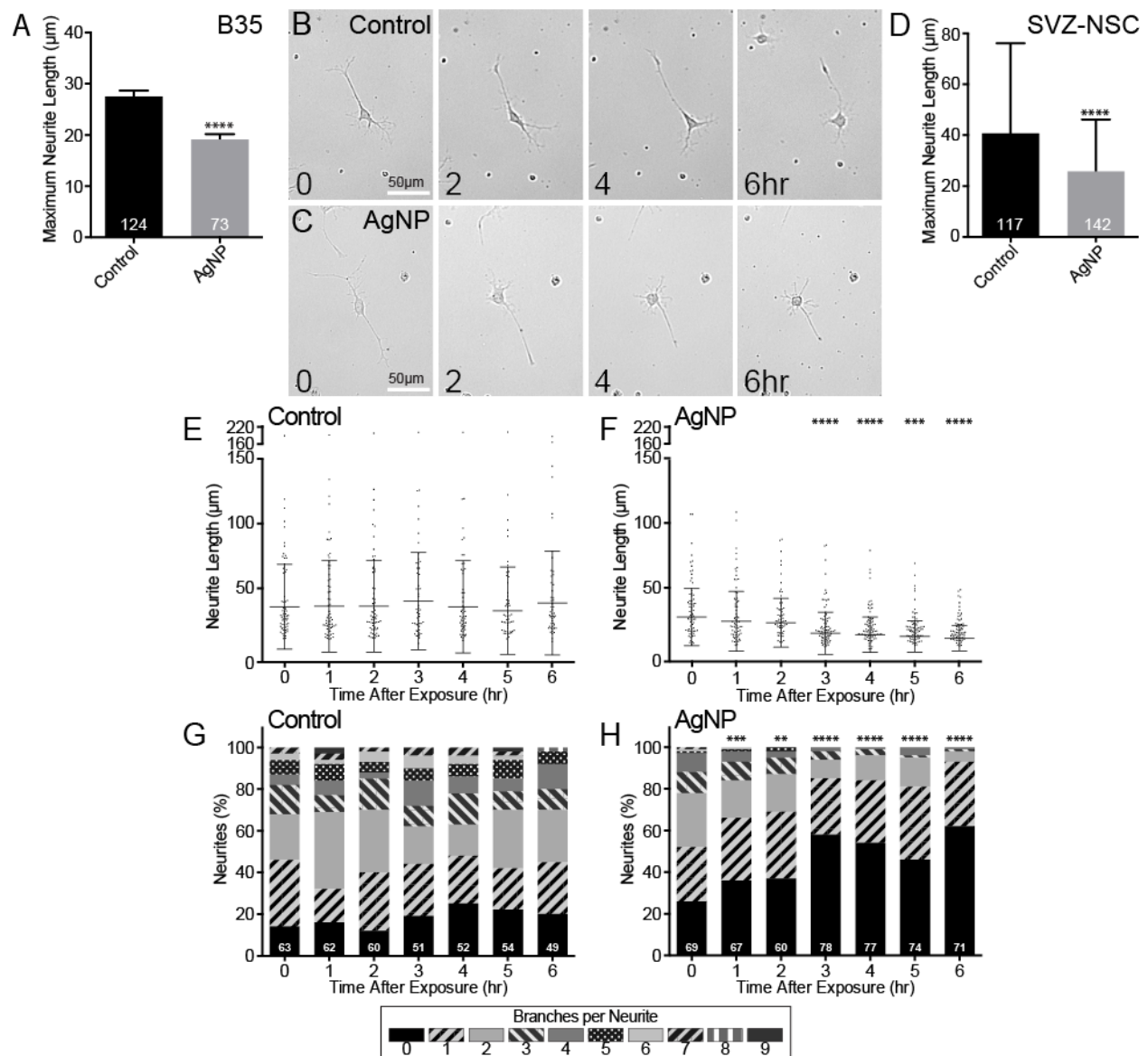
Figure 6: **Low-level AgNP exposure disrupts neurite dynamics in cultured neural cells.**
Time lapse experiments with B35 neuroblastoma cells revealed maximum neurite length was
significantly reduced following 1µg/mL AgNP exposure (A; ****$p<0.0001$, two-tailed t-test,
n=2). In SVZ NSC, control cells (B) became morphologically distinct from AgNP-exposed cells
(C), exhibiting similar reduction of maximum neurite length (D; ****$p<0.0001$, two-tailed t-test,
n=3). Over time, neurites on control cells were highly dynamic and variable (E), while neurites
on AgNP-exposed cells began similarly but quickly underwent significant collapse (F).
Similarly, neurites on control cells were generally well-arborized (G), while AgNP-exposed cells
underwent significant loss of arborization until most neurites contained one or no branch points
(H). Numbers in bars indicate number of neurites measured. ($p>0.01$, Two-way ANOVA of at
least 3 independent experiments; **$p<0.01$, ***$p<0.001$, ****$p<0.0001$ compared to same time
point in control; Sidak's multiple comparisons)

especially prudent to investigate the possible effects of low-level, sub-toxic AgNP exposure on brain health. Here, SVZ NSC, a population of cells vital for normal brain function, were isolated and cultured as an *in vitro* model for adult neurogenesis, neurodevelopment, and mature neural cells in general.

Concentrations between 0.05-2.0μg/mL AgNP were used for this study in an effort to elicit robust effects while staying below toxicity thresholds. These concentrations have previously been reported as below the threshold for apoptosis and necrosis for cultured neurons (Haase et al., 2012; Xu et al., 2013) and PC12 cells (Hadrup et al., 2012; Hussain et al., 2006). Additionally, AgNP administered to rats at levels that did not cause any obvious toxicity (10-25nm, 100 and 500mg/kg/day) over the course of one month of treatment accumulated in the brain at concentrations up to 0.3-0.4μg/mL (Lee et al., 2013), in some cases even increased to 0.4-0.5μg/mL during the four month recovery period. The chosen concentrations are also comparable to exposure estimates from consumer products. Analysis of AgNP release from antimicrobial socks revealed they were capable of leaching 1.5-650μg AgNP into a 1hr wash (Benn and Westerhoff, 2008). Additional studies estimated human exposure to AgNP from food packaging to be 0.06-13μg/kg/day (Cushen et al., 2013, 2014). Also, release of AgNP from coated catheters has been found to be approximately 0.6μg/day (Bidgoli et al., 2013). Though these values may not be enough to individually account for the concentration used in these experiments, consideration of multiple simultaneous sources and the bioaccumulative nature of AgNP make it significantly more feasible. Finally, comet assay, a method of assessing DNA damage on a single-cell basis, confirmed that the two highest concentrations used in this study, 1μg/mL and 2μg/mL, did not significantly increase apoptosis (Figure 4F). Therefore, any changes observed in NSC differentiation or behavior are due to sub-toxic effects of AgNP.

Here, low-level AgNP exposure resulted in an increase of the proportion of cells containing f-actin inclusions in a dose- and time-dependent manner (Figure 5). These inclusions appear similar to structures observed when cells are exposed to the actin-stabilizing toxin jasplakinolide (Lazaro-Dieguez et al., 2008) or the actin-depolymerizing toxin cytochalasin D (Muller et al., 2013). This suggests that the inclusions could be indicative of a disruption of actin dynamics. However, AgNP within cells can be equally distributed throughout the cytosol (Marano et al., 2011), or they can be agglomerated and sequestered within membrane-bound compartments (Gliga et al., 2014; Schrand et al., 2008). As the observed f-actin inclusions only very rarely co-localized with enhanced AgNP (Figure 5), formation of these inclusions indicates AgNP-mediated disruption of actin dynamics or other cellular processes.

Finally, time lapse experiments showed that AgNP-exposed cells undergo a collapse of existing neurites, a reduction in neurite arborization, and a significant decrease of neurite dynamics overall (Figure 6). As these processes are cytoskeleton-driven, their loss further supports that low-level AgNP exposure disrupts actin dynamics in differentiating NSC. Actin dynamics are vital for neurogenesis, as a motor for neurite extension and an anchor for adhesion (Bray and Chapman, 1985; Hotulainen and Lappalainen, 2006). Similarly, neurite extension and arborization are themselves vital for neurogenesis, aiding in migration, differentiation, and integration. Therefore disruption of these cytoskeleton-mediated processes and actin-dynamics in general could lead to a loss of neurogenesis and impairment of normal brain function.

As neurogenesis contributes to the basic processes of learning and memory (Snyder et al., 2001; van Praag et al., 1999), one would expect to observe their impairment following AgNP treatment. However, results reported to date are conflicting. One experiment exposed mice to AgNP (25nm, 10-50mg/kg/day) for 7 days and found no changes to neurogenesis or cognitive

function (Liu et al., 2013). Alternatively, rats exposed to sub-toxic levels of AgNP (50-100nm, 3-30mg/kg/day) for 14 days exhibited a significant loss of spatial memory and learning (Liu et al., 2012). While this study did not examine neurogenesis directly, it instead proposed AgNP-driven production of reactive oxygen species (ROS) as a possible mechanism. Minute modulations of intracellular ROS are known to be vital for regulation of NSC proliferation and differentiation (Le Belle et al., 2011; Prozorovski et al., 2015; Vieira et al., 2011), and AgNP at toxic concentrations are known to produce excess ROS (Carlson et al., 2008; Haase et al., 2012; Manke et al., 2013). AgNP at lower concentrations can also influence ROS signaling, and the ERK and Akt pathways in a neuroblastoma cell line (Dayem et al., 2014). ERK aids in control of NSC proliferation and differentiation (Huang et al., 2014; Liu et al., 2014), while Akt promotes proliferation and survival during differentiation (Conti et al., 2001; Jin et al., 2005). Interestingly, when SH-SY5Y neuroblastoma cells were exposed to low-level AgNP, neuronal differentiation increased (Dayem et al., 2014). These results highlight that it is especially important to understand how AgNP interact with NSC and the pathways governing their behavior. Any changes could result in a corresponding malfunction of neurogenesis, and lead to losses of basic processes such as learning, memory, and endogenous repair.

CHAPTER 3: LOW-LEVEL SILVER NANOPARTICLE EXPOSURE ALTERS β-CATENIN SIGNALING AND LOCALIZATION.

3.1 INTRODUCTION

Numerous intracellular signaling pathways are involved in the regulation of adult neural stem cells (NSC) and their activity. Chief among these are Akt, MAPK (ERK), and Wnt signaling (Faigle and Song, 2013; Ma et al., 2004). Akt signaling, known to promote cell survival in mature neurons (Dudek et al., 1997), increases NSC survival and proliferation (Kalluri et al., 2007). However, while some have shown Akt activation to promote proliferation over differentiation (Jin et al., 2005; Peltier et al., 2007), others have found that Akt activation can enhance neuronal differentiation of NSC (Conti et al., 2001). The key difference appears to be which downstream effectors are involved, with CREB and GSK3β promoting survival and proliferation (Jin et al., 2005; Pap and Cooper, 1998; Peltier et al., 2007) and Bad promoting neuronal differentiation (Conti et al., 2001). ERK signaling is similarly complex, promoting oligodendrocyte (Hu et al., 2004) and neural differentiation (Conti et al., 2001; Lim et al., 2007; Liu et al., 2014), neurite extension (Arevalo et al., 2012; Lim et al., 2007; Robinson et al., 1998), and NSC proliferation (Huang et al., 2014; Tocharus et al., 2014). Finally, Wnt signaling is known to be necessary for neurogenesis (Lie et al., 2005), promoting NSC survival (Sinha et al., 2005; Toledo et al., 2008), neurite extension (Lee et al., 2014; Pino et al., 2011), synaptogenesis (Inestrosa and Arenas, 2010), proliferation (Adachi et al., 2007; Marinaro et al., 2012; Wexler et al., 2008), and differentiation (Kuwabara et al., 2009; Marinaro et al., 2012).

Intracellular transduction of Wnt signaling may proceed through several different pathways: canonical and non-canonical. Non-canonical Wnt signaling is very diverse, involved in protection from the Alzheimer's-related protein amyloid-β (Toledo et al., 2008) and stem cell

differentiation in the developing (Toledo et al., 2008) and adult (Pino et al., 2011) brain, and acts through many various intracellular pathways. Conversely, canonical Wnt signaling is always mediated by β-catenin (Hinck et al., 1994), a protein that acts as a bridge between the cadherin complex and the f-actin cytoskeleton (Wheelock and Knudsen, 1991), anchoring the adhesion complex to the cytoskeleton. Under normal circumstances, β-catenin is phosphorylated by GSK3β (Peifer et al., 1994; Yost et al., 1996), marking it for degradation (Aberle et al., 1997) and replacement by newly-translated β-catenin. However, when canonical Wnt signaling is activated, the activity of GSK3β is inhibited, leading to a reduction in this turnover and an increase in intracellular β-catenin levels (Munemitsu et al., 1995). This free β-catenin binds the transcription factors TCF/LEF (Molenaar et al., 1996), shuttling them into the nucleus to initiate transcription of genes related to metabolism, proliferation, and stem cell differentiation (Sinha et al., 2005; Wisniewska, 2013). Aside from Wnt, β-catenin signaling can be activated by Akt signaling (Pap and Cooper, 1998) or by increased reactive oxygen species (ROS) generation (Essers et al., 2005; Funato et al., 2006).

Reduced β-catenin signaling decreases cell survival (Almeida et al., 2011; Newnham et al., 2015), and inhibition of β-catenin translation induces apoptosis (Dong et al., 2015). Conversely, both overexpression of β-catenin (Chou et al., 2015; Greco et al., 2016; Wang et al., 2014; Zhang et al., 2015b) and the inability to degrade constitutively translated β-catenin (Abdelmaksoud-Damak et al., 2015; Wu et al., 2001) are associated with a cancer state in many cell types. However, normal β-catenin signaling is vital for proliferation (Adachi et al., 2007) and differentiation (Wang et al., 2016) of NSC, and for neurite extension (Lee et al., 2014; Yu and Malenka, 2004) and arborization (Yu and Malenka, 2003). Therefore, control of β-catenin

36

transcription (Shackleford et al., 2013), translation (Chou et al., 2015; Yoon et al., 2012), and activity (Iaconelli et al., 2015) are tightly regulated.

Low-level silver nanoparticles (AgNP) disrupt cytoskeleton and neurite dynamics (Cooper and Spitzer, 2015), both processes controlled by β-catenin (Lee et al., 2014; Yu and Malenka, 2003). Further, AgNP are known to affect Akt and ROS signaling (Dayem et al., 2014) at low-level exposures, two pathways that are linked with β-catenin signaling (Funato et al., 2006; Pap and Cooper, 1998). Therefore, this work investigates β-catenin signaling in NSC as a likely target for disruption following low-level AgNP exposure.

<div align="center">

3.2 MATERIALS AND METHODS

</div>

3.2.1 Cell Culture

NSC cultures were harvested, maintained as spheres, and plated as described in (2.2.1) and (2.2.2).

3.2.2 Immunocytochemistry

Immunocytochemistry experiments were used to examine changes to the cellular localization of β-catenin within differentiated SVZ NSC exposed to AgNP. Cells were allowed to differentiate on poly-L-lysine (0.01%) and laminin (10μg/mL) coated coverslips for 2-3 days before media was replaced. Following media replacement, stock 40nm AgNP solution (20μg/mL) was added to wells to a concentration of 1μg/mL at 24, 6, 2, and 1hr before fixation, with 2mM sterile-filtered sodium citrate added to control cells at the 24hr timepoint. Processing was conducted as described in (2.2.4). Primary antibody used was rabbit-α-β-catenin (1:500; Santa Cruz, Dallas, Texas, United States), with goat-α-rabbit Alexa 488 (1:500; Life Technologies) as secondary. Phalloidin Alexa 568 (1:100; Life) was used to stain the f-actin cytoskeleton, and DAPI (Sigma) was used as a nuclear counterstain.

3.2.3 Western Blot

Immunoblot analysis was run on whole protein homogenates from cells exposed to 1.0μg/mL AgNP for 24hr to investigate changes to intracellular signaling pathways. Briefly, cells were collected using Laemmli solution (2% SDS, 6M Urea, 625mM Tris, 160mM DTT, 160mM DTE), heated to 70°C for 15min and triturated to homogenize, cooled, and homogenates stored at -20°C. 10μL protein was mixed with 5μL fresh loading buffer (58% glycerol, 0.36M Tris, 6% Tris, 6% β-mercaptoethanol, 0.01% bromophenol blue) and loaded into 10% poly-acrylamide gels. Gels were run in running buffer (40mM Trizma Base, 200mM Glycine, 0.1% SDS) at 85V for 90min. Gels were washed in transfer buffer (25mM Tris, 192mM Glycine, pH 8.3) and proteins were transferred to PVDF (Biorad) at 85V for 1hr at 4°C. Membrane was washed in TTBS (20mM Tris, 0.5M NaCl, 0.1% Tween 20, pH 7.5) then blocked for 2hr (4% skim milk in TTBS). After washing again with TTBS, membrane was incubated overnight with primary antibody in TTBS with 5% bovine serum albumin (BSA). Primary antibodies used were rabbit-α-phospho-Akt (pAkt; 1:2000; Cell Signaling Technologies (CST), Danvers, Massachusetts), rabbit-α-phospho-MAPK (pMAPK; 1:2000; CST), or rabbit-α-β-catenin (1:5000; Santa Cruz). Membranes were washed in TTBS and incubated with goat-α-rabbit conjugated with horse radish peroxidase (1:1000; CST) as secondary antibody in TTBS with 5%BSA for 1hr. After secondary incubation, membranes were washed and imaged in a darkroom using film (GE Healthcare Life Sciences, Pittsburgh, Pennsylvania) and WesternBright ECL solutions (Advansta, Menlo Park, California). After imaging, membranes were stripped using stripping buffer (Fisher) before blocking again and incubating with either a second primary or HRP-conjugated α-pan-actin (1:5000; CST) for loading control. Membranes were stripped two times at most. Photographs were scanned for quantification.

3.2.4 Analysis

All images were analyzed using ImageJ (NIH). Cells in immunocytochemistry experiments were counted, then analyzed to assess cells containing only f-actin inclusions, only β-catenin puncta, both not co-localized, and both co-localized. Each category was placed within a hierarchy (β-catenin puncta and f-actin inclusion co-localization > both f-actin inclusions and β-catenin puncta present, not co-localized > β-catenin puncta only > f-actin inclusions only) and each cell only assigned to one category to ensure no cell was counted twice. Immunoblots were analyzed for intensity values, then normalized to pan-actin, and finally experimental values normalized to control values. All statistical analysis was performed in PRISM.

3.3 RESULTS

3.3.1 Low-Level AgNP Induce Punctate β-Catenin Expression in SVZ NSC.

After being allowed to differentiate for 2-3 days, SVZ NSC were exposed to 1µg/mL AgNP for 1-24hr and immunostained for expression patterns of the canonical Wnt mediator β-catenin. Control cells contained a relatively uniform localization of β-catenin within each cell (Figure 7A), with very few cells exhibiting a punctate pattern of expression (Figure 7A). When cells were exposed to AgNP (Figure 7B), there was a noticeable formation of bright puncta at the plasma membrane containing β-catenin. The proportion of cells containing β-catenin puncta increases significantly in a time-dependent manner following AgNP exposure (Figure 7C).

3.3.2 β-Catenin Puncta Co-localize With f-Actin Inclusions.

When AgNP-treated are immunostained for β-catenin (Figure 8A) and stained for f-actin (Figure 8B), cells with β-catenin puncta generally contain f-actin inclusions. Further, β-catenin puncta co-localize with f-actin inclusions (Figure 8C), and the proportion of cells with co-localizations increases significantly with longer low-level AgNP exposure time. A significantly

39
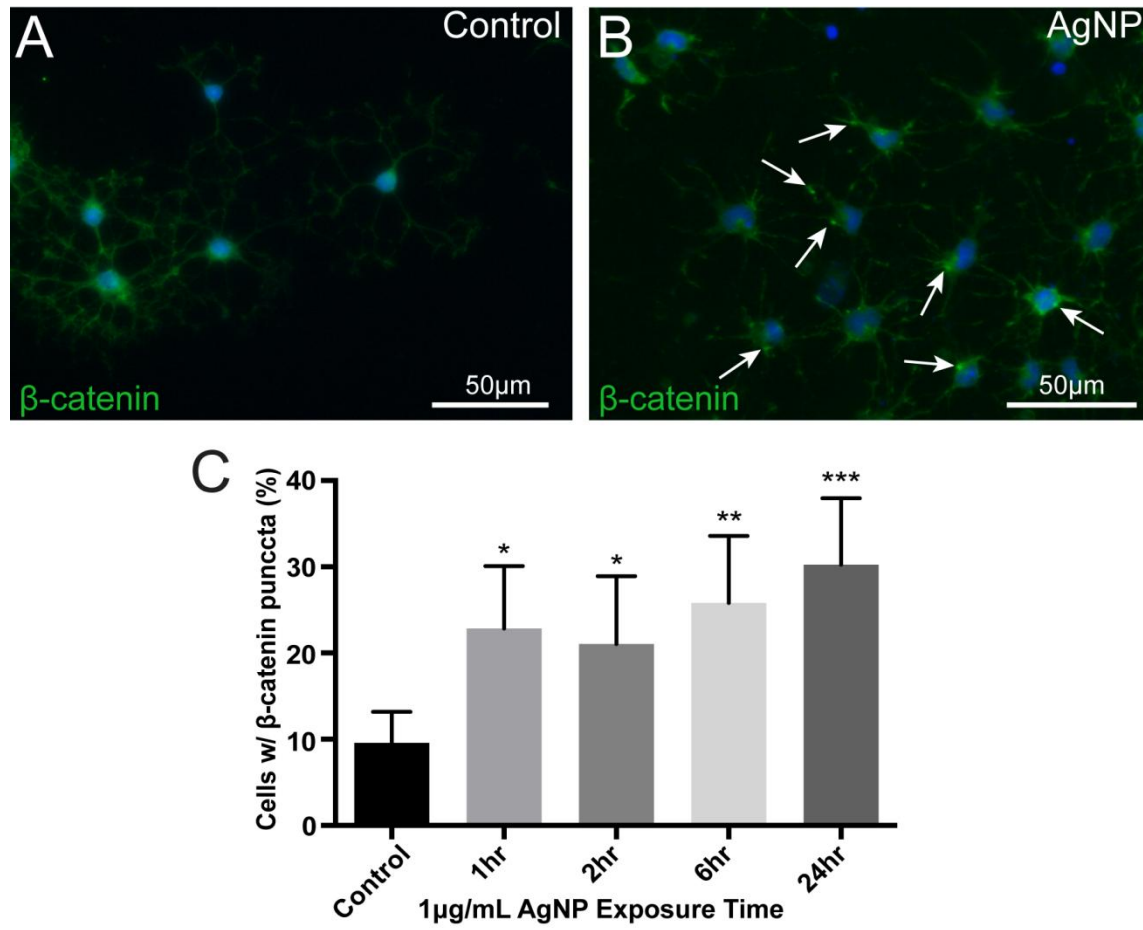
Figure 7: **AgNP exposure induces punctate β-catenin expression in differentiating NSC.** Control cells expressing β-catenin in immunocytochemistry experiments typically exhibit uniform distribution, with very few cells having a punctate expression pattern (A). Following 1μg/mL AgNP exposure, differentiating NSC undergo a qualitative increase in the proportion of cells with punctate expression (B; arrows). The increase in cells with punctate β-catenin expression is significant and time-dependent. $p=0.0005$, ANOVA, $n=6$. *$p<0.05$, **$p<0.01$, ***$p<0.001$ compared to control, Tukey's multiple comparisons. Blue is DAPI.
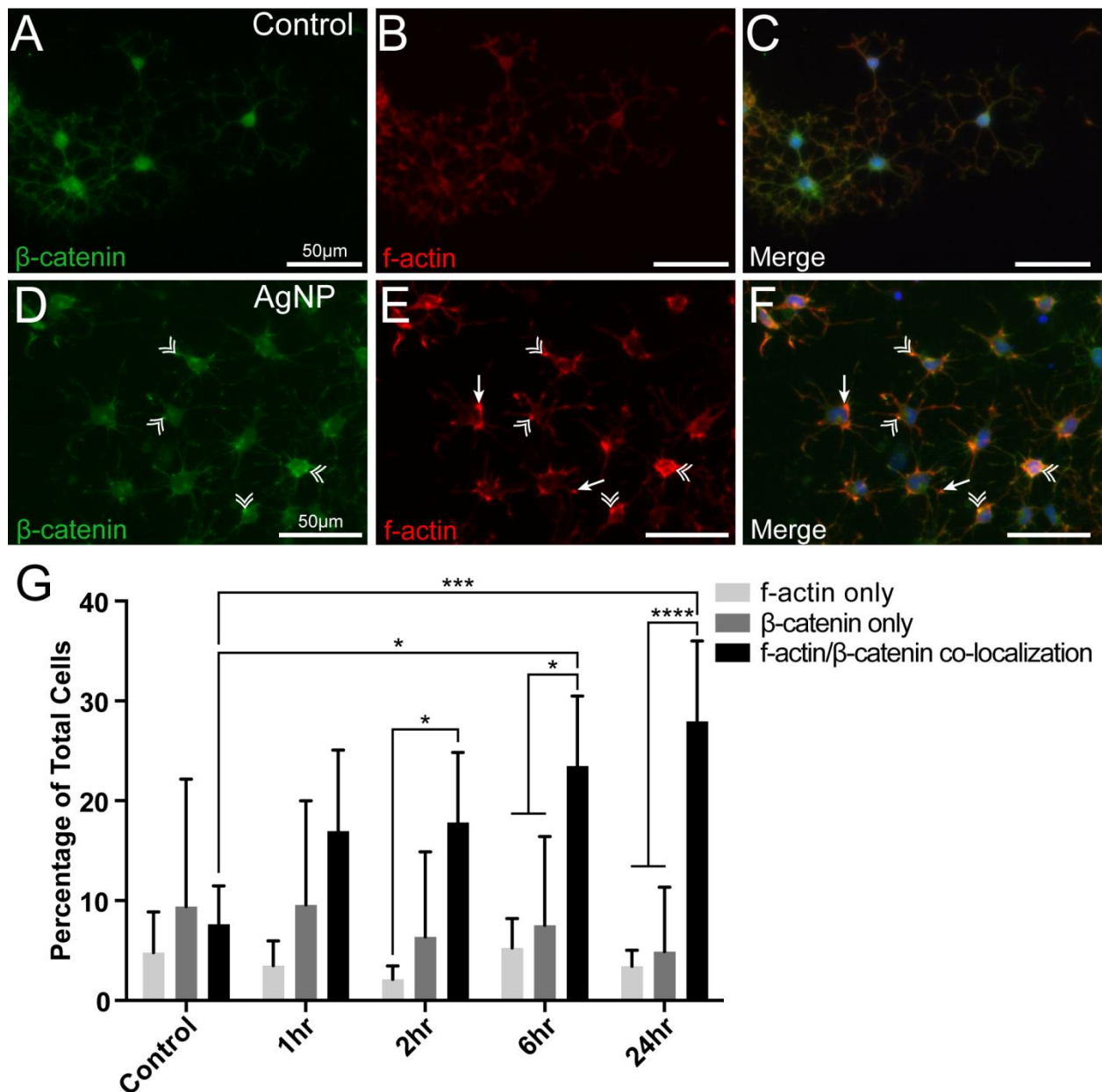
Figure 8: **Following AgNP exposure, β-catenin puncta and f-actin inclusions co-localize.** β-catenin (A) and f-actin (B) distribution within control cells (A-C) is relatively uniform. However, 1μg/mL AgNP induced the formation of β-catenin puncta (D) and f-actin inclusions (E). When overlaid (F), puncta and inclusions (arrow) often co-localize (double arrowhead). The proportion of total cells with co-localized f-actin inclusions and β-catenin puncta increases significantly over time and is significantly different from those that contain only f-actin inclusions or β-catenin puncta after AgNP (G; $p=0.0047$, Two-way ANOVA, n=6; *$p<0.05$, ***$p<0.001$, ****$p<0.0001$; Sidak's multiple comparisons). Blue is DAPI. Scale bars are 50μm.

higher proportion of total cells exhibit co-localization than those with just f-actin inclusions or β-catenin puncta (Figure 8D). No significant change was observed in the proportion of cells with either only f-actin inclusions or only β-catenin puncta. The proportion of cells containing both β-catenin puncta and f-actin inclusions, but lacking co-localization, was less than 1% across all conditions (data not shown), indicating that β-catenin puncta and f-actin inclusions appear together. This also validates our method of counting total cells within a hierarchy.

3.3.3 Low-Level AgNP Exposure Increases Intracellular β-Catenin.

Differentiating SVZ NSC were exposed to 1μg/mL AgNP for 24hr before whole-cell homogenates were collected for Western blot analysis. Preliminary data suggest that low-level AgNP exposure does not alter levels of pAkt or pMAPK (data not shown), which might suggest that neither pathway is affected by AgNP in NSC. However, intracellular β-catenin levels increased significantly following low-level AgNP exposure (Figure 9). Unlike Akt and MAPK, where different degrees of Akt and MAPK phosphorylation to pAkt and pMAPK respectively are the results of pathway activation, β-catenin signaling activation causes increased intracellular levels of β-catenin itself (Munemitsu et al., 1995). Therefore, these results suggest an activation of β-catenin signaling following AgNP exposure.

3.4 DISCUSSION

Tightly controlled β-catenin signaling is involved in regulation of almost every stage of neurogenesis, including proliferation, survival, differentiation, and neurite development (Adachi et al., 2007; Kuwabara et al., 2009; Lee et al., 2014; Lie et al., 2005; Marinaro et al., 2012; Yu and Malenka, 2003). Here, we show that both β-catenin localization and signaling are affected by low-level AgNP exposure. Following exposure to 1μg/mL AgNP for up to 24 hours,
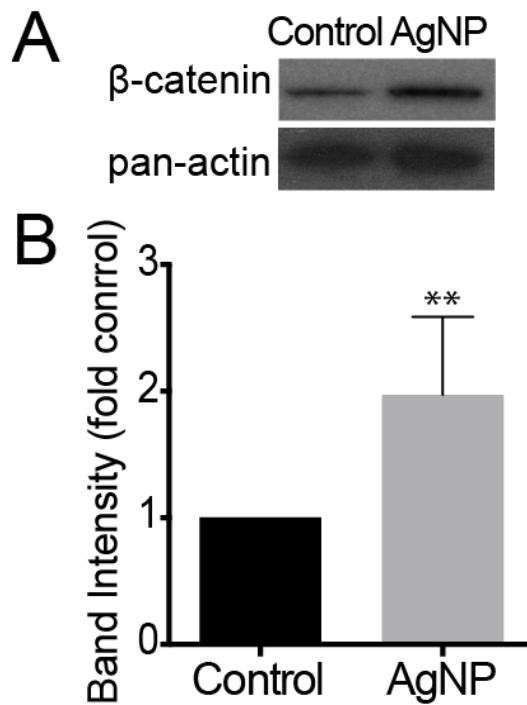
Figure 9: **Low-level AgNP exposure increases intracellular β-catenin in SVZ NSC.**
Representative images of membranes following analysis of intracellular β-catenin content by
Western blot (A). After differentiating SVZ-NSC were exposed to 1μg/mL AgNP for 24hr,
intracellular β-catenin levels increased significantly when normalized tocorresponding control
conditions (B; **p<0.01, two-tailed t-test, n=3), indicating an activation of β-catenin signaling.
Pan-actin used as loading control. Data and images courtesy of Dr. Nadja Spitzer.

differentiating NSC experienced a time-dependent aggregation of intracellular β-catenin into

puncta (Figure 7). Further, cells that contain β-catenin puncta also tend to contain previously-

observed f-actin inclusions, with the two almost always co-localizing (Figure 8). Finally, the

increase in β-catenin puncta is accompanied by increased intracellular β-catenin levels (Figure

9), indicative of activated β-catenin signaling (Munemitsu et al., 1995). This finding is contrary

to what would be expected given previous data showing that neurite dynamics and arborization

are inhibited following AgNP exposure (Figure 6), as β-catenin activation promotes both neurite

extension and arborization (Lee et al., 2014; Yu and Malenka, 2003). However, β-catenin's

effects are context-dependent (Summarized in Fig 3.4). Wnt/β-catenin signaling induces cell

proliferation in NSC in the absence of Hipk1, but the presence of Hipk1 actively inhibits NSC

proliferation and instead promotes neuronal differentiation (Marinaro et al., 2012). β-catenin can

also bind to transcription factors from the forkhead box O (FOXO) family under stressful

conditions, inhibiting TCF/LEF signaling and instead prioritizing cell survival over proliferation

or differentiation (Almeida et al., 2007; Hoogeboom et al., 2008). Clearly, further work is needed

to elucidate β-catenin's role in mediating the observed changes to NSC behavior (Figure 6).

Additionally, β-catenin signaling can be activated by several intracellular signaling pathways,

including Wnt (Hinck et al., 1994; Peifer et al., 1994) and Akt (Fukumoto et al., 2001; Haq et al.,

2003; Sharma et al., 2002). AgNP have previously been shown to increase Akt signaling at low-

level exposures (Dayem et al., 2014), which could correspond to an increase in β-catenin

signaling. However, preliminary experiments found no significant change to Akt signaling.

Therefore, the increase in intracellular β-catenin following AgNP exposure (Figure 8) may be

mediated by some mechanism other than Akt signaling. Future experiments should focus on
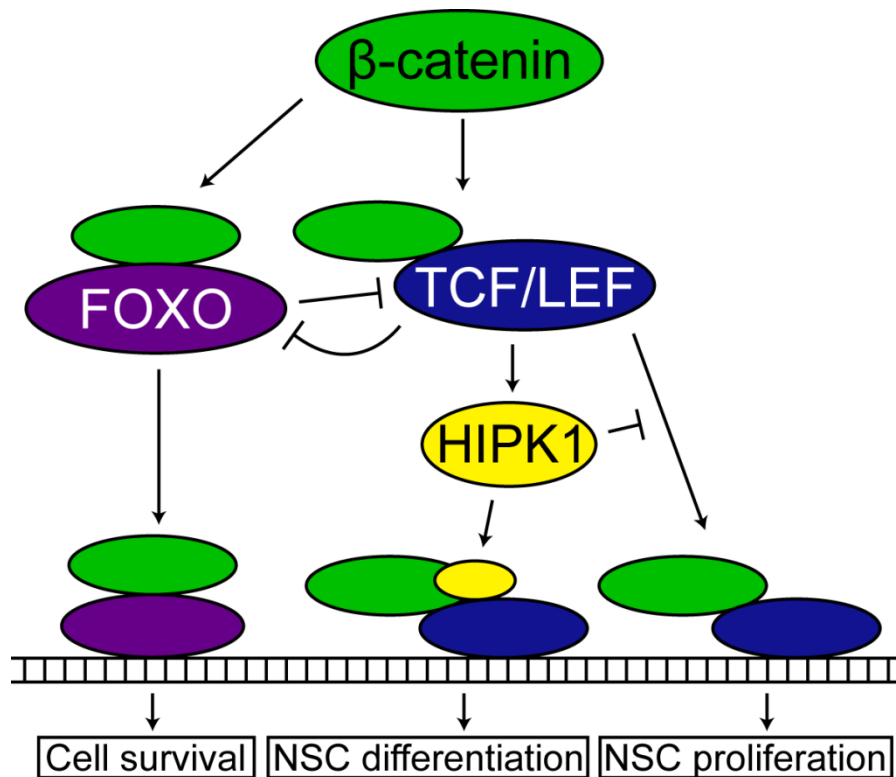
Figure 10: **Summary of several β-catenin-transcription factor interactions in NSC.**
Following β-catenin signaling activation, intracellular β-catenin becomes available to bind
transcription factors. Two possible targets are transcription factors in the TCF/LEF family or the
FOXO family. β-catenin-TCF/LEF signaling, more closely associated with canonical β-catenin
signaling under favorable conditions, is modulated by HIPK1, and promotes NSC differentiation
in the presence of HIPK1 or NSC proliferation in the absence of HIPK1. Conversely, β-catenin
will bind FOXO under stressful conditions, inhibiting β-catenin-TCF/LEF signaling and
transcribing genes to promote cell survival rather than differentiation or proliferation.
Illustration © Robert Cooper, 2016.

on determining the mechanism behind AgNP-induced β-catenin signaling activation and other

consequences of β-catenin's altered localization.

CHAPTER 4: SILVER NANOPARTICLES CROSS THE BLOOD-BRAIN BARRIER AND ACCUMULATE *IN VIVO*.

4.1 INTRODUCTION

Silver nanoparticles (AgNP) are known to be found in numerous consumer products, such as food packaging, toothpaste, and drinkware (Benn et al., 2010; Quadros et al., 2013; von Goetz et al., 2013). Therefore, implications of oral exposure are especially important. AgNP are known to survive the gastro-intestinal tract intact, agglomerating or dissolving in the stomach and then separating from agglomerates or re-forming from ions following bicarbonate neutralization in the duodenum (Walczak et al., 2013). From there, they can enter the bloodstream , migrate to various organs, and accumulate and persist long-term (Lee et al., 2013). In the brain, AgNP retain their nanoparticle form (Tang et al., 2008), bypass and damage the blood brain barrier (Sharma et al., 2010; Tang et al., 2008; Tang et al., 2010; Xu et al., 2015a) and accumulate (Wen et al., 2016) with a half life greater than four months (Lee et al., 2013).

Multiple studies have shown adverse effects following AgNP exposure *in vivo*. In rats, two-week exposure to AgNP (0.2mg/kg) caused degeneration of synaptic structure and downregulation of synaptic proteins (Skalska et al., 2014). Another two-week study (1-10mg/kg) found neuron shrinkage, astrocyte swelling, and induction of inflammatory response (Xu et al., 2015b). No changes in hippocampal neurogenesis or cognitive performance were observed following seven days' AgNP exposure (10-50mg/kg) in mice, either immediately or after 28 days of recovery (Liu et al., 2013). Conversely, two weeks' exposure to AgNP (3-30mg/kg) was found to reduce spatial cognition in rats (Liu et al., 2012). The reduction of long-term potentiation, a process normally increased during learning, and increased oxidative stress were both identified as possible mechanisms for these effects (Liu et al., 2012). However, the authors

did not examine associated changes to neurogenesis. As AgNP are found in numerous products encountered on a daily basis (Benn et al., 2010; Quadros et al., 2013; Yang and Westerhoff, 2014) and previous work demonstrates that low-level AgNP exposure may disrupts neural stem cell physiology (Cooper and Spitzer, 2015), possible changes to neurogenesis following longer-term *in vivo* exposure should be examined.

Another area in need to study is AgNP's effects on the electrical activity of newly differentiated cells. Adult neural stem cells (NSC), the proliferative cells found in the subventricular zone of adult mammals, are originally hyperpolarized and have high potassium permeability (Scheffler et al., 2005; Stewart et al., 1999). During differentiation, they undergo a series of complex changes during which their resting potential rises, making them more excitable (Scheffler et al., 2005). Though they undergo few spontaneous synaptic events before the completion of differentiation, they eventually gain voltage-gated sodium channels that allow them to fire action potentials (Belluzzi et al., 2003; Carleton et al., 2003; Scheffler et al., 2005; Stewart et al., 1999; Wang et al., 2003). Therefore, this change in membrane properties from hyperpolarized to excitable is a vital part of NSC differentiation into mature neuronal phenotypes (Scheffler et al., 2005). AgNP can inhibit voltage-gated sodium channels (Busse et al., 2013; Liu et al., 2009b). Further, they can inhibit voltage-gated potassium channels, both transient and delayed-rectifier types (Liu et al., 2011). However, these studies have all been carried out on primary cultures, on cells that had previously been allowed to develop mature membrane properties. Changes to membrane properties following AgNP exposure during cell differentiation have not yet been investigated.

4.2 MATERIALS AND METHODS

4.2.1 *In Vivo* **AgNP Exposure and BrdU Treatment**

Young adult Sprague-Dawley rats were purchased from Hilltop and cared for under

Marshall University IACUC protocol 598. Animals were maintained in environmentally-

controlled cages on a 12-hour day/night cycle with access to standard chow and water *ad libitum*.

As detailed in Figure 11, after being allowed to acclimate, animals were trained daily for 7d to

take 10% sucrose (Fisher) solution orally from a syringe when presented (Atcha et al., 2010) at

1:00pm plus or minus 2hr. Following training, control animals (n=16, 8 male, 8 female) were

maintained on daily feedings of 10% sucrose. Experimental animals (n=16, 8 male, 8 female)

were given 100mg/kg 40nm uncoated AgNP (NanoAmor, Houston, Texas) suspended in 10%

sucrose. Dosing volume was 2mL/kg. Each group of animals consisted of equal numbers of

males and females, with equal numbers of each treated with AgNP or sucrose vehicle for 28d.

Sucrose solutions and AgNP suspensions were prepared fresh daily as 20% sucrose and

100mg/mL AgNP in diH$_2$O. AgNP suspensions were made by fifteen minutes of sonication and

cooled to room temperature on ice. Solutions for feeding were made as a 1-to-1 mixture of

100mg/mL AgNP and 20% sucrose for AgNP-treated animals or as 20% sucrose with diH$_2$O for

control animals.

To label the entire subventricular zone-rostral migratory stream-olfactory bulb (SVZ-

RMS-OB) system, animals were given intraperitoneal injections of BrdU at 14, 7, 2, and 1d

before collection. Injections were administered following brief anesthesia with isofluorane (Kent

Scientific) to reduce animal stress. Tissue from half of each group was collected following 28d

of treatment as described below. Other animals in each group were allowed 28d recovery, with

Begin treatment
Control: 2M 2F
AgNP: 2M 2F

Collect half
Control: 1M 1F
AgNP: 1M 1F

Collect recovery
Control: 1M 1F
AgNP: 1M 1F

Begin training
1 week

BrdU (50mg/kg)

BrdU (50mg/kg)

Treatment Period (4 weeks)
-Control given 10% sucrose
-Experimental given 100mg/kg
 AgNP in 10% sucrose

Recovery Period (4 weeks)
-No treatments
-Weight monitored
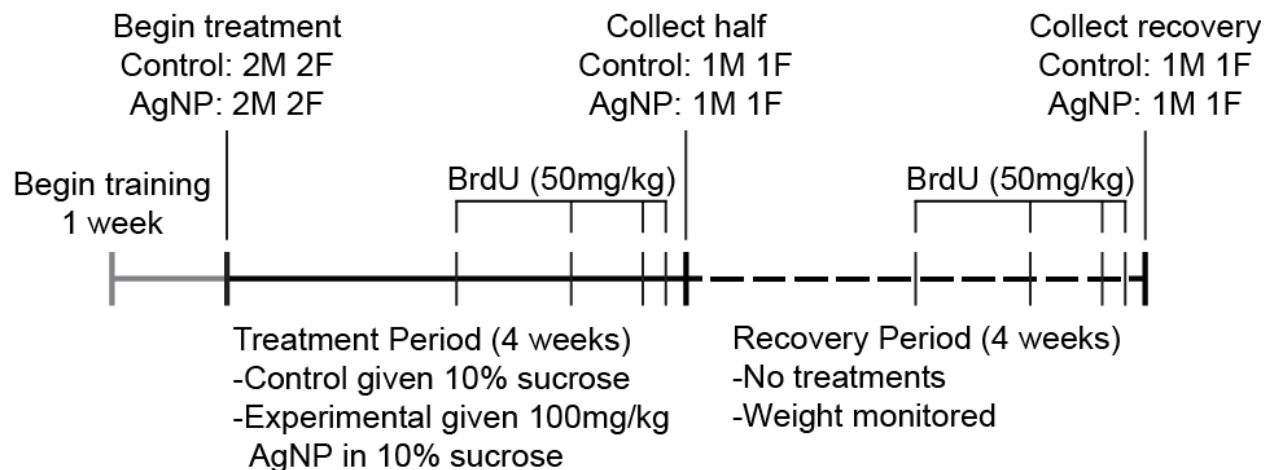
Repeat, staggered by 3 weeks to avoid overlap of collection dates.
8 animals per group (4M, 4F), 4 groups; total 32 animals (16M 16F)
n=4 (n=8 if pooling sexes)

Figure 11: **Schedule of animal experiments.** All stages and steps were performed on equal numbers of males and females. All animals were trained for one week to accept 10% sucrose from a syringe. Daily for 4 weeks, half of each group was given 100mg/kg AgNP in 10% sucrose at a dosing volume of 2mL/kg, with the other half given vehicle control. Tissue was collected from half of each treatment group immediately following treatment completion, with the other half collected after 4 weeks of recovery. All animals were given intraperitoneal injections of BrdU at 50mg/kg 14, 7, 2, and 1d before collection in an attempt to label the entire SVZ-RMS-OB system (Figure 1B). Weight and behavior were monitored daily throughout treatment.

no AgNP or sucrose treatment. Animal weight and behavior were monitored daily during treatment.

4.2.2 Tissue Collection and Sectioning

Animals were euthanized with deep isofluorane followed by bilateral pneumothorax. Cardiac perfusion was performed first with 150mL PBS1 (2.2.1) to ensure exsanguination followed by perfusion with 500mL of fresh 4% paraformaldehyde (PFA) in PBS1. Upon completion, heads were removed and brains collected. As AgNP are known to accumulate in cerebellum at levels similar to neurogenic niches (Wen et al., 2016), cerebella were removed using a razor blade and placed in tared tubes for silver content analysis, and brains were placed in 4% PFA postfix for one day. After postfix, brains were moved to 30% sucrose with 0.01% sodium azide (Sigma) in PBS2 (2.2.4) and stored at 4°C. Fixed tissue was embedded in Tissue Tek OCT Compound (Sakura Finetek, Torrance, California,), sectioned at 30µm using a Leica CM3050 S cryostat (Leica), and stored as free-floating sections in cryoprotectant (30% Glycerol (AMRESCO), 30% Ethylene Glycol (AMRESCO), 40% PBS2) at -20°C.

4.2.3 Immunohistochemistry

Sections were placed in four 5min washes with PBS2, then immersed in 1% $NaBH_4$ (Sigma) in PBS2 for 20 minutes to reduce background autofluoresence (Spitzer et al., 2011). After washing six times with PBS2 and once with diH_2O, sections were immersed in 2N HCl for 30min at 48°C and neutralized in 0.1M Borate (pH 8.5; Fisher) for 12 minutes, followed by washing once with diH_2O, then three times with PBS2. Sections were blocked in 10% normal goat serum (NGS; Life) in PBS2 + 0.3% Triton-X (PBTx) for 1hr, followed by PBS2 washes. Sections were placed in tubes with primary antibody at 1:500 in 1% NGS in PBTx overnight. Primary antibodies used were mouse-α-BrdU (Abcam) and rabbit-α-β-tubulinIII (Abcam),

rabbit-α-nestin (Abcam), rabbit-α-DCX (Millipore), or rabbit-α-NeuN (Abcam). Sections were washed four times, then placed in tubes with secondary antibody at 1:500 in 1% NGS and PBTx overnight. Secondary antibodies were goat-α-rabbit-Alexa 488 (Life) and goat-α-mouse Alexa 568 (Life). After washing with PBS2, sections were immersed in $CuSO_4$ solution (1mM $CuSO_4$ (Sigma), 50mM Ammonium Acetate (Fisher)) for 1hr, washed again with diH_2O and PBS2, and then counterstained with DAPI in PBS2 for 1hr. Sections were floated onto Fisherbrand Superfrost Plus slides (Fisher) and sealed in Prolong Gold and allowed to cure overnight. Sections were imaged using an epifluorescent microscope (Leica).

4.2.4 Silver Content Analysis

Wet silver content of cerebella was analyzed by Dr. John W. Olesik in the Trace Element Research Laboratory at Ohio State University School of Earth Sciences by inductively coupled plasma mass spectrometry.

4.2.5 Patch Clamp Electrophysiology

Cells were cultured and plated as described in (2.2.1) and (2.2.2). For experiments, cells were constantly perfused with warm sterile bath solution (130mM NaCl (Fisher); 3mM KCl (BioExpress); 4mM $MgCl_2$ (Sigma); 1mM $CaCl_2$ (Avantor; Center Valley, Pennsylvania, United States); 2.5mM EGTA (Sigma); 10mM HEPES (Fisher); 5mM Glucose (BioExpress); pH 7.4) and maintained at approximately 35°C. Whole-cell recordings were taken using an Axopatch 200B (Molecular Devices; Sunnyvale, California, United States) with CV 203BU headstage (Molecular Devices), with the program CLAMPEX 10.3 (Molecular Devices) delivering command potentials. Electrodes were 2-3 MΩ and pulled from thin-wall capillary glass (A-M Systems; Sequim, Washington, United States) using a P-97 Flaming/Brown micropipette puller (Sutter Instruments; Novato, California, United States). In-electrode solution consisted of

140mM KCl, 2mM MgCl$_2$, 1mM CaCl$_2$, 2.5mM EGTA, 1mM HEPES, and 3mM ATP at pH 7.4 with a final 287mOsm. A step protocol was applied that held cells between -80 and +60mV for 100ms following 50ms prepulse at -80mV. Tail currents were analyzed with 50ms voltage steps between -100mV and -50mV following a 75ms prepulse at +20mV. Both protocols utilized a holding potential of -80mV. Inactivation/activation dynamics were analyzed using a step protocol that held cells between -100 and +60mV for 100ms from a holding potential of -40mV.

<div align="center">

4.3 RESULTS

</div>

4.3.1 Silver Nanoparticle Treatment Does Not Alter Rat Growth

During the course of treatment and recovery, animal weight and behavior were monitored for signs of stress or toxicity. With only one exception, animals readily took sucrose solution or AgNP-containing sucrose solution from syringes after 7 days of training. The one exception was placed in the control group and eventually did take sucrose solution after several more days, and no changes were observed in the animal's growth compared to other control animals. Qualitatively, presence of AgNP in feeding solutions seemed to have no adverse effects on health or behavior in treated animals. No animals performed behaviors characteristic of stress or pain, such as head-pressing. Neither male nor female AgNP-treated animals' weights were significantly different from control at any time point during treatment or recovery (Figure 12).

4.3.2 Silver Nanoparticles Cause Silver Accumulation and Persistence in Rat Brains

Following perfusion, cerebella were removed and placed in tared tubes for Ag wet content analysis by ICP-MS. AgNP-treated animals had significantly higher Ag load than control animals, both immediately after treatment and after 28 days of recovery (Figure 13). Though there was a decrease in Ag content of AgNP-treated animals' brains during recovery (mean decrease of 8ppb), it was not a significant decrease (Figure 13). Further, the average Ag content
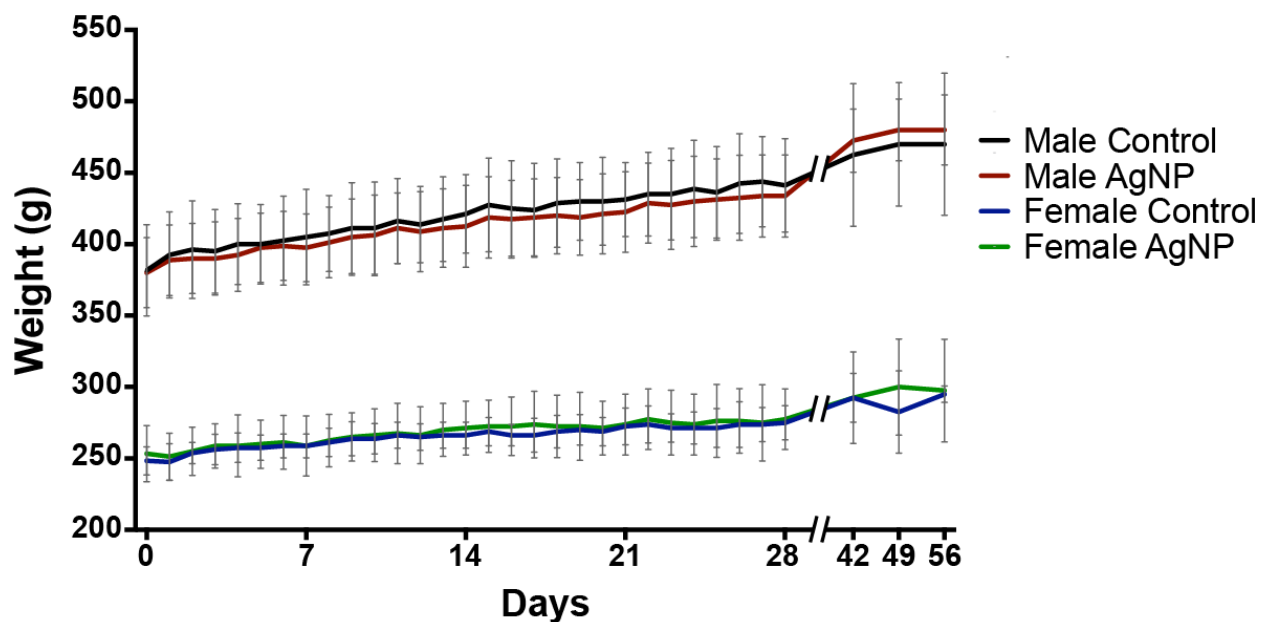
Figure 12: **Growth curve of animal subjects by sex and treatment.** Animal weights were recorded daily during treatment, then at 14, 21, and 28d during recovery (42, 49, and 56d). Weight of AgNP-treated animals did not differ significantly during treatment (n=8) or recovery (n=4). (p=0.9995, 2-way ANOVA; no significance between treatment groups at any timepoint; Sidak's multiple comparisons)
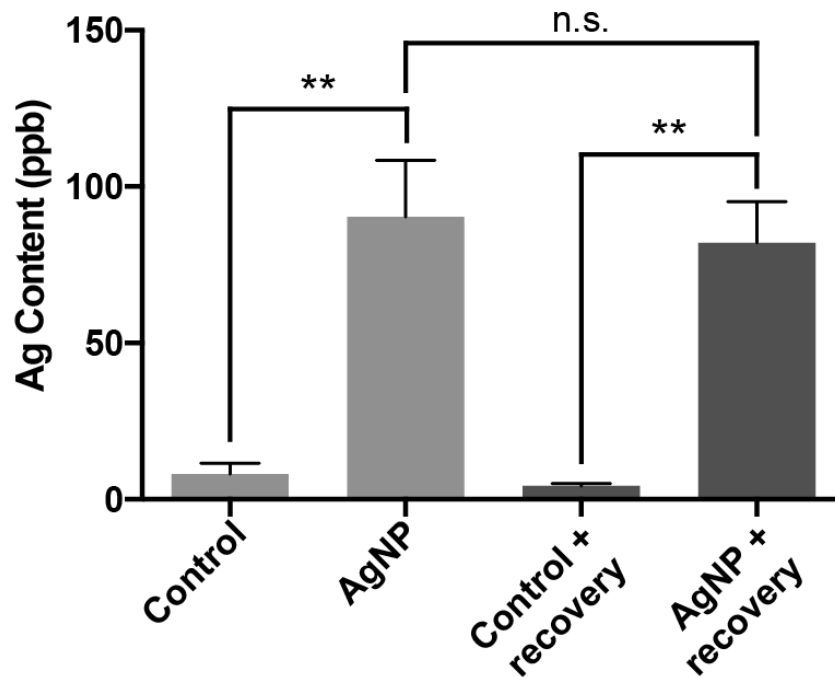
Figure 13: **Ag accumulates and persists in animal brains following AgNP exposure.** After 28 days of treatment, AgNP-treated animal's brains contained significantly more Ag than untreated animals. This difference was maintained even after recovery, with Ag loads of AgNP-exposed animals not decreasing significantly after a 28-day recovery period. ($p < 0.001$, ANOVA, n=3; **$p < 0.01$, Tukey's multiple comparisons)

of AgNP-treated animals (90.25ppb, or 0.09ppm) falls within the range of concentrations used for pilot immunocytochemistry experiments (0.05-2.0ppm; 2.2.2). It is also approximately one order of magnitude away from concentrations used in comet assay (2.2.5), time lapse experiments (2.2.7), later immunocytochemistry experiments (3.2.2), and cells collected for Western blot (3.2.3) (1ppm).

4.3.3 Immunohistochemistry of Brain Sections Reveals Inconclusive BrdU Label

Animals were given injections of BrdU at 14, 7, 2, and 1 days pre-collection to label dividing cells in the SVZ and the differentiated cells derived from them in the entire SVZ-RMS-OB system. Sections were immunolabeled for markers of NSC differentiation and BrdU to assess co-labeling and determine fate of differentiating NSC during treatment and recovery. However, while labeling of differentiation markers like nestin (Figure 14A, green) and NeuN (Figure 14B, green) was successful, BrdU labeling revealed inconsistent areas of BrdU+ cells. While most times $BrdU^+$ cells were present in the SVZ, cells in the OB only occasionally labeled as $BrdU^+$, and cells in the RMS rarely labeled as $BrdU^+$ (Figure 14). A different α-BrdU antibody was tested, but ultimately did not produce significantly different results (data not shown).

4.3.4 Patch Clamp Electrophysiology Results Are Incomplete

Electrophysiology experiments encountered numerous technical setbacks. Only four recordings were successfully obtained from control cells. Of these four, all show evidence of a slow-activating, slow-inactivating outward current, possibly from K^+ outward delayed rectifier channels (Figure 15). Similarly, three show evidence of a fast-activating, fast-inactivating outward current, possibly from A-type K^+ channels. Also, there is high variability between the measured cells, with peak currents from the slow-activating current varying from 110pA to
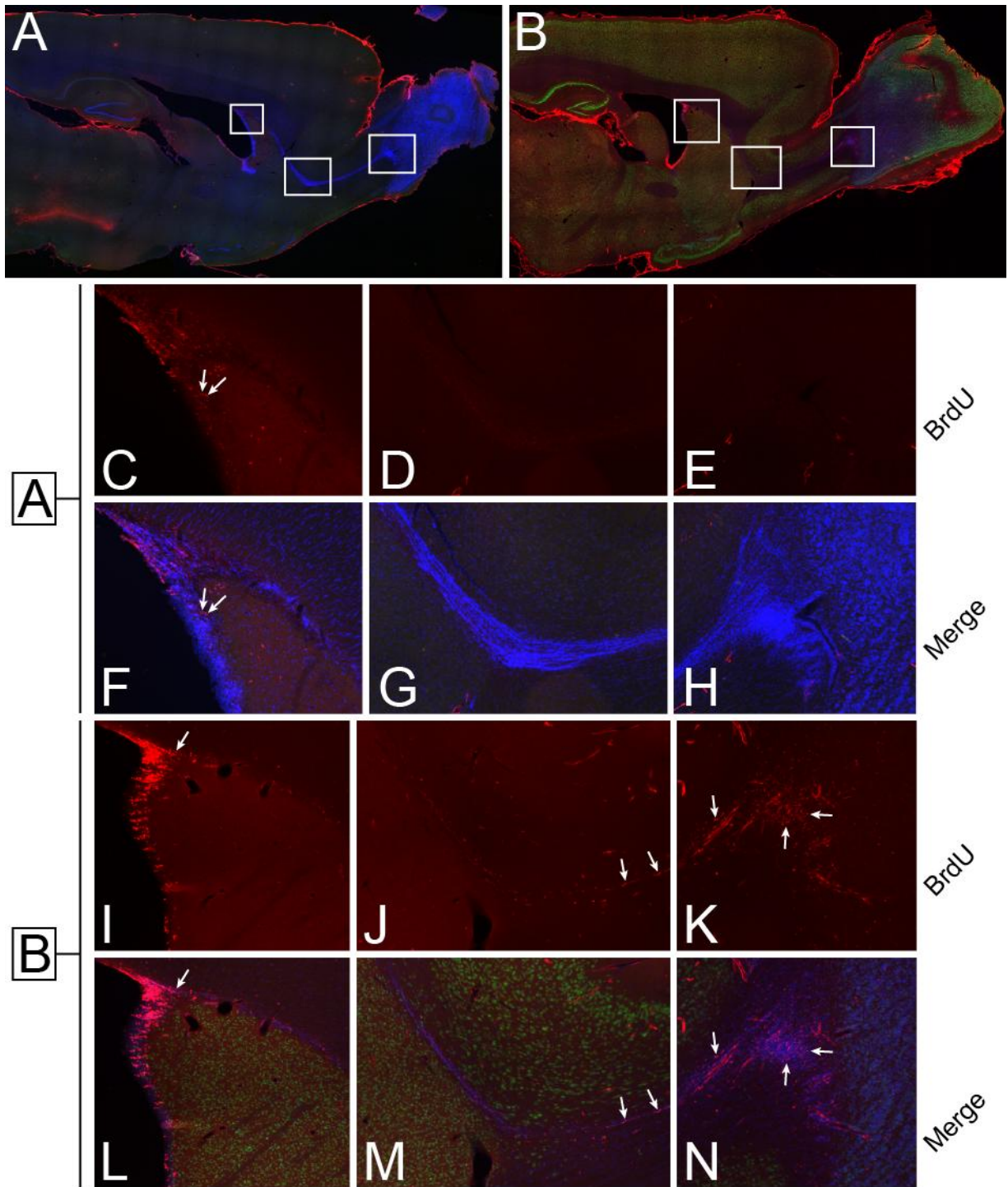
Figure 14: **BrdU label is inconsistent in SVZ-RMS-OB system.** Sections were processed using immunohistochemistry for BrdU (red) and, among others, Nestin (A; green) or NeuN (B; green). While BrdU label (arrows) was generally present in the SVZ (C, F, I, L), labeling in the RMS (D, G, J, M) and OB (E, H, K, N) was only present in some sections, even when the corresponding structures were visible with DAPI staining of nuclei (blue). Inconsistent staining was present in both control (A) and AgNP-exposed (B) brains.

57
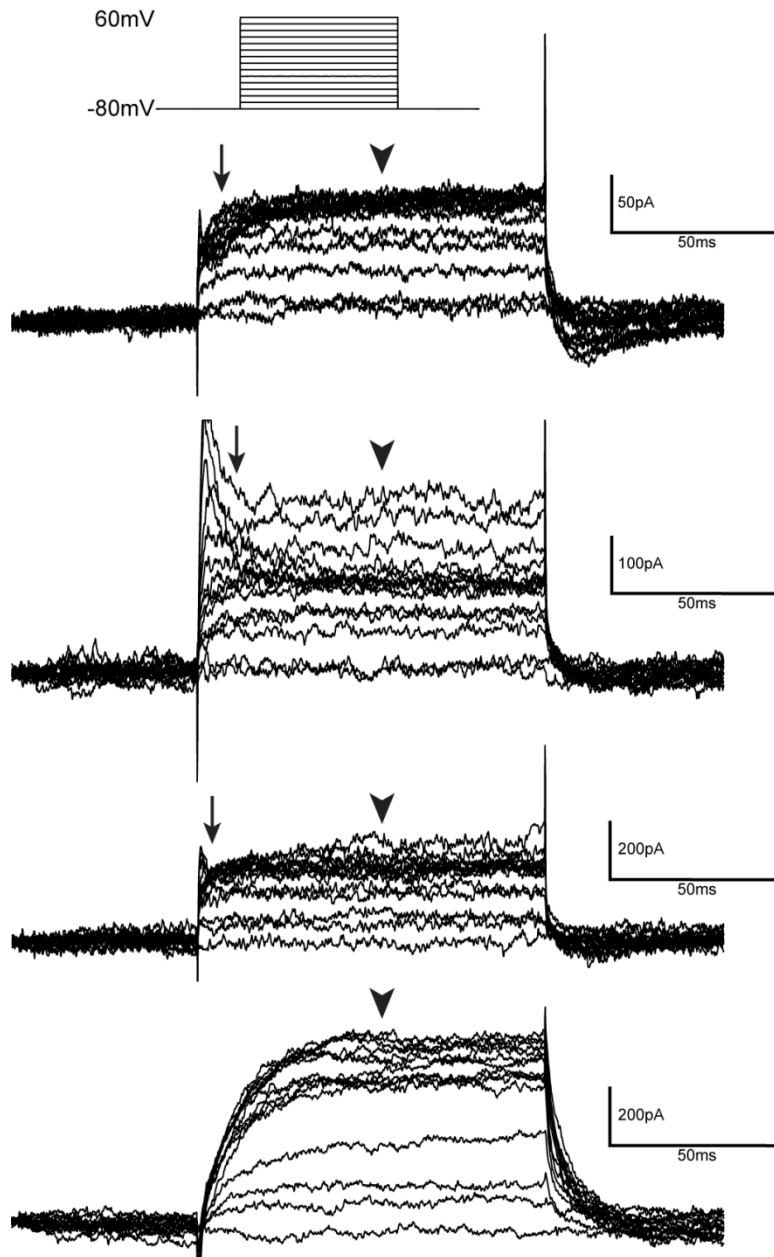
Figure 15: **Control cell voltage clamp traces following IV-curve protocols.** Cells were held at -80mV subjected to 10mV steps from -80mV to +60mV. All cells appear to contain slow-activating, slow-inactivating outward currents (arrowheads), possibly delayed rectifier K^+ channels. Three show evidence of fast-activating, fast-inactivating A-type K^+ currents (arrows). However, the current amplitudes are too variable (I_{max} from 110pA to 650 pA) to plot a meaningful IV-curve. Attempts to further elucidate activation/deactivation dynamics with a tail current protocol and inactivation holding voltage (+40mV) failed due to repeated gigaseal loss.

almost 650pA. Therefore, attempts to plot an IV-curve of the data were inconclusive. No

recordings were successfully obtained from AgNP-treated cells.

4.4 DISCUSSION

AgNP accumulate in various tissues *in vivo*, including the brain (Buzulukov Iu et al.,

2014; Ji et al., 2007; Kim et al., 2008b; Lee et al., 2013; Wen et al., 2016). Reports of their

effects *in vivo* vary, with some studies claiming no observable effects (Ji et al., 2007; Liu et al.,

2013; Munger et al., 2015; Munger et al., 2014), while others have found evidence of adverse

effects in mammal models (Hadrup et al.; Kim et al., 2008b; Kovvuru et al., 2015; Li et al.,

2014; Liu et al., 2012; Skalska et al., 2014; Tang et al., 2008; Tiwari et al., 2011; Xu et al.,

2015a; Yin et al., 2015a) in the absence of overt signs of stress like changes to body weight, food

and water intake, and behavior. Even then, few studies have analyzed AgNP's effects on adult

neurogenesis *in vivo*, and none following more than seven days' exposure (Liu et al., 2013).

Therefore, investigations into AgNP's effects on adult neurogenesis *in vivo* are especially

prudent, as several studies have shown that AgNP are capable of altering neurogenesis *in vitro* at

various exposure levels ranging from 0.1μM (Dayem et al., 2014), to 1μg/mL (Cooper and

Spitzer, 2015), to 25μg/mL (Oh et al., 2015). This work attempted to bridge this gap by

analyzing NSC proliferation, migration, and differentiation of newly-generated NSC within the

SVZ-RMS-OB system in young-adult rats following AgNP exposure.

Twenty-eight-days' treatment with 100mg/kg uncoated 40nm AgNP produced

significantly elevated Ag levels in brain tissue (Figure 13) without altering growth (Figure 12) or

inducing signs of stress. Immediately following treatment, brains contained an average of 90ppb

Ag, and after 28 days of recovery contained approximately 82ppb (Figure 13), though this

decrease was not statistically significant. Identical dosing parameters with 10nm AgNP resulted

in brain Ag content of approximately 300ppb, whereas Ag content from 25nm AgNP treatment

was closer to 200ppb (Lee et al., 2013). In other studies, intragastric exposure to 6nm AgNP at

100μg/kg for 28 days resulted in brain Ag content of 36ppb (Buzulukov Iu et al., 2014), while

subcutaneous injection of 50-100nm AgNP at 62.8mg/kg for 2-24 weeks resulted in brain Ag

levels ranging from 200-400ppb (Tang et al., 2008). However, accumulation dynamics of AgNP

differ with size, with smaller AgNP tending to have greater accumulation (Anderson et al., 2015;

Boudreau et al., 2016; Lee et al., 2013). Therefore, Ag levels observed in brain tissue from this

study using 40nm AgNP are in line with the results of other studies. Further, the lack of a

significant decrease in Ag content after 28 days' recovery is consistent with many studies

demonstrating the high longitudinal retention of AgNP in the brain (Lankveld et al., 2010; Lee et

al., 2013; Wen et al., 2016).

Analysis of NSC fate *in vivo* following AgNP treatment or recovery was hampered by

lack of consistent BrdU labeling throughout the SVZ-RMS-OB system (Figure 14). BrdU was

administered at 14, 7, 2, and 1 days pre-collection, as previous work has shown that, following a

single BrdU injection to label diving cells and their progeny, most BrdU-positive cells have

migrated from the SVZ to the OB after 15 days (Lois and Alvarez-Buylla, 1994). However, cells

positive for BrdU and other temporally-specific markers of cell division can appear in the OB as

quickly as two to four days after treatment (Lois and Alvarez-Buylla, 1994; Parent et al., 2002;

Perez-Asensio et al., 2013). Indeed, migrating neuroblasts from the SVZ take 2-7 days to

traverse the RMS, up to 2 days to migrate to their final location within the OB, and then

anywhere from 2 to 21 days to complete differentiation into mature neurons (Petreanu and

Alvarez-Buylla, 2002). However, a period of 8-12 days appears to be sufficient to see convincing

label of cells in the OB (Zigova et al., 1998). Perhaps instead of the BrdU protocol used in these

experiments, a more effective method would be a series of seven 50mg/kg treatments, once every

two days beginning twelve days before collection, with the final three treatments administered

three, two, and one days before collection. This should allow sufficient time for labeled cells to

reach the OB and begin differentiation, while also ensuring that labeled cells are still present in

the RMS. Additional administrations may be necessary, as BrdU is present in the blood and

labels CNS tissue for only two hours following IP injection (Hayes and Nowakowski, 2000;

Matiasova et al., 2014; Packard et al., 1973). Whether such measures would be necessary to label

the entire SVZ-RMS-OB system in rats is presently unknown.

This experiment also proposed to analyze altered electrophysiological properties of

differentiating NSC in response to AgNP treatment. Normally, differentiating NSC proceed

through a series of tightly-controlled electrophysiological events (Scheffler et al., 2005). AgNP

inhibit both voltage-gated sodium (Busse et al., 2013; Liu et al., 2009b) and potassium (Liu et

al., 2011) channel activity, validating their ability to interfere with membrane properties in

mature neural cells. However, AgNP exposure occurs throughout life, while NSC are in various

stages of differentiation. Indeed, interference of NSC electrophysiological development due to

disease state can lead to a loss of NSC proliferation and development of aberrant membrane

properties during differentiation (DiFebo et al., 2012). Therefore, though this study did not

achieve its goal, determining how NSC membrane properties can be altered during

differentiation by AgNP exposure remains an important, necessary field of investigation.

CHAPTER 5: CONCLUSIONS AND FUTURE DIRECTIONS

Previous work has convincingly established that silver nanoparticles (AgNP) have potential use as an antimicrobial agent (Samuel and Guggenbichler, 2004; Sondi and Salopek-Sondi, 2004). They perforate the bacterial membrane (Kora and Sashidhar, 2014; Li et al., 2013; Su et al., 2009), bind to and disrupt proteins involved in cellular processes (Choi et al., 2008; Du et al., 2012; Wigginton et al., 2010), and damage DNA (Radzig et al., 2013; Vishnupriya et al., 2013), eventually resulting in the death of the cell. They successfully inhibit the growth of even highly antibiotic-resistant strains of pathogenic bacteria (Abdel Rahim and Ali Mohamed, 2015; Actis et al., 2015; Jun et al., 2015; Li et al., 2013). Beyond bacteria, AgNP inhibit the growth of fungal pathogens (Hwang et al., 2012; Kim et al., 2008a; Monteiro et al., 2011; Panacek et al., 2009), even those that are resistant to traditional antimycotics (Artunduaga Bonilla et al., 2015), and have been suggested as a treatment for fungal infections of the skin (Anwar et al., 2016). Further, AgNP can prevent the spread of key viruses such as human immunodeficiency virus (Elechiguerra et al., 2005; Lara et al., 2010a; Lara et al., 2010b; Sun et al., 2005b), herpes simplex virus (Baram-Pinto et al., 2009; Gaikwad et al., 2013), multiple strains of influenza virus (Xiang et al., 2013; Xiang et al., 2011), and many others (Chen et al., 2013a; Lu et al., 2008; Rogers et al., 2008; Sun et al., 2008; Trefry and Wooley, 2013). Indeed, AgNP have been proposed as a coating for contraceptive devices to prevent the spread of sexually-transmitted infections, both viral and bacterial (Mohammed Fayaz et al., 2012). They have also been incorporated into catheter coatings to prevent infection (Samuel and Guggenbichler, 2004), and are used in burn dressings to speed healing (Bidgoli et al., 2013).

Despite the potential of these applications, AgNP-treated products result in direct consumer exposure (Benn et al., 2010; Benn and Westerhoff, 2008; Cushen et al., 2013; Kaegi et

al., 2010; Quadros and Marr, 2011; Quadros et al., 2013; von Goetz et al., 2013). AgNP will also leach into the environment, eventually ending up in waste water, the atmosphere, and soil (Blaser et al., 2008; Hashimoto et al., 2015; Ji et al., 2007; Quadros and Marr, 2010; Sekhon, 2014; Tugulea et al., 2014). In water and soil, AgNP can persist for months, possibly even years (Dale et al., 2015; Loza et al., 2014; Sekine et al., 2015; Tugulea et al., 2014) by dynamic dissolution and reformation (Yu et al., 2014) dependent upon local conditions and particle coating (Levard et al., 2012; Sekine et al., 2015; Yin et al., 2015c). Given the lack of studies examining environmental levels of AgNP in soil or water, variability in AgNP-containing product use within the population, and their highly location-dependent behavior, an estimate of actual exposure is difficult at best (Whiteley et al., 2013).

A great deal of research has focused on AgNP's toxic effects in numerous eukaryotic cell types at high concentrations (Reviewed in Bartlomiejczyk et al., 2013 and Kruszewski et al., 2011). They generate reactive oxygen species, break down the cytoskeleton and membrane, damage DNA, and disrupt protein function (Ahamed et al., 2008; Ahlberg et al., 2014; Arora et al., 2008; Dubey et al.; Gliga et al., 2014; Haase et al., 2012; Jiang et al., 2013; Kawata et al., 2009; Kim et al., 2012; Kim et al., 2009; Miura and Shinohara, 2009; Wise et al., 2010; Xu et al., 2013). Further, they are capable of crossing biological defenses such as the blood-air barrier in the lungs (Ji et al., 2007; Oberdorster et al., 2004), the intestinal barrier (Boudreau et al., 2016; Gaillet and Rouanet, 2015; Kovvuru et al., 2015; Xu et al., 2015b), the blood-testis barrier (Lee et al., 2013; Sleiman et al., 2013), the placental barrier (Melnik et al., 2013), and the blood-brain barrier (Lee et al., 2013; Sosedova et al., 2015; Tang et al., 2008; Tang et al., 2010). AgNP can bypass these defenses altogether, such as following their nasal inhalation and subsequent retrograde transport down the olfactory nerve to the brain (Danscher and Locht, 2010;

63

Oberdorster et al., 2004; Simko and Mattsson, 2010), thereby bypassing the blood-brain barrier. Once they have entered the body, AgNP accumulate in many tissues including the liver, kidneys, and brain (Lee et al., 2013). Numerous studies have noted that retention times in the brain are significantly higher than other organs (Lankveld et al., 2010; Wen et al., 2016). Therefore, studying the effects of AgNP on brain health is especially prudent. Further, the majority of studies concerned with the biological effects of AgNP have focused on their toxicity and its underlying mechanisms, with little research focused on the consequences of AgNP exposure at levels that do not cause loss of cell viability.

This research aimed to fill that gap, using adult neural stem cells (NSC) from the brains of young adult rats as an accepted *in vitro* model of neurodevelopment, NSC behavior, and neural cell function in general (Aimone et al., 2014; Gage, 2000; Ge et al., 2008). NSC were exposed to uncoated 40nm AgNP *in vitro* at concentrations ranging from 0.05-2.0μg/mL, levels previously shown to not reduce viability in cultured mammalian cells (Table 1). This was confirmed here via alkaline comet assay, where AgNP exposure did not change Olive moment distribution compared to negative controls (Figure 4), indicating no damage to DNA beyond basal levels (Olive and Banath, 2006; Olive et al., 1990). However, low-level AgNP exposure induced the formation of f-actin inclusions in a dose- and time-dependent manner, irrespective of AgNP localization within cells (Figure 5) that appear visually similar to those seen following f-actin disrupting toxins (Lazaro-Dieguez et al., 2008; Muller et al., 2013). Further, AgNP exposure resulted in β-catenin puncta (Figure 8) that co-localized with f-actin inclusions (Figure 9), hinting at recruitment or disruption of β-catenin signaling accompanied by loss of f-actin dynamics. This was supported by the loss of neurite dynamics and arborization, both

64

cytoskeleton-driven processes mediated by β-catenin (Lee et al., 2014; Yu and Malenka, 2003), in time-lapse experiments following AgNP exposure (Figure 6).

Questions remain concerning the composition of these f-actin inclusions, the mechanism of their formation, and whether or not their presence mediates observed deficits in cytoskeleton dynamics. AgNP are capable of reacting with and disrupting structures of membrane components (Ansari et al., 2014), so f-actin inclusion formation may begin with disruption to localized chemistry of the membrane itself. β-catenin is known to bind to several proteins with variable function, such as the actin-bundling protein fascin (Tao et al., 1996) and cadherin adhesion complexes (Wheelock and Knudsen, 1991). During canonical signaling, β-catenin enters the nucleus and binds transcription factors in the T-Cell Factor/Lymphoid Enhancer Factor (TCF/LEF) family (Molenaar et al., 1996), promoting either proliferation or neuronal differentiation in NSC in a context-dependent manner (Marinaro et al., 2012; Qu et al., 2010; Wisniewska, 2013). Alternatively, β-catenin can bind factors from the Forkhead Box O (FOXO) family (Essers et al., 2005) under conditions associated with stress, especially oxidative stress, to promote antioxidant response, DNA repair, cell quiescence, and cell survival (Almeida et al., 2007; Martins et al., 2016). However, upregulation of E-cadherin can reduce the activity of β-catenin by sequestering β-catenin at the membrane (Huels et al., 2015), even under conditions that promote activation of β-catenin signaling. Adenomatous polyposis coli (APC), a protein usually involved in degradation of β-catenin (Munemitsu et al., 1995), can also recruit β-catenin to the membrane, thereby allowing APC to aid in cellular migration (Sharma et al., 2006). Therefore, the formation of observed f-actin inclusions with co-localized β-catenin puncta following AgNP exposure may be mediated by the dysregulation of these mechanisms. β-catenin may be recruited through its canonical cadherin-associated linkage to the f-actin cytoskeleton

(Wheelock and Knudsen, 1991), or perhaps β-catenin is involved in the recruitment of f-actin through fascin binding (Tao et al., 1996).

Fascin is necessary for neurite dynamics and migration in SVZ NSC (Sonego et al., 2013), and its recruitment to and sequestration within f-actin inclusions could explain the observed loss of neurite dynamics and arborization following AgNP exposure (Figure 6). Alternatively, if β-catenin is sequestered while bound to TCF/LEF transcription factors, this would result in a loss of function. As temporally- and spatially-regulated TCF/LEF signaling is vital for proper proliferation and differentiation of NSC (Wisniewska, 2013), the resulting lack of proper signaling could also explain observed changes to NSC behavior following AgNP exposure. Further, β-catenin sequestration within f-actin inclusions may explain why AgNP exposure induced an increase in intracellular β-catenin (Figure 9), yet analysis of NSC behavior is more consistent with aberrant or decreased β-catenin signaling (Lee et al., 2014; Marinaro et al., 2012; Yu and Malenka, 2003). Therefore, this work collectively suggests that low-level AgNP exposure disrupts β-catenin function in differentiating NSC, possibly through sequestration of β-catenin and subsequent sequestration of its associated proteins. Future research should therefore examine localization of these partner proteins. If possible, it should also determine the degree of β-catenin-associated transcription factor binding in response to the observed increase in intracellular β-catenin, especially to genes known to be involved in neuronal differentiation like *NeuroD1* and *Prox1* (Wisniewska, 2013).

In addition to being visually similar to cytoskeletal changes seen after treatment with f-actin-disrupting toxins (Lazaro-Dieguez et al., 2008; Muller et al., 2013), f-actin inclusions also appear similar to structures termed actin patches (Gallo, 2013). Actin patches are transient nucleations of f-actin normally observed during neurite initiation, neurite branching, and axon

66

retraction (Gallo, 2006; Ketschek and Gallo, 2010; Spillane and Gallo, 2014; Spillane et al., 2011). They are also found in the initial segmentof axons, where they are thought to prevent the trafficking of dendritic proteins (Chen et al., 2013b; Watanabe et al., 2012). Similarly, actin patches are thought to act as promoters of axon branching by halting the transport of and recruiting mitochondria, translational machinery, and protein components necessary for branching (Spillane and Gallo, 2014; Spillane et al., 2013). However, actin patches are normally only present for short periods of time, approximately 20-50 seconds (Spillane et al., 2011), and act as the foundations for initial extension of filopodia that may later be stabilized by microtubules to form branches (Spillane and Gallo, 2014). If AgNP inhibit actin dynamics, then f-actin inclusions may be failed attempts by NSC to form neurites or branches. Alternatively, as not all actin patches give rise to filopodia (Spillane et al., 2013), f-actin inclusions may be actin patches that would not have produced filopodia but still failed to depolymerize. The only complication is the presence of β-catenin within f-actin inclusions. Though Arp2/3, their p35 and p21 subunits, the Arp2/3 recruiter WAVE1, and the actin bundler cortactin have all been reported in actin patches (Spillane et al., 2012; Spillane et al., 2011), β-catenin has not been reported in actin patches specifically. However, β-catenin is known to be localized to the sites of process extension in dendritic spines and axon branches, and is locally transcribed in growth cones (Elul et al., 2003; Kundel et al., 2009; Yu and Malenka, 2004). Therefore, β-catenin may be recruited to actin patches to mediate extension, but AgNP interference instead prevents functionalization and depolymerization, giving rise to f-actin inclusions containing β-catenin.

Given the relative novelty of AgNP as an environmental contaminant, further consideration should also be given to the effects of alternate products generated from AgNP in the environment on NSC behavior and physiology. Traditionally, the breakdown and sulfidation

of AgNP into insoluble Ag_2S has been thought to remove AgNP from the environment and largely mitigate their toxicity (Levard et al., 2013). Recently, AgNP in wastewater treatment plants have been found to not only break down into Ag_2S, but also form into Ag_2S nanoparticles (Ag_2S-NP) through bacterial processes that are common in natural waters (Kim et al., 2010). There is a distinct lack of research addressing the possible environmental levels of Ag_2S-NP, or what their possible physiological effects might be. Ag_2S-NP persist in soil for at least seven months (Sekine et al., 2015), and have some comparable antimicrobial action to AgNP (Kumari et al., 2014). Studies in algae (Jagadeesh et al., 2015) and plants (Wang et al., 2015) have found toxic effects following Ag_2S-NP exposure. Further, experiments using zebrafish have found that, though 0.1 μg/mL Ag_2S-NP are not as toxic as AgNP, they can still exert physiological effects such as interference in antioxidant pathways (Devi et al., 2015). Conversely, studies in a fish cell line did not reveal any overt genotoxicity following 0.01-1.0μg/mL Ag_2S-NP exposure (Munari et al., 2014). Further research is needed to determine what, if any, physiological effects Ag_2S-NP could have at low concentrations, especially whether or not they share AgNP's ability to translocate to and accumulate in tissues like the brain.

Altogether, these data add to the existing body of knowledge concerning AgNP's effects on NSC function. They confirm AgNP's bioaccumulative nature within the brain and confirm they are capable of disrupting cellular processes such as neurite dynamics and β-catenin signaling even at low exposure levels that do not cause loss of cell viability. However, they also raise further questions regarding the composition of observed f-actin inclusions and how their formation relates to observed changes to NSC physiology and behavior. As these effects are all observed at levels of AgNP that do not reduce cell viability, they raise serious concerns about other effects of AgNP on the brain, and possible effects of increasing environmental AgNP-

68

derived Ag_2S-NP following the rise in AgNP use within society. Overall, this research

demonstrates that low-level AgNP pose a significant risk to basic neural functions, and that long-

term exposure could result in deficits in learning, brain repair, and neurodevelopment.

REFERENCES

Abdel Rahim KA, Ali Mohamed AM. Bactericidal and Antibiotic Synergistic Effect of Nanosilver Against Methicillin-Resistant Staphylococcus aureus. Jundishapur J Microbiol. 2015;8:e25867.

Abdelmaksoud-Damak R, Miladi-Abdennadher I, Triki M, Khabir A, Charfi S, Ayadi L, et al. Expression and mutation pattern of beta-catenin and adenomatous polyposis coli in colorectal cancer patients. Arch Med Res. 2015;46:54-62.

Aberle H, Bauer A, Stappert J, Kispert A, Kemler R. beta-catenin is a target for the ubiquitin-proteasome pathway. EMBO J. 1997;16:3797-804.

Actis L, Srinivasan A, Lopez-Ribot JL, Ramasubramanian AK, Ong JL. Effect of silver nanoparticle geometry on methicillin susceptible and resistant Staphylococcus aureus, and osteoblast viability. J Mater Sci Mater Med. 2015;26:215.

Adachi K, Mirzadeh Z, Sakaguchi M, Yamashita T, Nikolcheva T, Gotoh Y, et al. Beta-catenin signaling promotes proliferation of progenitor cells in the adult mouse subventricular zone. Stem cells. 2007;25:2827-36.

Ahamed M, Karns M, Goodson M, Rowe J, Hussain SM, Schlager JJ, et al. DNA damage response to different surface chemistry of silver nanoparticles in mammalian cells. Toxicology and applied pharmacology. 2008;233:404-10.

Ahlberg S, Antonopulos A, Diendorf J, Dringen R, Epple M, Flock R, et al. PVP-coated, negatively charged silver nanoparticles: A multi-center study of their physicochemical characteristics, cell culture and in vivo experiments. Beilstein journal of nanotechnology. 2014;5:1944-65.

Aimone JB, Li Y, Lee SW, Clemenson GD, Deng W, Gage FH. Regulation and Function of Adult Neurogenesis: From Genes to Cognition. Physiological reviews. 2014;94:991-1026.

Almeida M, Han L, Ambrogini E, Weinstein RS, Manolagas SC. Glucocorticoids and tumor necrosis factor alpha increase oxidative stress and suppress Wnt protein signaling in osteoblasts. The Journal of biological chemistry. 2011;286:44326-35.

Almeida M, Han L, Martin-Millan M, O'Brien CA, Manolagas SC. Oxidative stress antagonizes Wnt signaling in osteoblast precursors by diverting beta-catenin from T cell factor- to forkhead box O-mediated transcription. The Journal of biological chemistry. 2007;282:27298-305.

Altman J, Das GD. Autoradiographic and histological evidence of postnatal hippocampal neurogenesis in rats. The Journal of comparative neurology. 1965;124:319-35.

Altman J, Das GD. Autoradiographic and histological studies of postnatal neurogenesis. I. A longitudinal investigation of the kinetics, migration and transformation of cells incorporating tritiated thymidine in neonate rats, with special reference to postnatal neurogenesis in some brain regions. The Journal of comparative neurology. 1966;126:337-89.

Altman J, Das GD. Postnatal neurogenesis in the guinea-pig. Nature. 1967;214:1098-101.

Alvarez-Buylla A. Mechanism of neurogenesis in adult avian brain. Experientia. 1990;46:948-55.

Alvarez-Buylla A. Neurogenesis and plasticity in the CNS of adult birds. Exp Neurol. 1992;115:110-4.

Alvarez-Buylla A, Nottebohm F. Migration of young neurons in adult avian brain. Nature. 1988;335:353-4.

Alvarez-Buylla A, Theelen M, Nottebohm F. Proliferation "hot spots" in adult avian ventricular zone reveal radial cell division. Neuron. 1990;5:101-9.

Anderson DS, Patchin ES, Silva RM, Uyeminami DL, Sharmah A, Guo T, et al. Influence of particle size on persistence and clearance of aerosolized silver nanoparticles in the rat lung. Toxicological sciences : an official journal of the Society of Toxicology. 2015;144:366-81.

Anderson MJ, Waxman SG. Neurogenesis in tissue cultures of adult teleost spinal cord. Brain research. 1985;352:203-12.

Angel BM, Batley GE, Jarolimek CV, Rogers NJ. The impact of size on the fate and toxicity of nanoparticulate silver in aquatic systems. Chemosphere. 2013;93:359-65.

Ansari MA, Khan HM, Khan AA, Ahmad MK, Mahdi AA, Pal R, et al. Interaction of silver nanoparticles with Escherichia coli and their cell envelope biomolecules. J Basic Microbiol. 2014;54:905-15.

Anwar MF, Yadav D, Jain S, Kapoor S, Rastogi S, Arora I, et al. Size- and shape-dependent clinical and mycological efficacy of silver nanoparticles on dandruff. International journal of nanomedicine. 2016;11:147-61.

Arevalo MA, Ruiz-Palmero I, Scerbo MJ, Acaz-Fonseca E, Cambiasso MJ, Garcia-Segura LM. Molecular mechanisms involved in the regulation of neuritogenesis by estradiol: Recent advances. The Journal of steroid biochemistry and molecular biology. 2012;131:52-6.

Arora S, Jain J, Rajwade JM, Paknikar KM. Cellular responses induced by silver nanoparticles: In vitro studies. Toxicology letters. 2008;179:93-100.

Artunduaga Bonilla JJ, Paredes Guerrero DJ, Sanchez Suarez CI, Ortiz Lopez CC, Torres Saez RG. In vitro antifungal activity of silver nanoparticles against fluconazole-resistant Candida species. World J Microbiol Biotechnol. 2015;31:1801-9.

Atcha Z, Rourke C, Neo AH, Goh CW, Lim JS, Aw CC, et al. Alternative method of oral dosing for rats. Journal of the American Association for Laboratory Animal Science : JAALAS. 2010;49:335-43.

Atli G, Canli M. Metals (Ag(+) , Cd(2+) , Cr(6+)) affect ATPase activity in the gill, kidney, and muscle of freshwater fish Oreochromis niloticus following acute and chronic exposures. Environ Toxicol. 2013;28:707-17.

Baker C, Pradhan A, Pakstis L, Pochan DJ, Shah SI. Synthesis and antibacterial properties of silver nanoparticles. Journal of nanoscience and nanotechnology. 2005;5:244-9.

Baker SA, Baker KA, Hagg T. Dopaminergic nigrostriatal projections regulate neural precursor proliferation in the adult mouse subventricular zone. The European journal of neuroscience. 2004;20:575-9.

Baram-Pinto D, Shukla S, Perkas N, Gedanken A, Sarid R. Inhibition of herpes simplex virus type 1 infection by silver nanoparticles capped with mercaptoethane sulfonate. Bioconjug Chem. 2009;20:1497-502.

Bartlomiejczyk T, Lankoff A, Kruszewski M, Szumiel I. Silver nanoparticles -- allies or adversaries? Annals of agricultural and environmental medicine : AAEM. 2013;20:48-54.

Belluzzi O, Benedusi M, Ackman J, LoTurco JJ. Electrophysiological differentiation of new neurons in the olfactory bulb. The Journal of neuroscience : the official journal of the Society for Neuroscience. 2003;23:10411-8.

Benn T, Cavanagh B, Hristovski K, Posner JD, Westerhoff P. The release of nanosilver from consumer products used in the home. J Environ Qual. 2010;39:1875-82.

Benn TM, Westerhoff P. Nanoparticle silver released into water from commercially available sock fabrics. Environmental science & technology. 2008;42:4133-9.

Benninghoff J, Gritti A, Rizzi M, Lamorte G, Schloesser RJ, Schmitt A, et al. Serotonin depletion hampers survival and proliferation in neurospheres derived from adult neural stem cells. Neuropsychopharmacology : official publication of the American College of Neuropsychopharmacology. 2010;35:893-903.

Bianchini A, Playle RC, Wood CM, Walsh PJ. Mechanism of acute silver toxicity in marine invertebrates. Aquatic toxicology. 2005;72:67-82.

Bianchini A, Wood CM. Mechanism of acute silver toxicity in Daphnia magna. Environmental toxicology and chemistry / SETAC. 2003;22:1361-7.

Bidgoli SA, Mahdavi M, Rezayat SM, Korani M, Amani A, Ziarati P. Toxicity assessment of nanosilver wound dressing in Wistar rat. Acta medica Iranica. 2013;51:203-8.

Blaser SA, Scheringer M, Macleod M, Hungerbuhler K. Estimation of cumulative aquatic exposure and risk due to silver: contribution of nano-functionalized plastics and textiles. The Science of the total environment. 2008;390:396-409.

Boudreau MD, Imam MS, Paredes AM, Bryant MS, Cunningham CK, Felton RP, et al. Differential Effects of Silver Nanoparticles and Silver Ions on Tissue Accumulation, Distribution, and Toxicity in the Sprague Dawley Rat Following Daily Oral Gavage Administration for 13-Weeks. Toxicological sciences : an official journal of the Society of Toxicology. 2016.

Bragg PD, Rainnie DJ. The effect of silver ions on the respiratory chain of Escherichia coli. Can J Microbiol. 1974;20:883-9.

Braunschweig L, Meyer AK, Wagenfuhr L, Storch A. Oxygen regulates proliferation of neural stem cells through Wnt/beta-catenin signalling. Molecular and cellular neurosciences. 2015;67:84-92.

Bray D, Chapman K. Analysis of microspike movements on the neuronal growth cone. The Journal of neuroscience : the official journal of the Society for Neuroscience. 1985;5:3204-13.

Braydich-Stolle L, Hussain S, Schlager JJ, Hofmann MC. In vitro cytotoxicity of nanoparticles in mammalian germline stem cells. Toxicological sciences : an official journal of the Society of Toxicology. 2005;88:412-9.

Bury NR, Wood CM. Mechanism of branchial apical silver uptake by rainbow trout is via the proton-coupled Na(+) channel. Am J Physiol. 1999;277:R1385-91.

Busse M, Stevens D, Kraegeloh A, Cavelius C, Vukelic M, Arzt E, et al. Estimating the modulatory effects of nanoparticles on neuronal circuits using computational upscaling. International journal of nanomedicine. 2013;8:3559-72.

Buzulukov Iu P, Arianova EA, Demin VF, Safenkova IV, Gmoshinskii IV, Tutel'ian VA. [Bioaccumulation of silver and gold nanoparticles in organs and tissues of rats by neutron activation analysis]. Izv Akad Nauk Ser Biol. 2014:286-95.

Carleton A, Petreanu LT, Lansford R, Alvarez-Buylla A, Lledo PM. Becoming a new neuron in the adult olfactory bulb. Nature neuroscience. 2003;6:507-18.

Carlson C, Hussain SM, Schrand AM, Braydich-Stolle LK, Hess KL, Jones RL, et al. Unique cellular interaction of silver nanoparticles: size-dependent generation of reactive oxygen species. J Phys Chem B. 2008;112:13608-19.

Caubit X, Arsanto JP, Figarella-Branger D, Thouveny Y. Expression of polysialylated neural cell adhesion molecule (PSA-N-CAM) in developing, adult and regenerating caudal spinal cord of the urodele amphibians. Int J Dev Biol. 1993;37:327-36.

Chen N, Zheng Y, Yin J, Li X, Zheng C. Inhibitory effects of silver nanoparticles against adenovirus type 3 in vitro. J Virol Methods. 2013a;193:470-7.

Chen X, Schluesener HJ. Nanosilver: a nanoproduct in medical application. Toxicology letters. 2008;176:1-12.

Chen Z, Lee H, Henle SJ, Cheever TR, Ekker SC, Henley JR. Primary neuron culture for nerve growth and axon guidance studies in zebrafish (Danio rerio). PloS one. 2013b;8:e57539.

Chirumamilla S, Sun D, Bullock MR, Colello RJ. Traumatic brain injury induced cell proliferation in the adult mammalian central nervous system. J Neurotrauma. 2002;19:693-703.

Choi O, Deng KK, Kim NJ, Ross L, Jr., Surampalli RY, Hu Z. The inhibitory effects of silver nanoparticles, silver ions, and silver chloride colloids on microbial growth. Water Res. 2008;42:3066-74.

Chou SD, Murshid A, Eguchi T, Gong J, Calderwood SK. HSF1 regulation of beta-catenin in mammary cancer cells through control of HuR/elavL1 expression. Oncogene. 2015;34:2178-88.

Conti L, Sipione S, Magrassi L, Bonfanti L, Rigamonti D, Pettirossi V, et al. Shc signaling in differentiating neural progenitor cells. Nature neuroscience. 2001;4:579-86.

Cooper RJ, Spitzer N. Silver nanoparticles at sublethal concentrations disrupt cytoskeleton and neurite dynamics in cultured adult neural stem cells. Neurotoxicology. 2015;48:231-8.

Cremer H, Lange R, Christoph A, Plomann M, Vopper G, Roes J, et al. Inactivation of the N-CAM gene in mice results in size reduction of the olfactory bulb and deficits in spatial learning. Nature. 1994;367:455-9.

Cushen M, Kerry J, Morris M, Cruz-Romero M, Cummins E. Migration and exposure assessment of silver from a PVC nanocomposite. Food chemistry. 2013;139:389-97.

Cushen M, Kerry J, Morris M, Cruz-Romero M, Cummins E. Evaluation and simulation of silver and copper nanoparticle migration from polyethylene nanocomposites to food and an associated exposure assessment. Journal of agricultural and food chemistry. 2014;62:1403-11.

Dale AL, Lowry GV, Casman EA. Stream dynamics and chemical transformations control the environmental fate of silver and zinc oxide nanoparticles in a watershed-scale model. Environmental science & technology. 2015;49:7285-93.

Danscher G, Locht LJ. In vivo liberation of silver ions from metallic silver surfaces. Histochemistry and cell biology. 2010;133:359-66.

Dash PK, Mach SA, Moore AN. Enhanced neurogenesis in the rodent hippocampus following traumatic brain injury. Journal of neuroscience research. 2001;63:313-9.

Dayem AA, Kim B, Gurunathan S, Choi HY, Yang G, Saha SK, et al. Biologically synthesized silver nanoparticles induce neuronal differentiation of SH-SY5Y cells via modulation of reactive oxygen species, phosphatases, and kinase signaling pathways. Biotechnology journal. 2014;9:934-43.

de Lima R, Seabra AB, Duran N. Silver nanoparticles: a brief review of cytotoxicity and genotoxicity of chemically and biogenically synthesized nanoparticles. Journal of applied toxicology : JAT. 2012;32:867-79.

De Matteis V, Malvindi MA, Galeone A, Brunetti V, De Luca E, Kote S, et al. Negligible particle-specific toxicity mechanism of silver nanoparticles: The role of Ag(+) ion release in the cytosol. Nanomedicine. 2015;11:731-9.

Devi GP, Ahmed KB, Varsha MK, Shrijha BS, Lal KK, Anbazhagan V, et al. Sulfidation of silver nanoparticle reduces its toxicity in zebrafish. Aquatic toxicology. 2015;158:149-56.

DiFebo F, Curti D, Botti F, Biella G, Bigini P, Mennini T, et al. Neural precursors (NPCs) from adult L967Q mice display early commitment to "in vitro" neuronal differentiation and hyperexcitability. Exp Neurol. 2012;236:307-18.

Dobias J, Bernier-Latmani R. Silver release from silver nanoparticles in natural waters. Environmental science & technology. 2013;47:4140-6.

Doetsch F, Alvarez-Buylla A. Network of tangential pathways for neuronal migration in adult mammalian brain. Proceedings of the National Academy of Sciences of the United States of America. 1996;93:14895-900.

Doetsch F, Caille I, Lim DA, Garcia-Verdugo JM, Alvarez-Buylla A. Subventricular zone astrocytes are neural stem cells in the adult mammalian brain. Cell. 1999;97:703-16.

Doetsch F, Garcia-Verdugo JM, Alvarez-Buylla A. Cellular composition and three-dimensional organization of the subventricular germinal zone in the adult mammalian brain. The Journal of neuroscience : the official journal of the Society for Neuroscience. 1997;17:5046-61.

Doetsch F, Petreanu L, Caille I, Garcia-Verdugo JM, Alvarez-Buylla A. EGF converts transit-amplifying neurogenic precursors in the adult brain into multipotent stem cells. Neuron. 2002;36:1021-34.

Dong L, Deng J, Sun ZM, Pan AP, Xiang XJ, Zhang L, et al. Interference with the beta-catenin gene in gastric cancer induces changes to the miRNA expression profile. Tumour Biol. 2015;36:6973-83.

Du H, Lo TM, Sitompul J, Chang MW. Systems-level analysis of Escherichia coli response to silver nanoparticles: the roles of anaerobic respiration in microbial resistance. Biochemical and biophysical research communications. 2012;424:657-62.

Dubey P, Matai I, Kumar SU, Sachdev A, Bhushan B, Gopinath P. Perturbation of cellular mechanistic system by silver nanoparticle toxicity: Cytotoxic, genotoxic and epigenetic potentials. Adv Colloid Interface Sci. 2015;221:4-21.

Dudek H, Datta SR, Franke TF, Birnbaum MJ, Yao R, Cooper GM, et al. Regulation of neuronal survival by the serine-threonine protein kinase Akt. Science. 1997;275:661-5.

Elechiguerra JL, Burt JL, Morones JR, Camacho-Bragado A, Gao X, Lara HH, et al. Interaction of silver nanoparticles with HIV-1. J Nanobiotechnology. 2005;3:6.

Elul TM, Kimes NE, Kohwi M, Reichardt LF. N- and C-terminal domains of beta-catenin, respectively, are required to initiate and shape axon arbors of retinal ganglion cells in vivo. The Journal of neuroscience : the official journal of the Society for Neuroscience. 2003;23:6567-75.

Eriksson PS, Perfilieva E, Bjork-Eriksson T, Alborn AM, Nordborg C, Peterson DA, et al. Neurogenesis in the adult human hippocampus. Nature medicine. 1998;4:1313-7.

Essers MA, de Vries-Smits LM, Barker N, Polderman PE, Burgering BM, Korswagen HC. Functional interaction between beta-catenin and FOXO in oxidative stress signaling. Science. 2005;308:1181-4.

Faigle R, Song H. Signaling mechanisms regulating adult neural stem cells and neurogenesis. Biochimica et biophysica acta. 2013;1830:2435-48.

Fukumoto S, Hsieh CM, Maemura K, Layne MD, Yet SF, Lee KH, et al. Akt participation in the Wnt signaling pathway through Dishevelled. The Journal of biological chemistry. 2001;276:17479-83.

Funato Y, Michiue T, Asashima M, Miki H. The thioredoxin-related redox-regulating protein nucleoredoxin inhibits Wnt-beta-catenin signalling through dishevelled. Nature cell biology. 2006;8:501-8.

Gage FH. Mammalian neural stem cells. Science. 2000;287:1433-8.

Gaikwad S, Ingle A, Gade A, Rai M, Falanga A, Incoronato N, et al. Antiviral activity of mycosynthesized silver nanoparticles against herpes simplex virus and human parainfluenza virus type 3. International journal of nanomedicine. 2013;8:4303-14.

Gaillet S, Rouanet JM. Silver nanoparticles: Their potential toxic effects after oral exposure and underlying mechanisms - A review. Food and chemical toxicology : an international journal published for the British Industrial Biological Research Association. 2015;77C:58-63.

Gallo G. RhoA-kinase coordinates F-actin organization and myosin II activity during semaphorin-3A-induced axon retraction. Journal of cell science. 2006;119:3413-23.

Gallo G. Mechanisms underlying the initiation and dynamics of neuronal filopodia: from neurite formation to synaptogenesis. Int Rev Cell Mol Biol. 2013;301:95-156.

Garcia-Reyero N, Kennedy AJ, Escalon BL, Habib T, Laird JG, Rawat A, et al. Differential effects and potential adverse outcomes of ionic silver and silver nanoparticles in vivo and in vitro. Environmental science & technology. 2014;48:4546-55.

Garcia-Verdugo JM, Llahi S, Ferrer I, Lopez-Garcia C. Postnatal neurogenesis in the olfactory bulbs of a lizard. A tritiated thymidine autoradiographic study. Neurosci Lett. 1989;98:247-52.

Ge S, Sailor KA, Ming GL, Song H. Synaptic integration and plasticity of new neurons in the adult hippocampus. The Journal of physiology. 2008;586:3759-65.

Gerard C, Langlois X, Gingrich J, Doucet E, Verge D, Kia HK, et al. Production and characterization of polyclonal antibodies recognizing the intracytoplasmic third loop of the 5-hydroxytryptamine1A receptor. Neuroscience. 1994;62:721-39.

Gliga AR, Skoglund S, Wallinder IO, Fadeel B, Karlsson HL. Size-dependent cytotoxicity of silver nanoparticles in human lung cells: the role of cellular uptake, agglomeration and Ag release. Particle and fibre toxicology. 2014;11:11.

Greco A, De Virgilio A, Rizzo MI, Pandolfi F, Rosati D, de Vincentiis M. The prognostic role of E-cadherin and beta-catenin overexpression in laryngeal squamous cell carcinoma. Laryngoscope. 2016;126:E148-55.

Guggenbichler JP, Boswald M, Lugauer S, Krall T. A new technology of microdispersed silver in polyurethane induces antimicrobial activity in central venous catheters. Infection. 1999;27 Suppl 1:S16-23.

Gyori BM, Venkatachalam G, Thiagarajan PS, Hsu D, Clement MV. OpenComet: an automated tool for comet assay image analysis. Redox Biol. 2014;2:457-65.

Haase A, Rott S, Mantion A, Graf P, Plendl J, Thunemann AF, et al. Effects of silver nanoparticles on primary mixed neural cell cultures: uptake, oxidative stress and acute calcium responses. Toxicological sciences : an official journal of the Society of Toxicology. 2012;126:457-68.

Hackenberg S, Scherzed A, Kessler M, Hummel S, Technau A, Froelich K, et al. Silver nanoparticles: evaluation of DNA damage, toxicity and functional impairment in human mesenchymal stem cells. Toxicology letters. 2011;201:27-33.

Hadrup N, Loeschner K, Mortensen A, Sharma AK, Qvortrup K, Larsen EH, et al. The similar neurotoxic effects of nanoparticulate and ionic silver in vivo and in vitro. Neurotoxicology. 2012;33:416-23.

Hansen U, Thunemann AF. Considerations using silver nitrate as a reference for in vitro tests with silver nanoparticles. Toxicology in vitro : an international journal published in association with BIBRA. 2016;34:120-2.

Haq S, Michael A, Andreucci M, Bhattacharya K, Dotto P, Walters B, et al. Stabilization of beta-catenin by a Wnt-independent mechanism regulates cardiomyocyte growth. Proceedings of the National Academy of Sciences of the United States of America. 2003;100:4610-5.

Hashimoto Y, Takeuchi S, Mitsunobu S, Ok YS. Chemical speciation of silver (Ag) in soils under aerobic and anaerobic conditions: Ag nanoparticles vs. ionic Ag. J Hazard Mater. 2015.

Hayes NL, Nowakowski RS. Exploiting the dynamics of S-phase tracers in developing brain: interkinetic nuclear migration for cells entering versus leaving the S-phase. Developmental neuroscience. 2000;22:44-55.

Hinck L, Nathke IS, Papkoff J, Nelson WJ. Beta-catenin: a common target for the regulation of cell adhesion by Wnt-1 and Src signaling pathways. Trends Biochem Sci. 1994;19:538-42.

Hoogeboom D, Essers MA, Polderman PE, Voets E, Smits LM, Burgering BM. Interaction of FOXO with beta-catenin inhibits beta-catenin/T cell factor activity. The Journal of biological chemistry. 2008;283:9224-30.

Hotulainen P, Lappalainen P. Stress fibers are generated by two distinct actin assembly mechanisms in motile cells. The Journal of cell biology. 2006;173:383-94.

Hsiao IL, Hsieh YK, Wang CF, Chen IC, Huang YJ. Trojan-horse mechanism in the cellular uptake of silver nanoparticles verified by direct intra- and extracellular silver speciation analysis. Environmental science & technology. 2015;49:3813-21.

Hu X, Jin L, Feng L. Erk1/2 but not PI3K pathway is required for neurotrophin 3-induced oligodendrocyte differentiation of post-natal neural stem cells. Journal of neurochemistry. 2004;90:1339-47.

Huang JH, Cai WJ, Zhang XM, Shen ZY. Icariin promotes self-renewal of neural stem cells: an involvement of extracellular regulated kinase signaling pathway. Chinese journal of integrative medicine. 2014;20:107-15.

Huels DJ, Ridgway RA, Radulescu S, Leushacke M, Campbell AD, Biswas S, et al. E-cadherin can limit the transforming properties of activating beta-catenin mutations. EMBO J. 2015;34:2321-33.

Hussain S, Meneghini E, Moosmayer M, Lacotte D, Anner BM. Potent and reversible interaction of silver with pure Na,K-ATPase and Na,K-ATPase-liposomes. Biochimica et biophysica acta. 1994;1190:402-8.

Hussain SM, Hess KL, Gearhart JM, Geiss KT, Schlager JJ. In vitro toxicity of nanoparticles in BRL 3A rat liver cells. Toxicology in vitro : an international journal published in association with BIBRA. 2005;19:975-83.

Hussain SM, Javorina AK, Schrand AM, Duhart HM, Ali SF, Schlager JJ. The interaction of manganese nanoparticles with PC-12 cells induces dopamine depletion. Toxicological sciences : an official journal of the Society of Toxicology. 2006;92:456-63.

Hwang IS, Lee J, Hwang JH, Kim KJ, Lee DG. Silver nanoparticles induce apoptotic cell death in Candida albicans through the increase of hydroxyl radicals. The FEBS journal. 2012;279:1327-38.

Iaconelli J, Huang JH, Berkovitch SS, Chattopadhyay S, Mazitschek R, Schreiber SL, et al. HDAC6 inhibitors modulate Lys49 acetylation and membrane localization of beta-catenin in human iPSC-derived neuronal cells. ACS Chem Biol. 2015;10:883-90.

Inestrosa NC, Arenas E. Emerging roles of Wnts in the adult nervous system. Nature reviews Neuroscience. 2010;11:77-86.

Jacobs BL, van Praag H, Gage FH. Adult brain neurogenesis and psychiatry: a novel theory of depression. Molecular psychiatry. 2000;5:262-9.

Jagadeesh E, Khan B, Chandran P, Khan SS. Toxic potential of iron oxide, CdS/Ag(2)S composite, CdS and Ag(2)S NPs on a fresh water alga Mougeotia sp. Colloids and surfaces B, Biointerfaces. 2015;125:284-90.

Jang MH, Bae SJ, Lee SK, Lee YJ, Hwang YS. Effect of material properties on stability of silver nanoparticles in water. Journal of nanoscience and nanotechnology. 2014;14:9665-9.

Jedynak P, Kos T, Sandi C, Kaczmarek L, Filipkowski RK. Mice with ablated adult brain neurogenesis are not impaired in antidepressant response to chronic fluoxetine. J Psychiatr Res. 2014;56:106-11.

Ji JH, Jung JH, Kim SS, Yoon JU, Park JD, Choi BS, et al. Twenty-eight-day inhalation toxicity study of silver nanoparticles in Sprague-Dawley rats. Inhalation toxicology. 2007;19:857-71.

Jiang X, Foldbjerg R, Miclaus T, Wang L, Singh R, Hayashi Y, et al. Multi-platform genotoxicity analysis of silver nanoparticles in the model cell line CHO-K1. Toxicology letters. 2013;222:55-63.

Jin L, Hu X, Feng L. NT3 inhibits FGF2-induced neural progenitor cell proliferation via the PI3K/GSK3 pathway. Journal of neurochemistry. 2005;93:1251-61.

Jun SH, Cha SH, Kim JH, Yoon M, Cho S, Park Y. Silver Nanoparticles Synthesized Using Caesalpinia sappan Extract as Potential Novel Nanoantibiotics Against Methicillin-Resistant Staphylococcus aureus. Journal of nanoscience and nanotechnology. 2015;15:5543-52.

Jung WK, Koo HC, Kim KW, Shin S, Kim SH, Park YH. Antibacterial activity and mechanism of action of the silver ion in Staphylococcus aureus and Escherichia coli. Applied and environmental microbiology. 2008;74:2171-8.

Kaegi R, Sinnet B, Zuleeg S, Hagendorfer H, Mueller E, Vonbank R, et al. Release of silver nanoparticles from outdoor facades. Environ Pollut. 2010;158:2900-5.

Kalluri HS, Vemuganti R, Dempsey RJ. Mechanism of insulin-like growth factor I-mediated proliferation of adult neural progenitor cells: role of Akt. The European journal of neuroscience. 2007;25:1041-8.

Kargov SI, Korolev NI, Stanislavskii OB, Kuznetsov IA. [Interaction of immobilized DNA with silver ions]. Mol Biol (Mosk). 1986;20:1499-505.

Kawata K, Osawa M, Okabe S. In Vitro Toxicity of Silver Nanoparticles at Noncytotoxic Doses to HepG2 Human Hepatoma Cells. Environmental science & technology. 2009;43:6046-51.

Ketschek A, Gallo G. Nerve growth factor induces axonal filopodia through localized microdomains of phosphoinositide 3-kinase activity that drive the formation of cytoskeletal precursors to filopodia. The Journal of neuroscience : the official journal of the Society for Neuroscience. 2010;30:12185-97.

Kim AS, Chae CH, Kim J, Choi JY, Kim SG, Baciut G. Silver nanoparticles induce apoptosis through the toll-like receptor 2 pathway. Oral surgery, oral medicine, oral pathology and oral radiology. 2012;113:789-98.

Kim B, Park CS, Murayama M, Hochella MF. Discovery and characterization of silver sulfide nanoparticles in final sewage sludge products. Environmental science & technology. 2010;44:7509-14.

Kim KJ, Sung WS, Moon SK, Choi JS, Kim JG, Lee DG. Antifungal effect of silver nanoparticles on dermatophytes. J Microbiol Biotechnol. 2008a;18:1482-4.

Kim S, Choi JE, Choi J, Chung KH, Park K, Yi J, et al. Oxidative stress-dependent toxicity of silver nanoparticles in human hepatoma cells. Toxicology in vitro : an international journal published in association with BIBRA. 2009;23:1076-84.

Kim YS, Kim JS, Cho HS, Rha DS, Kim JM, Park JD, et al. Twenty-eight-day oral toxicity, genotoxicity, and gender-related tissue distribution of silver nanoparticles in Sprague-Dawley rats. Inhalation toxicology. 2008b;20:575-83.

Kora AJ, Sashidhar RB. Biogenic silver nanoparticles synthesized with rhamnogalacturonan gum: Antibacterial activity, cytotoxicity and its mode of action. Arabian Journal of Chemistry. 2014.

Kovvuru P, Mancilla PE, Shirode AB, Murray TM, Begley TJ, Reliene R. Oral ingestion of silver nanoparticles induces genomic instability and DNA damage in multiple tissues. Nanotoxicology. 2015;9:162-71.

Kruszewski M, Brzoska K, Brunborg G, Asare N, Dobrzyńska M, Dušinská M, et al. Toxicity of Silver Nanomaterials in Higher Eukaryotes. In: James CF, editor. Advances in Molecular Toxicology: Elsevier; 2011. p. 179-218.

Kumari P, Chandran P, Khan SS. Synthesis and characterization of silver sulfide nanoparticles for photocatalytic and antimicrobial applications. J Photochem Photobiol B. 2014;141:235-40.

Kundel M, Jones KJ, Shin CY, Wells DG. Cytoplasmic polyadenylation element-binding protein regulates neurotrophin-3-dependent beta-catenin mRNA translation in developing hippocampal neurons. The Journal of neuroscience : the official journal of the Society for Neuroscience. 2009;29:13630-9.

Kuwabara T, Hsieh J, Muotri A, Yeo G, Warashina M, Lie DC, et al. Wnt-mediated activation of NeuroD1 and retro-elements during adult neurogenesis. Nature neuroscience. 2009;12:1097-105.

Lankveld DP, Oomen AG, Krystek P, Neigh A, Troost-de Jong A, Noorlander CW, et al. The kinetics of the tissue distribution of silver nanoparticles of different sizes. Biomaterials. 2010;31:8350-61.

Lara HH, Ayala-Nunez NV, Ixtepan-Turrent L, Rodriguez-Padilla C. Mode of antiviral action of silver nanoparticles against HIV-1. J Nanobiotechnology. 2010a;8:1.

Lara HH, Ixtepan-Turrent L, Garza-Trevino EN, Rodriguez-Padilla C. PVP-coated silver nanoparticles block the transmission of cell-free and cell-associated HIV-1 in human cervical culture. J Nanobiotechnology. 2010b;8:15.

Lazaro-Dieguez F, Aguado C, Mato E, Sanchez-Ruiz Y, Esteban I, Alberch J, et al. Dynamics of an F-actin aggresome generated by the actin-stabilizing toxin jasplakinolide. Journal of cell science. 2008;121:1415-25.

Le Belle JE, Orozco NM, Paucar AA, Saxe JP, Mottahedeh J, Pyle AD, et al. Proliferative neural stem cells have high endogenous ROS levels that regulate self-renewal and neurogenesis in a PI3K/Akt-dependant manner. Cell stem cell. 2011;8:59-71.

Lee JH, Kim YS, Song KS, Ryu HR, Sung JH, Park JD, et al. Biopersistence of silver nanoparticles in tissues from Sprague-Dawley rats. Particle and fibre toxicology. 2013;10:36.

Lee SH, Ko HM, Kwon KJ, Lee J, Han SH, Han DW, et al. tPA regulates neurite outgrowth by phosphorylation of LRP5/6 in neural progenitor cells. Molecular neurobiology. 2014;49:199-215.

Levard C, Hotze EM, Colman BP, Dale AL, Truong L, Yang XY, et al. Sulfidation of silver nanoparticles: natural antidote to their toxicity. Environmental science & technology. 2013;47:13440-8.

Levard C, Hotze EM, Lowry GV, Brown GE, Jr. Environmental transformations of silver nanoparticles: impact on stability and toxicity. Environmental science & technology. 2012;46:6900-14.

Li LH, Yen MY, Ho CC, Wu P, Wang CC, Maurya PK, et al. Non-cytotoxic nanomaterials enhance antimicrobial activities of cefmetazole against multidrug-resistant Neisseria gonorrhoeae. PloS one. 2013;8:e64794.

Li Y, Bhalli JA, Ding W, Yan J, Pearce MG, Sadiq R, et al. Cytotoxicity and genotoxicity assessment of silver nanoparticles in mouse. Nanotoxicology. 2014;8 Suppl 1:36-45.

Lie DC, Colamarino SA, Song HJ, Desire L, Mira H, Consiglio A, et al. Wnt signalling regulates adult hippocampal neurogenesis. Nature. 2005;437:1370-5.

Lim MS, Nam SH, Kim SJ, Kang SY, Lee YS, Kang KS. Signaling pathways of the early differentiation of neural stem cells by neurotrophin-3. Biochemical and biophysical research communications. 2007;357:903-9.

Liu F, Xuan A, Chen Y, Zhang J, Xu L, Yan Q, et al. Combined effect of nerve growth factor and brainderived neurotrophic factor on neuronal differentiation of neural stem cells and the potential molecular mechanisms. Molecular medicine reports. 2014;10:1739-45.

Liu P, Huang Z, Gu N. Exposure to silver nanoparticles does not affect cognitive outcome or hippocampal neurogenesis in adult mice. Ecotoxicology and environmental safety. 2013;87:124-30.

Liu XS, Chopp M, Zhang XG, Zhang RL, Buller B, Hozeska-Solgot A, et al. Gene profiles and electrophysiology of doublecortin-expressing cells in the subventricular zone after ischemic stroke. Journal of cerebral blood flow and metabolism : official journal of the International Society of Cerebral Blood Flow and Metabolism. 2009a;29:297-307.

Liu Y, Guan W, Ren G, Yang Z. The possible mechanism of silver nanoparticle impact on hippocampal synaptic plasticity and spatial cognition in rats. Toxicology letters. 2012;209:227-31.

Liu Z, Ren G, Zhang T, Yang Z. Action potential changes associated with the inhibitory effects on voltage-gated sodium current of hippocampal CA1 neurons by silver nanoparticles. Toxicology. 2009b;264:179-84.

Liu Z, Ren G, Zhang T, Yang Z. The inhibitory effects of nano-Ag on voltage-gated potassium currents of hippocampal CA1 neurons. Environ Toxicol. 2011;26:552-8.

Lois C, Alvarez-Buylla A. Long-distance neuronal migration in the adult mammalian brain. Science. 1994;264:1145-8.

Loza K, Diendorf J, Sengstock C, Ruiz-Gonzalez L, Gonzalez-Calbet JM, Vallet-Regi M, et al. The dissolution and biological effects of silver nanoparticles in biological media. Journal of Materials Chemistry B. 2014;2:1634-43.

Lu L, Sun RW, Chen R, Hui CK, Ho CM, Luk JM, et al. Silver nanoparticles inhibit hepatitis B virus replication. Antivir Ther. 2008;13:253-62.

Luskin MB. Restricted proliferation and migration of postnatally generated neurons derived from the forebrain subventricular zone. Neuron. 1993;11:173-89.

Luskin MB, Boone MS. Rate and pattern of migration of lineally-related olfactory bulb interneurons generated postnatally in the subventricular zone of the rat. Chem Senses. 1994;19:695-714.

Ma W, Li BS, Zhang L, Pant HC. Signaling cascades implicated in muscarinic regulation of proliferation of neural stem and progenitor cells. Drug News Perspect. 2004;17:258-66.

Malberg JE, Eisch AJ, Nestler EJ, Duman RS. Chronic antidepressant treatment increases neurogenesis in adult rat hippocampus. The Journal of neuroscience : the official journal of the Society for Neuroscience. 2000;20:9104-10.

Manke A, Wang L, Rojanasakul Y. Mechanisms of nanoparticle-induced oxidative stress and toxicity. Biomed Res Int. 2013;2013:942916.

Marano F, Hussain S, Rodrigues-Lima F, Baeza-Squiban A, Boland S. Nanoparticles: molecular targets and cell signalling. Archives of toxicology. 2011;85:733-41.

Marinaro C, Pannese M, Weinandy F, Sessa A, Bergamaschi A, Taketo MM, et al. Wnt signaling has opposing roles in the developing and the adult brain that are modulated by Hipk1. Cerebral cortex. 2012;22:2415-27.

Martins R, Lithgow GJ, Link W. Long live FOXO: unraveling the role of FOXO proteins in aging and longevity. Aging Cell. 2016;15:196-207.

Matiasova A, Sevc J, Mikes J, Jendzelovsky R, Daxnerova Z, Fedorocko P. Flow cytometric determination of 5-bromo-2'-deoxyuridine pharmacokinetics in blood serum after intraperitoneal administration to rats and mice. Histochemistry and cell biology. 2014;142:703-12.

Meijering E, Jacob M, Sarria JC, Steiner P, Hirling H, Unser M. Design and validation of a tool for neurite tracing and analysis in fluorescence microscopy images. Cytometry Part A : the journal of the International Society for Analytical Cytology. 2004;58:167-76.

Melnik EA, Buzulukov YP, Demin VF, Demin VA, Gmoshinski IV, Tyshko NV, et al. Transfer of Silver Nanoparticles through the Placenta and Breast Milk during in vivo Experiments on Rats. Acta naturae. 2013;5:107-15.

Miller BR, Hen R. The current state of the neurogenic theory of depression and anxiety. Current opinion in neurobiology. 2015;30:51-8.

Miura N, Shinohara Y. Cytotoxic effect and apoptosis induction by silver nanoparticles in HeLa cells. Biochemical and biophysical research communications. 2009;390:733-7.

Mohammed Fayaz A, Ao Z, Girilal M, Chen L, Xiao X, Kalaichelvan P, et al. Inactivation of microbial infectiousness by silver nanoparticles-coated condom: a new approach to inhibit HIV- and HSV-transmitted infection. International journal of nanomedicine. 2012;7:5007-18.

Mokry J, Subrtova D, Nemecek S. Cultivation of neural EGF-responsive precursor cells. Sb Ved Pr Lek Fak Karlovy Univerzity Hradci Kralove. 1995;38:167-74.

Mokry J, Subrtova D, Nemecek S. Differentiation of epidermal growth factor-responsive neural precursor cells within neurospheres. Acta Medica (Hradec Kralove). 1996;39:7-20.

Molenaar M, van de Wetering M, Oosterwegel M, Peterson-Maduro J, Godsave S, Korinek V, et al. XTcf-3 transcription factor mediates beta-catenin-induced axis formation in Xenopus embryos. Cell. 1996;86:391-9.

Money ES, Barton LE, Dawson J, Reckhow KH, Wiesner MR. Validation and sensitivity of the FINE Bayesian network for forecasting aquatic exposure to nano-silver. The Science of the total environment. 2014;473-474:685-91.

Monteiro DR, Gorup LF, Silva S, Negri M, de Camargo ER, Oliveira R, et al. Silver colloidal nanoparticles: antifungal effect against adhered cells and biofilms of Candida albicans and Candida glabrata. Biofouling. 2011;27:711-9.

Moyer CA, Brentano L, Gravens DL, Margraf HW, Monafo WW, Jr. Treatment of Large Human Burns with 0.5 Per Cent Silver Nitrate Solution. Arch Surg. 1965;90:812-67.

Mu Y, Lee SW, Gage FH. Signaling in adult neurogenesis. Current opinion in neurobiology. 2010;20:416-23.

Muller P, Langenbach A, Kaminski A, Rychly J. Modulating the actin cytoskeleton affects mechanically induced signal transduction and differentiation in mesenchymal stem cells. PloS one. 2013;8:e71283.

Munari M, Sturve J, Frenzilli G, Sanders MB, Brunelli A, Marcomini A, et al. Genotoxic effects of CdS quantum dots and Ag2S nanoparticles in fish cell lines (RTG-2). Mutat Res Genet Toxicol Environ Mutagen. 2014;775-776:89-93.

Munemitsu S, Albert I, Souza B, Rubinfeld B, Polakis P. Regulation of intracellular beta-catenin levels by the adenomatous polyposis coli (APC) tumor-suppressor protein. Proceedings of the National Academy of Sciences of the United States of America. 1995;92:3046-50.

Munger MA, Hadlock G, Stoddard G, Slawson MH, Wilkins DG, Cox N, et al. Assessing orally bioavailable commercial silver nanoparticle product on human cytochrome P450 enzyme activity. Nanotoxicology. 2015;9:474-81.

Munger MA, Radwanski P, Hadlock GC, Stoddard G, Shaaban A, Falconer J, et al. In vivo human time-exposure study of orally dosed commercial silver nanoparticles. Nanomedicine. 2014;10:1-9.

Muraoka K, Shingo T, Yasuhara T, Kameda M, Yuen WJ, Uozumi T, et al. Comparison of the therapeutic potential of adult and embryonic neural precursor cells in a rat model of Parkinson disease. Journal of neurosurgery. 2008;108:149-59.

Newnham LE, Wright MJ, Holdsworth G, Kostarelos K, Robinson MK, Rabbitts TH, et al. Functional inhibition of beta-catenin-mediated Wnt signaling by intracellular VHH antibodies. MAbs. 2015;7:180-91.

Nordeen EJ, Nordeen KW. Neurogenesis and sensitive periods in avian song learning. Trends in neurosciences. 1990;13:31-6.

Nottebohm F. From bird song to neurogenesis. Sci Am. 1989;260:74-9.

Oberdorster G, Sharp Z, Atudorei V, Elder A, Gelein R, Kreyling W, et al. Translocation of inhaled ultrafine particles to the brain. Inhalation toxicology. 2004;16:437-45.

Oh JH, Son MY, Choi MS, Kim S, Choi AY, Lee HA, et al. Integrative analysis of genes and miRNA alterations in human embryonic stem cells-derived neural cells after exposure to silver nanoparticles. Toxicology and applied pharmacology. 2015.

Olive PL, Banath JP. The comet assay: a method to measure DNA damage in individual cells. Nat Protoc. 2006;1:23-9.

Olive PL, Banath JP, Durand RE. Heterogeneity in radiation-induced DNA damage and repair in tumor and normal cells measured using the "comet" assay. Radiat Res. 1990;122:86-94.

Packard DS, Jr., Menzies RA, Skalko RG. Incorportaiton of thymidine and its analogue, bromodeoxyuridine, into embryos and maternal tissues of the mouse. Differentiation. 1973;1:397-404.

Pal S, Tak YK, Song JM. Does the antibacterial activity of silver nanoparticles depend on the shape of the nanoparticle? A study of the Gram-negative bacterium Escherichia coli. Applied and environmental microbiology. 2007;73:1712-20.

Panacek A, Kolar M, Vecerova R, Prucek R, Soukupova J, Krystof V, et al. Antifungal activity of silver nanoparticles against Candida spp. Biomaterials. 2009;30:6333-40.

Panacek A, Kvitek L, Prucek R, Kolar M, Vecerova R, Pizurova N, et al. Silver colloid nanoparticles: synthesis, characterization, and their antibacterial activity. J Phys Chem B. 2006;110:16248-53.

Pap M, Cooper GM. Role of glycogen synthase kinase-3 in the phosphatidylinositol 3-Kinase/Akt cell survival pathway. The Journal of biological chemistry. 1998;273:19929-32.

Parent JM, Valentin VV, Lowenstein DH. Prolonged seizures increase proliferating neuroblasts in the adult rat subventricular zone-olfactory bulb pathway. The Journal of neuroscience : the official journal of the Society for Neuroscience. 2002;22:3174-88.

Peifer M, Pai LM, Casey M. Phosphorylation of the Drosophila adherens junction protein Armadillo: roles for wingless signal and zeste-white 3 kinase. Dev Biol. 1994;166:543-56.

Peltier J, O'Neill A, Schaffer DV. PI3K/Akt and CREB regulate adult neural hippocampal progenitor proliferation and differentiation. Developmental neurobiology. 2007;67:1348-61.

Perez-Asensio FJ, Perpina U, Planas AM, Pozas E. Interleukin-10 regulates progenitor differentiation and modulates neurogenesis in adult brain. Journal of cell science. 2013;126:4208-19.

Petreanu L, Alvarez-Buylla A. Maturation and death of adult-born olfactory bulb granule neurons: role of olfaction. The Journal of neuroscience : the official journal of the Society for Neuroscience. 2002;22:6106-13.

Pino D, Choe Y, Pleasure SJ. Wnt5a controls neurite development in olfactory bulb interneurons. ASN neuro. 2011;3:e00059.

Powers CM, Badireddy AR, Ryde IT, Seidler FJ, Slotkin TA. Silver nanoparticles compromise neurodevelopment in PC12 cells: critical contributions of silver ion, particle size, coating, and composition. Environmental health perspectives. 2011;119:37-44.

Prozorovski T, Schneider R, Berndt C, Hartung HP, Aktas O. Redox-regulated fate of neural stem progenitor cells. Biochimica et biophysica acta. 2015;1850:1543-54.

Qu Q, Sun G, Li W, Yang S, Ye P, Zhao C, et al. Orphan nuclear receptor TLX activates Wnt/beta-catenin signalling to stimulate neural stem cell proliferation and self-renewal. Nature cell biology. 2010;12:31-40; sup pp 1-9.

Quadros ME, Marr LC. Environmental and human health risks of aerosolized silver nanoparticles. Journal of the Air & Waste Management Association. 2010;60:770-81.

Quadros ME, Marr LC. Silver nanoparticles and total aerosols emitted by nanotechnology-related consumer spray products. Environmental science & technology. 2011;45:10713-9.

Quadros ME, Pierson R, Tulve NS, Willis R, Rogers K, Thomas TA, et al. Release of Silver from Nanotechnology-Based Consumer Products for Children. Environmental science & technology. 2013;47:8894-901.

Radzig MA, Nadtochenko VA, Koksharova OA, Kiwi J, Lipasova VA, Khmel IA. Antibacterial effects of silver nanoparticles on gram-negative bacteria: influence on the growth and biofilms formation, mechanisms of action. Colloids and surfaces B, Biointerfaces. 2013;102:300-6.

Reynolds BA, Weiss S. Generation of neurons and astrocytes from isolated cells of the adult mammalian central nervous system. Science. 1992;255:1707-10.

Rice AC, Khaldi A, Harvey HB, Salman NJ, White F, Fillmore H, et al. Proliferation and neuronal differentiation of mitotically active cells following traumatic brain injury. Exp Neurol. 2003;183:406-17.

Ricketts CR, Lowbury EJ, Lawrence JC, Hall M, Wilkins MD. Mechanism of prophylaxis by silver compounds against infection of burns. Br Med J. 1970;1:444-6.

Robinson MJ, Stippec SA, Goldsmith E, White MA, Cobb MH. A constitutively active and nuclear form of the MAP kinase ERK2 is sufficient for neurite outgrowth and cell transformation. Current biology : CB. 1998;8:1141-50.

Rogers JV, Parkinson CV, Choi YW, Speshock JL, Hussain SM. A Preliminary Assessment of Silver Nanoparticle Inhibition of Monkeypox Virus Plaque Formation. Nanoscale Research Letters. 2008;3:129-33.

Rungby J, Danscher G. Localization of exogenous silver in brain and spinal cord of silver exposed rats. Acta neuropathologica. 1983;60:92-8.

Russell AD, Hugo WB. Antimicrobial activity and action of silver. Prog Med Chem. 1994;31:351-70.

Ryu JM, Lee HJ, Jung YH, Lee KH, Kim DI, Kim JY, et al. Regulation of Stem Cell Fate by ROS-mediated Alteration of Metabolism. Int J Stem Cells. 2015;8:24-35.

Samuel U, Guggenbichler JP. Prevention of catheter-related infections: the potential of a new nano-silver impregnated catheter. Int J Antimicrob Agents. 2004;23 Suppl 1:S75-8.

Scheffler B, Walton NM, Lin DD, Goetz AK, Enikolopov G, Roper SN, et al. Phenotypic and functional characterization of adult brain neuropoiesis. Proceedings of the National Academy of Sciences of the United States of America. 2005;102:9353-8.

Schrand AM, Braydich-Stolle LK, Schlager JJ, Dai L, Hussain SM. Can silver nanoparticles be useful as potential biological labels? Nanotechnology. 2008;19:235104.

Sekhon BS. Nanotechnology in agri-food production: an overview. Nanotechnol Sci Appl. 2014;7:31-53.

Sekine R, Brunetti G, Donner E, Khaksar M, Vasilev K, Jamting AK, et al. Speciation and lability of Ag-, AgCl-, and Ag2S-nanoparticles in soil determined by X-ray absorption spectroscopy and diffusive gradients in thin films. Environmental science & technology. 2015;49:897-905.

Shackleford G, Makoukji J, Grenier J, Liere P, Meffre D, Massaad C. Differential regulation of Wnt/beta-catenin signaling by Liver X Receptors in Schwann cells and oligodendrocytes. Biochem Pharmacol. 2013;86:106-14.

Sharma HS, Hussain S, Schlager J, Ali SF, Sharma A. Influence of nanoparticles on blood-brain barrier permeability and brain edema formation in rats. Acta neurochirurgica Supplement. 2010;106:359-64.

Sharma M, Chuang WW, Sun Z. Phosphatidylinositol 3-kinase/Akt stimulates androgen pathway through GSK3beta inhibition and nuclear beta-catenin accumulation. The Journal of biological chemistry. 2002;277:30935-41.

Sharma M, Leung L, Brocardo M, Henderson J, Flegg C, Henderson BR. Membrane localization of adenomatous polyposis coli protein at cellular protrusions: targeting sequences and regulation by beta-catenin. The Journal of biological chemistry. 2006;281:17140-9.

Silvestry-Rodriguez N, Sicairos-Ruelas EE, Gerba CP, Bright KR. Silver as a disinfectant. Reviews of environmental contamination and toxicology. 2007;191:23-45.

Simko M, Mattsson MO. Risks from accidental exposures to engineered nanoparticles and neurological health effects: a critical review. Particle and fibre toxicology. 2010;7:42.

Singh NP, McCoy MT, Tice RR, Schneider EL. A simple technique for quantitation of low levels of DNA damage in individual cells. Experimental cell research. 1988;175:184-91.

Sinha D, Wang Z, Ruchalski KL, Levine JS, Krishnan S, Lieberthal W, et al. Lithium activates the Wnt and phosphatidylinositol 3-kinase Akt signaling pathways to promote cell survival in the absence of soluble survival factors. American journal of physiology Renal physiology. 2005;288:F703-13.

Skalska J, Frontczak-Baniewicz M, Struzynska L. Synaptic degeneration in rat brain after prolonged oral exposure to silver nanoparticles. Neurotoxicology. 2014.

Sleiman HK, Romano RM, Oliveira CA, Romano MA. Effects of prepubertal exposure to silver nanoparticles on reproductive parameters in adult male Wistar rats. Journal of toxicology and environmental health Part A. 2013;76:1023-32.

Snyder JS, Kee N, Wojtowicz JM. Effects of adult neurogenesis on synaptic plasticity in the rat dentate gyrus. Journal of neurophysiology. 2001;85:2423-31.

Sondi I, Salopek-Sondi B. Silver nanoparticles as antimicrobial agent: a case study on E. coli as a model for Gram-negative bacteria. Journal of colloid and interface science. 2004;275:177-82.

Sonego M, Gajendra S, Parsons M, Ma Y, Hobbs C, Zentar MP, et al. Fascin regulates the migration of subventricular zone-derived neuroblasts in the postnatal brain. The Journal of neuroscience : the official journal of the Society for Neuroscience. 2013;33:12171-85.

Sosedova LM, Novikov MA, Titov EA, Rukavishnikov VS. [Evaluation of biologic effects caused by nano-silver influence on brain tissue of experimental animals]. Med Tr Prom Ekol. 2015:26-30.

Spillane M, Gallo G. Involvement of Rho-family GTPases in axon branching. Small GTPases. 2014;5:e27974.

Spillane M, Ketschek A, Donnelly CJ, Pacheco A, Twiss JL, Gallo G. Nerve growth factor-induced formation of axonal filopodia and collateral branches involves the intra-axonal synthesis of regulators of the actin-nucleating Arp2/3 complex. The Journal of neuroscience : the official journal of the Society for Neuroscience. 2012;32:17671-89.

Spillane M, Ketschek A, Jones SL, Korobova F, Marsick B, Lanier L, et al. The actin nucleating Arp2/3 complex contributes to the formation of axonal filopodia and branches through the regulation of actin patch precursors to filopodia. Developmental neurobiology. 2011;71:747-58.

Spillane M, Ketschek A, Merianda TT, Twiss JL, Gallo G. Mitochondria coordinate sites of axon branching through localized intra-axonal protein synthesis. Cell Rep. 2013;5:1564-75.

Spitzer N, Sammons GS, Price EM. Autofluorescent cells in rat brain can be convincing impostors in green fluorescent reporter studies. Journal of neuroscience methods. 2011;197:48-55.

Stewart RR, Zigova T, Luskin MB. Potassium currents in precursor cells isolated from the anterior subventricular zone of the neonatal rat forebrain. Journal of neurophysiology. 1999;81:95-102.

Su HL, Chou CC, Hung DJ, Lin SH, Pao IC, Lin JH, et al. The disruption of bacterial membrane integrity through ROS generation induced by nanohybrids of silver and clay. Biomaterials. 2009;30:5979-87.

Sui Y, Horne MK, Stanic D. Reduced proliferation in the adult mouse subventricular zone increases survival of olfactory bulb interneurons. PloS one. 2012;7:e31549.

Sun D, Bullock MR, McGinn MJ, Zhou Z, Altememi N, Hagood S, et al. Basic fibroblast growth factor-enhanced neurogenesis contributes to cognitive recovery in rats following traumatic brain injury. Exp Neurol. 2009;216:56-65.

Sun D, Colello RJ, Daugherty WP, Kwon TH, McGinn MJ, Harvey HB, et al. Cell proliferation and neuronal differentiation in the dentate gyrus in juvenile and adult rats following traumatic brain injury. J Neurotrauma. 2005a;22:95-105.

Sun L, Singh AK, Vig K, Pillai SR, Singh SR. Silver Nanoparticles Inhibit Replication of Respiratory Syncytial Virus. Journal of Biomedical Nanotechnology. 2008;4:149-58.

Sun RW, Chen R, Chung NP, Ho CM, Lin CL, Che CM. Silver nanoparticles fabricated in Hepes buffer exhibit cytoprotective activities toward HIV-1 infected cells. Chem Commun (Camb). 2005b:5059-61.

Sun Y, Hu J, Zhou L, Pollard SM, Smith A. Interplay between FGF2 and BMP controls the self-renewal, dormancy and differentiation of rat neural stem cells. Journal of cell science. 2011;124:1867-77.

Tanapat P, Galea LA, Gould E. Stress inhibits the proliferation of granule cell precursors in the developing dentate gyrus. Int J Dev Neurosci. 1998;16:235-9.

Tang J, Xiong L, Wang J, Liu L, Li J, Wan Z, et al. Influence of silver nanoparticles on neurons and blood-brain barrier via subcutaneous injection in rats. Applied Surface Science. 2008;255:502-4.

Tang J, Xiong L, Zhou G, Wang S, Wang J, Liu L, et al. Silver nanoparticles crossing through and distribution in the blood-brain barrier in vitro. Journal of nanoscience and nanotechnology. 2010;10:6313-7.

Tao YS, Edwards RA, Tubb B, Wang S, Bryan J, McCrea PD. beta-Catenin associates with the actin-bundling protein fascin in a noncadherin complex. The Journal of cell biology. 1996;134:1271-81.

Tiwari DK, Jin T, Behari J. Dose-dependent in-vivo toxicity assessment of silver nanoparticle in Wistar rats. Toxicol Mech Methods. 2011;21:13-24.

Tocharus C, Puriboriboon Y, Junmanee T, Tocharus J, Ekthuwapranee K, Govitrapong P. Melatonin enhances adult rat hippocampal progenitor cell proliferation via ERK signaling pathway through melatonin receptor. Neuroscience. 2014;275:314-21.

Toledo EM, Colombres M, Inestrosa NC. Wnt signaling in neuroprotection and stem cell differentiation. Prog Neurobiol. 2008;86:281-96.

Trefry JC, Wooley DP. Silver nanoparticles inhibit vaccinia virus infection by preventing viral entry through a macropinocytosis-dependent mechanism. J Biomed Nanotechnol. 2013;9:1624-35.

Tugulea AM, Berube D, Giddings M, Lemieux F, Hnatiw J, Priem J, et al. Nano-silver in drinking water and drinking water sources: stability and influences on disinfection by-product formation. Environmental science and pollution research international. 2014;21:11823-31.

Tulve NS, Stefaniak AB, Vance ME, Rogers K, Mwilu S, LeBouf RF, et al. Characterization of silver nanoparticles in selected consumer products and its relevance for predicting children's potential exposures. Int J Hyg Environ Health. 2015;218:345-57.

Van Breemen VL, Clemente CD. Silver deposition in the central nervous system and the hematoencephalic barrier studied with the electron microscope. J Biophys Biochem Cytol. 1955;1:161-6.

van Praag H, Christie BR, Sejnowski TJ, Gage FH. Running enhances neurogenesis, learning, and long-term potentiation in mice. Proceedings of the National Academy of Sciences of the United States of America. 1999;96:13427-31.

Vieira HL, Alves PM, Vercelli A. Modulation of neuronal stem cell differentiation by hypoxia and reactive oxygen species. Prog Neurobiol. 2011;93:444-55.

Vishnupriya S, Chaudhari K, Jagannathan R, Pradeep T. Single-Cell Investigations of Silver Nanoparticle-Bacteria Interactions. Particle & Particle Systems Characterization. 2013;30:1056-62.

von Goetz N, Fabricius L, Glaus R, Weitbrecht V, Gunther D, Hungerbuhler K. Migration of silver from commercial plastic food containers and implications for consumer exposure assessment. Food additives & contaminants Part A, Chemistry, analysis, control, exposure & risk assessment. 2013;30:612-20.

Wachs FP, Couillard-Despres S, Engelhardt M, Wilhelm D, Ploetz S, Vroemen M, et al. High efficacy of clonal growth and expansion of adult neural stem cells. Laboratory investigation; a journal of technical methods and pathology. 2003;83:949-62.

Walczak AP, Fokkink R, Peters R, Tromp P, Herrera Rivera ZE, Rietjens IM, et al. Behaviour of silver nanoparticles and silver ions in an in vitro human gastrointestinal digestion model. Nanotoxicology. 2013;7:1198-210.

Wang DD, Krueger DD, Bordey A. Biophysical properties and ionic signature of neuronal progenitors of the postnatal subventricular zone in situ. Journal of neurophysiology. 2003;90:2291-302.

Wang L, Zhang X, Li Z, Chai J, Zhang G, Yu Z, et al. Overexpression of nuclear beta-catenin at invasive front in rectal carcinoma is associated with lymph node metastasis and poor prognosis. Clin Transl Oncol. 2014;16:488-94.

Wang P, Menzies NW, Lombi E, Sekine R, Blamey FP, Hernandez-Soriano MC, et al. Silver sulfide nanoparticles (Ag2S-NPs) are taken up by plants and are phytotoxic. Nanotoxicology. 2015;9:1041-9.

Wang RT, Halpern M. Neurogenesis in the vomeronasal epithelium of adult garter snakes: 3. Use of H3-thymidine autoradiography to trace the genesis and migration of bipolar neurons. Am J Anat. 1988;183:178-85.

Wang S, Li Z, Shen H, Zhang Z, Yin Y, Wang Q, et al. Quantitative Phosphoproteomic Study Reveals that PKA Regulates Neural Stem Cell Differentiation through Phosphorylation of Catenin beta-1 and Glycogen Synthase Kinase 3beta. Stem cells. 2016.

Watanabe K, Al-Bassam S, Miyazaki Y, Wandless TJ, Webster P, Arnold DB. Networks of polarized actin filaments in the axon initial segment provide a mechanism for sorting axonal and dendritic proteins. Cell Rep. 2012;2:1546-53.

Wen LS, Santschi PH, Gill GA, Tang D. Silver concentrations in Colorado, USA, watersheds using improved methodology. Environmental toxicology and chemistry / SETAC. 2002;21:2040-51.

Wen R, Yang X, Hu L, Sun C, Zhou Q, Jiang G. Brain-targeted distribution and high retention of silver by chronic intranasal instillation of silver nanoparticles and ions in Sprague-Dawley rats. Journal of applied toxicology : JAT. 2016;36:445-53.

Wexler EM, Geschwind DH, Palmer TD. Lithium regulates adult hippocampal progenitor development through canonical Wnt pathway activation. Molecular psychiatry. 2008;13:285-92.

Wexler EM, Paucer A, Kornblum HI, Palmer TD, Geschwind DH. Endogenous Wnt signaling maintains neural progenitor cell potency. Stem cells. 2009;27:1130-41.

Wheelock MJ, Knudsen KA. Cadherins and associated proteins. In Vivo. 1991;5:505-13.

Whiteley CM, Dalla Valle M, Jones KC, Sweetman AJ. Challenges in assessing release, exposure and fate of silver nanoparticles within the UK environment. Environmental science Processes & impacts. 2013;15:2050-8.

Wigginton NS, de Titta A, Piccapietra F, Dobias J, Nesatyy VJ, Suter MJ, et al. Binding of silver nanoparticles to bacterial proteins depends on surface modifications and inhibits enzymatic activity. Environmental science & technology. 2010;44:2163-8.

Wise JP, Sr., Goodale BC, Wise SS, Craig GA, Pongan AF, Walter RB, et al. Silver nanospheres are cytotoxic and genotoxic to fish cells. Aquatic toxicology. 2010;97:34-41.

Wisniewska MB. Physiological role of beta-catenin/TCF signaling in neurons of the adult brain. Neurochem Res. 2013;38:1144-55.

Wu R, Zhai Y, Fearon ER, Cho KR. Diverse mechanisms of beta-catenin deregulation in ovarian endometrioid adenocarcinomas. Cancer research. 2001;61:8247-55.

Xiang D, Zheng Y, Duan W, Li X, Yin J, Shigdar S, et al. Inhibition of A/Human/Hubei/3/2005 (H3N2) influenza virus infection by silver nanoparticles in vitro and in vivo. International journal of nanomedicine. 2013;8:4103-13.

Xiang DX, Chen Q, Pang L, Zheng CL. Inhibitory effects of silver nanoparticles on H1N1 influenza A virus in vitro. J Virol Methods. 2011;178:137-42.

Xu F, Piett C, Farkas S, Qazzaz M, Syed NI. Silver nanoparticles (AgNPs) cause degeneration of cytoskeleton and disrupt synaptic machinery of cultured cortical neurons. Molecular brain. 2013;6:29.

Xu L, Dan M, Shao A, Cheng X, Zhang C, Yokel RA, et al. Silver nanoparticles induce tight junction disruption and astrocyte neurotoxicity in a rat blood-brain barrier primary triple coculture model. International journal of nanomedicine. 2015a;10:6105-19.

Xu L, Shao A, Zhao Y, Wang Z, Zhang C, Sun Y, et al. Neurotoxicity of Silver Nanoparticles in Rat Brain After Intragastric Exposure. Journal of nanoscience and nanotechnology. 2015b;15:4215-23.

Xu L, Shi C, Shao A, Li X, Cheng X, Ding R, et al. Toxic responses in rat embryonic cells to silver nanoparticles and released silver ions as analyzed via gene expression profiles and transmission electron microscopy. Nanotoxicology. 2014:1-10.

Yamanaka M, Hara K, Kudo J. Bactericidal actions of a silver ion solution on Escherichia coli, studied by energy-filtering transmission electron microscopy and proteomic analysis. Applied and environmental microbiology. 2005;71:7589-93.

Yang Y, Westerhoff P. Presence in, and release of, nanomaterials from consumer products. Adv Exp Med Biol. 2014;811:1-17.

Yin N, Zhang Y, Yun Z, Liu Q, Qu G, Zhou Q, et al. Silver nanoparticle exposure induces rat motor dysfunction through decrease in expression of calcium channel protein in cerebellum. Toxicology letters. 2015a;237:112-20.

Yin Y, Shen M, Tan Z, Yu S, Liu J, Jiang G. Particle coating-dependent interaction of molecular weight fractionated natural organic matter: impacts on the aggregation of silver nanoparticles. Environmental science & technology. 2015b;49:6581-9.

Yin Y, Yang X, Zhou X, Wang W, Yu S, Liu J, et al. Water chemistry controlled aggregation and photo-transformation of silver nanoparticles in environmental waters. J Environ Sci (China). 2015c;34:116-25.

Yoon JH, Abdelmohsen K, Srikantan S, Yang X, Martindale JL, De S, et al. LincRNA-p21 suppresses target mRNA translation. Molecular cell. 2012;47:648-55.

Yost C, Torres M, Miller JR, Huang E, Kimelman D, Moon RT. The axis-inducing activity, stability, and subcellular distribution of beta-catenin is regulated in Xenopus embryos by glycogen synthase kinase 3. Genes & development. 1996;10:1443-54.

Yu SJ, Yin YG, Chao JB, Shen MH, Liu JF. Highly dynamic PVP-coated silver nanoparticles in aquatic environments: chemical and morphology change induced by oxidation of Ag(0) and reduction of Ag(+). Environmental science & technology. 2014;48:403-11.

Yu X, Malenka RC. Beta-catenin is critical for dendritic morphogenesis. Nature neuroscience. 2003;6:1169-77.

Yu X, Malenka RC. Multiple functions for the cadherin/catenin complex during neuronal development. Neuropharmacology. 2004;47:779-86.

Zhang L, Li X, He R, Wu L, Zhang L, Zeng J. Chloride-induced shape transformation of silver nanoparticles in a water environment. Environ Pollut. 2015a;204:145-51.

Zhang P, Cao HY, Bai LL, Li WN, Wang Y, Chen SY, et al. The high expression of TC1 (C8orf4) was correlated with the expression of beta-catenin and cyclin D1 and the progression of squamous cell carcinomas of the tongue. Tumour Biol. 2015b;36:7061-7.

Zhang RL, LeTourneau Y, Gregg SR, Wang Y, Toh Y, Robin AM, et al. Neuroblast division during migration toward the ischemic striatum: a study of dynamic migratory and proliferative characteristics of neuroblasts from the subventricular zone. The Journal of neuroscience : the official journal of the Society for Neuroscience. 2007;27:3157-62.

Zhang Z, Kong F, Vardhanabhuti B, Mustapha A, Lin M. Detection of engineered silver nanoparticle contamination in pears. Journal of agricultural and food chemistry. 2012;60:10762-7.

Zhang Z, Yang X, Shen M, Yin Y, Liu J. Sunlight-driven reduction of silver ion to silver nanoparticle by organic matter mitigates the acute toxicity of silver to Daphnia magna. J Environ Sci (China). 2015c;35:62-8.

Zheng W, ZhuGe Q, Zhong M, Chen G, Shao B, Wang H, et al. Neurogenesis in adult human brain after traumatic brain injury. J Neurotrauma. 2013;30:1872-80.

Zhou FC, Chiang YH. Long-term nonpassaged EGF-responsive neural precursor cells are stem cells. Wound Repair Regen. 1998;6:337-48.

Zigova T, Pencea V, Wiegand SJ, Luskin MB. Intraventricular administration of BDNF increases the number of newly generated neurons in the adult olfactory bulb. Molecular and cellular neurosciences. 1998;11:234-45.

Office of Research Integrity

February 9, 2016

Robert Cooper
Department of Biological Sciences
Marshall University

Dear Robert:

This letter is in response to the submitted thesis abstract entitled *"Adult Neural Stem Cell Differentiation and Signaling is Disrupted by Low-Level Silver nanoparticle Exposure in Vitro."* After assessing the abstract it has been deemed not to be human subject research and therefore exempt from oversight of the Marshall University Institutional Review Board (IRB). The Institutional Animal Care and Use Committee (IACUC) has reviewed and approved the study under protocols #530 and #598. The applicable human and animal federal regulations have set forth the criteria utilized in making this determination. If there are any changes to the abstract you provided then you would need to resubmit that information to the Office of Research Integrity for review and a determination.

I appreciate your willingness to submit the abstract for determination. Please feel free to contact the Office of Research Integrity if you have any questions regarding future protocols that may require IRB review.

Sincerely,

Bruce F. Day, ThD, CIP
Director